Development of New Methods to Study Cell Surface Glycosylation

Tríona M. O'Connell BSc. MSc.

submitted for the award of Ph.D

School of Biotechnology
Dublin City University

Under the supervision of

Dr. Brendan O'Connor Dr. Dermot Walls

Examined by
Dr. Tara Dalton
University of Limerick

Submitted for
examination
November 2015

I hereby certify that this material, which I now submit for assessment on the programme of study leading to the award of Ph.D is entirely my own work, that I have exercised reasonable care to ensure that the work is original, and does not to the best of my knowledge breach any law of copyright, and has not been taken from the work of others save and to the extent that such work has been cited and acknowledged within the text of my work.

Signed: _____

ID No. 10212138

Date: _____

This thesis is dedicated to the memory of my father, Ken O'Connell, who bears most of the responsibility for me growing up to be a scientist.

Contents

List of Figures

List of Tables

Common Terms

APS	Ammonium Persulphate
BCR	B-cell Receptor
BEMAD	Beta-elimination with Michael addition of DTT
BSA	Bovine Serum Albumin
CBP	Carbohydrate Binding Protein
CDG	Congenital Disorders of Glycosylation
CID	Collision Induced Dissociation
dH_2O	Distilled water
DTT	Dithiothreitol
FAB	Fast Atom Bombardment
ELLA	Enzyme Linked Lectin Assay
EPO	Erythropoietin
ER	Endoplasmic Reticulum
ETD	Electr
on Transfer Dissociation	
GalNAc	N-acetyl Galactosamine
GlcNAc	N-acetyl Glucosamine
LiaT	Lab in a Trench
NHS	N-Hydroxysuccinimide
O-GlcNAc	O-Linked β-N-acetylglucosamine
OGA	O-GlcNAc hydrolase
OGT	O-GlcNAc transferase
PBS	Phosphate Buffered Saline
PDMS	Poly DiMethyl Siloxane
PI	Propidium Iodide
PS	Phophatidyl Serine
PTM	Post Translational Modification
PVA	poly vinyl alcohol
SDS	Sodium Dodecylsulphate
SDS-PAGE	Sodium Dodecyl Sulphate PolyAcrylamide Gel Electrophoresis
TBS	Tris Buffered Saline
TBST	Tris Buffered Saline with 0.5 % Tween
TEMED	N,N,N',N'-Tetramethylethylenediamine
TFA	Trifluoroacetic acid

Abstract

Development of New Methods to Study Cell Surface Glycosylation

Tríona M. O'Connell

This thesis seeks to develop new methods to study the glycosylation of cell surfaces, with a particular interest in apoptosis. Existing methods in glycobiology include mass spectrometry and glycan identification by lectin binding. The use of new carbohydrate binding proteins (CBP) and microfluidic techniques will improve the field of glycobiology and its relevance in the area of apoptosis.

A method using the Lab in a Trench (LiaT) platform was developed to allow sequential labelling of cell surface glycans using lectins. Cells are captured in the trench, fluorescently labelled lectins are then added and allowed time to bind. The lectins are then released by their corresponding free sugar, allowing probing with subsequent lectins without steric hindrance due to adjacent sugars of interest. This study represents the first sequential labelling of the same cell surface by lectins.

It has been established, that exposure of terminal N-acetylglucosamine (GlcNAc) occurs in late apoptosis and has a role in immune recognition and clearance of dead cells. AAL-2 is a recombinantly produced lectin or CBP with an affinity for the terminal sugar N-acetyl glucosamine (GlcNAc). It has a binding profile matching that of the commercial GSL II in flow cytometry and western blot, but has the advantage of not requiring additional ions in its buffer. Using flow cytometry, this study has shown that AAL-2 binds exclusively to late apoptotic cells. GafD is another recombinantly produced CBP with an affinity for terminal O-linked GlcNAc (O-GlcNAc). It was determined by flow cytometry that GafD binds to a subset very late apoptotic cells. The proteins to which GafD binds were identified through isolation of the cell membrane followed by mass spectrometric analysis. The proteins were found to be predominantly cytosolic, indicating a migration of the intracellular membrane to the cell surface during late apoptosis.

Acknowledgements

I would like to thank Dr. Dermot Walls and Dr. Brendan O'Connor for their support and supervision over the course of this project.

I would also like to acknowledge Dr. Roya Hakimjavadi, Dr. Damien King, Dr. Ruth Larragy and Dr. Linda Hughes for their time, and all the skills and advice they have given me over the years. Special thanks go to my colleagues Jonathan Cawley and Donal Monaghan for patiently producing proteins for me.

Thanks to my many friends who have listened to me, and drank much coffee and light refreshments with me, and provided plenty of moral support.

Many thanks to my sisters and brother, for support and encouragement, and the odd bit of scientific advice.

I am especially grateful to my mother, for getting me to where I am today. As I grow older I realise how much of an inspiration she is to me.

And finally, thanks to John Barrett, for feeding me and minding me, and encouraging me to pursue a Ph.D in the first place.

Chapter 1

Introduction

In 2012, the National Academy of Sciences in conjunction with the National Institutes of Health, the National Science Foundation and other interested parties, published a document calling for improved methods and tools to transform glycoscience (of Sciences et al., 2012). Progress in the study of glycobiology has not matched the rapid advances in the fields of molecular biology and protein analysis in the last fifty years. This thesis aims to contribute new methods to further the field of glycobiology.

Complex sugar structures called glycans, bound to various proteins and lipids of the cell, have important roles in permitting cells to communicate with and adhere to one another. Problems with cell glycosylation may lead to disease (section 1.1.3), whereas correct glycosylation has a protective effect (section 1.1.4) and may indeed be useful for therapeutics (section 1.1.5). Understanding the role glycosylation plays in the complex process of apoptosis (section 1.2) could potentially lead to new understanding of and diagnostics for autoimmune disease (section 1.2.2).

The current methods for studying glycans are primarily limited to mass spectrometry (section 1.3.1), which may be expensive, and carbohydrate binding proteins called lectins (section 1.3.2) that may be used as probes for techniques such as flow cytometry or western blotting (section 1.3.3).

It is hoped, that by using microfludic systems such as Lab in a Trench (section 3.1), the use of lectin probes may finally be expanded beyond using a single probe on a single cell to using multiple probes in sequence on the same cell. Furthermore, novel carbohydrate binding proteins (section 1.4) could be used in conjunction with flow cytometry (section 1.6) to further

enhance our understanding of apoptosis.

Over the course of this work, new methods to analyse the sugars on the surface of cells will be devised, using advances in microfluidics and carbohydrate binding probes to further understand the nature of cell surface glycosylation.

1.1 Glycosylation

Glycosylation covers a range of post-translational modifications whereby carbohydrates are covalently attached to a protein or lipid. These carbohydrates may be in the complex form of long straight chains or branched tree-like structures, or in the more simple form of single sugar modifications. Glycosylation has been identified in all kingdoms of life, and is absolutely crucial for multi-cellular organisms. Apweiler et al. estimate that over half of all eukaryotic proteins are glycoproteins (Apweiler et al., 1999). Glycans are built in a stepwise manner through the addition of sugar subunits by enzymes called glycosyltransferases. This process is driven by the enzymes in the pathways and the available sugars, unlike protein production that is based strictly on an RNA template.

Glycoproteins and glycolipids are proteins or lipids with attached glycans. Where the mass of carbohydrate on a protein is greater than the mass of protein, it is referred to as a proteoglycan. The glycome represents the totality of glycans and their interactions in the cell and is many times more complex than the genome or proteome. As glycosylation can occur on a whole range of proteins and lipids, in many possible orientations, formed from tens of possible sugar subunits, the possible permutations of the glycome are staggering (Laine, 1997). Furthermore, glycosylation is not directly encoded on the genome. Although glycosyltransferases that mediate glycan construction are so encoded, many do not have known consensus sequences for their site of activity, causing bioinformatic modelling of the glycome to be highly challenging. Some limited predictions of glycosylation can be made based on these enzymes, however much of our knowledge of glycan structure and localisation is through experimental measurement (Bertozzi & Sasisekharan, 2009). Competing glycosyltransferases and variations in dietary monosaccharides have been demonstrated to affect the glycome (Bertozzi & Sasisekharan, 2009; Zachara & Hart, 2006), further

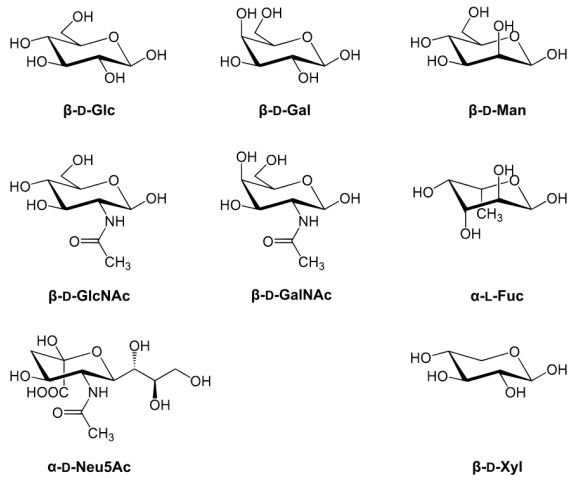

Figure 1.1: Glycans are composed of common monosaccharides. From top left: D-glucose, D-galactose, D-mannose, D-N-Acetylglucosamine, D-N-Acetylgalactosamine, L-fucose, D-N-Acetylneuraminic acid, D-Xylose. With the exception of fucose, the monosaccharides found in mammalian glycans are predominantly D-stereoisomers.
Image "Glykoproteine Zucker" by Yikrazuul, downloaded from WikiMedia.org 26/11/2015

increasing the challenges in its study.

Glycosylation may occur intracellularly as an antagonist for phosphorylation of proteins in the form of the addition of a single N-Acetylglucosamine (GlcNAc) (Zachara & Hart, 2006), or extracellularly where complex glycans are displayed on proteins and lipids and act as signalling and adhesion molecules (Figure 1.2)(Varki et al., 2009a).

Surface glycans generally fall into two categories, N-linked glycans and O-linked glycans. N-glycans represent approximately 90 % of multimeric glycan structures, with O-linked making up the remainder. N-linked glycans are found on asparagine residues and have a branched structure with a mannose at its core. O-linked glycans are frequently bound to a serine or threonine residue via an N-acetylgalactosamine (GalNAc) and can have a variety of glycan structures stemming from them. The glycans are attached to the proteins post-translationally in the endoplasmic reticulum and Golgi compartments. Glycosylation of proteins can confer solubility and thermal-stability on them (Schwarz & Aebi, 2011).

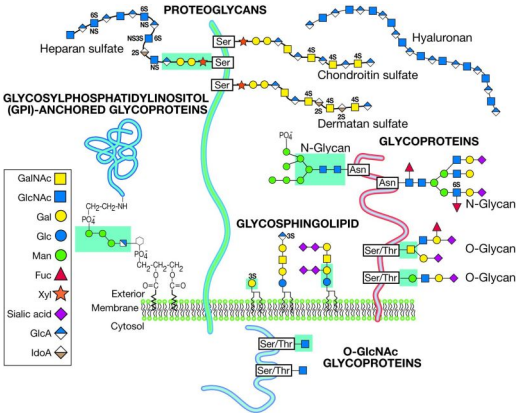

Figure 1.2: Glycan structures at the cell surface. Glycans on the surface of cells can be found attached to proteins or lipids and face the extracellular space where they act as signalling molecules or have roles in adhesion (Varki et al., 2009a).

1.1.1 Glycans are structurally diverse

Glycans have great structural diversity. Glycan modifications of proteins range from the single sugar addition of O-linked β-N-acetyl-glucosamine (O-GlcNAc), to the complex branching structures of the N-glycans, and the long chains of O-glycans. Although glycans can be attached to lipids also, glycoproteins are more commonly studied. The final capping structure of glycans is also important for their function, in particular in their various roles on the surface of a cell.

1.1.1.1 O-linked β-N-acetyl-glucosamine

O-linked β-N-acetyl-glucosamine (O-GlcNAc) is a very common post translational modification of nucleo-cytosolic proteins, with a role as an antagonist to phosphorylation (Hart & Akimoto, 2009). O-GlcNAc is attached to serine or threonine residues of proteins exclusively via O-GlcNAc transferase (OGT). There is no clear consensus site for the enzyme to bind, though about half of O-GlcNAcylated proteins have a proline-valine-serine sequence. Unlike N- and O- glycans it is not confined to the Golgi or extra cellular spaces. The addition of the single molecule of GlcNAc does not confer any change in charge on the protein, and likely acts through steric hindrance of phosphotase binding and may interfere with the proteins conformation (Banerjee et al., 2013).

O-GlcNAcylation was first discovered in 1983, and its importance wasn't

realised until 1990 when it was discovered to be involved in the regulation of ribosomal proteins (Torres & Hart, 1984; Hart & Akimoto, 2009). It cycles readily on and off proteins, through the complementary actions of OGT and O-GlcNAc hydrolase (OGA), the former catalysing the addition of O-GlcNAc from UDP-GlcNAc on to the protein and the latter enzyme its removal. As its addition does not alter charge, it does not change a protein's migration on electrophoresis, and, as it is readily hydrolysed by lysosomal hexosaminidases, the ubiquity of O-GlcNAcylation was slow to be recognised. It is now apparent that O-GlcNAcylation is essential for the survival of metazoans, and the OGT/OGA that manage its activity in the cell are highly conserved across many species. O-GlcNAc is likely to be found anywhere that serine/threonine phosphorylation occurs. OGT is cleaved during apoptosis by caspase-3, and lysosomal proteins cleave O-GlcNac from its protein sites.

Altered O-GlcNAcylation has been implicated in a number of diseases. O-GlcNAcylation is known to be widespread in nuclear and mitochondrial proteins in heart disease (Ma et al., 2015). Cycling of UDP-GlcNAc and GlcNAc has a role in regulating cellular metabolism. UDP is a potent feedback inhibitor of OGT, and UDP-GlcNAc appears to act as an "energy sensor" for the cell. UDP-GlcNAc is a by-product of glucose metabolism, and its overproduction leads to inappropriate GlcNAcylation of cellular proteins in diabetes, altering cellular metabolism (Hanover et al., 2010; Vosseller et al., 2002; McClain et al., 2002). O-GlcNAc has been demonstrated to be a key link between hyperglycaemia and cardiomyopathy through the increased O-GlcNAcylation of nuclear regulatory proteins (Clark et al., 2003).

Current methods for identification of O-GlcNAcylation are based around carbohydrate binding proteins such as sWGA or the antibody CTD 110.1, chemical modifications for mass spectrometry, and the addition of galactose based groups for easy of labelling (Banerjee et al., 2013; Ma & Hart, 2014). Affinity columns based on CTD 110.1 or sWGA have been used to enrich O-GlcNAcylated peptides for mass spectrometry, these methods rely on good specificity of binding and do not provide detail on the localisation of the O-GlcNAc modification on the peptide. Addition of modified galactoses to O-GlcNAc residues by a mutated galactosyl transferase also allows the O-GlcNAcylated proteins to be bound by the lectin ricin and enriched for. The modified galactoses can have radioactive elements or be derivatised

to allow "click" chemistry labelling of the protein. This method is useful for quantification of O-GlcNAc sites and enrichment of O-GlcNAcylated proteins but does not provide localisation data. Beta-elimination followed by Michael addition removes the OGlcNAc from the protein and replaces it with an easily detectable DTT or biotin molecule. The method was adapted from phosphorylation studies, and if using distinguishable labels can be run simultaneously with phosphorylation detection. This method has the advantage of being able to localise the OGlcNAc sites on the proteins of interest, though it does require expertise in mass spectrometry and careful sample preparation.

1.1.1.2 N-Glycosylation

N-glycans are branched glycans that are covalently attached to proteins at the nitrogen of the side group of asparagine residues. The asparagine is part of a recognised consensus sequence of asparagine - X - serine/threonine, where X can be any amino acid but proline. Although this sequence is necessary for N-glycosylation, it is not a guarantee that the site will have a glycan (Gavel & Heijne, 1990). N-glycans represent up to 90 % of the multimeric glycans found on cells and are exclusively found on the cell surface or attached to secreted proteins. N-glycosylation can be complex-biantennary, oligomannosylated, or a hybrid of the two.

The process of N-glycosylation begins on the cytoplasmic surface of the endoplasmic reticulum (ER), where a precursor 14-glycan core is built on the lipid dolichol-P-phosphate (DPP). The use of lipid carriers such as DPP for N-glycosylation appears to be highly conserved across eukaryotes (Schwarz & Aebi, 2011). The proto-N-glycan is then flipped to the luminal surface of the ER where it is transferred "en bloc" by oliggosaccharyl transferase to the nascent protein as it is produced by the ribosome. Some further modification of the glycan occurs in the late ER before the immature glycoprotein is transferred to the Golgi apparatus for final remodelling and maturation. Glycosyltransferases are spatially arranged as an enzymatic array in the golgi, with successive reactions catalysed by neighbouring transferases positioned in the fashion of an assembly line. After final capping, the glycoprotein is transferred to the cell surface where it remains or is secreted. There is no evidence for mature N-glycans in the intracellular space, even on the cytosolic portions of transmembrane proteins (Stanley et al., 2009).

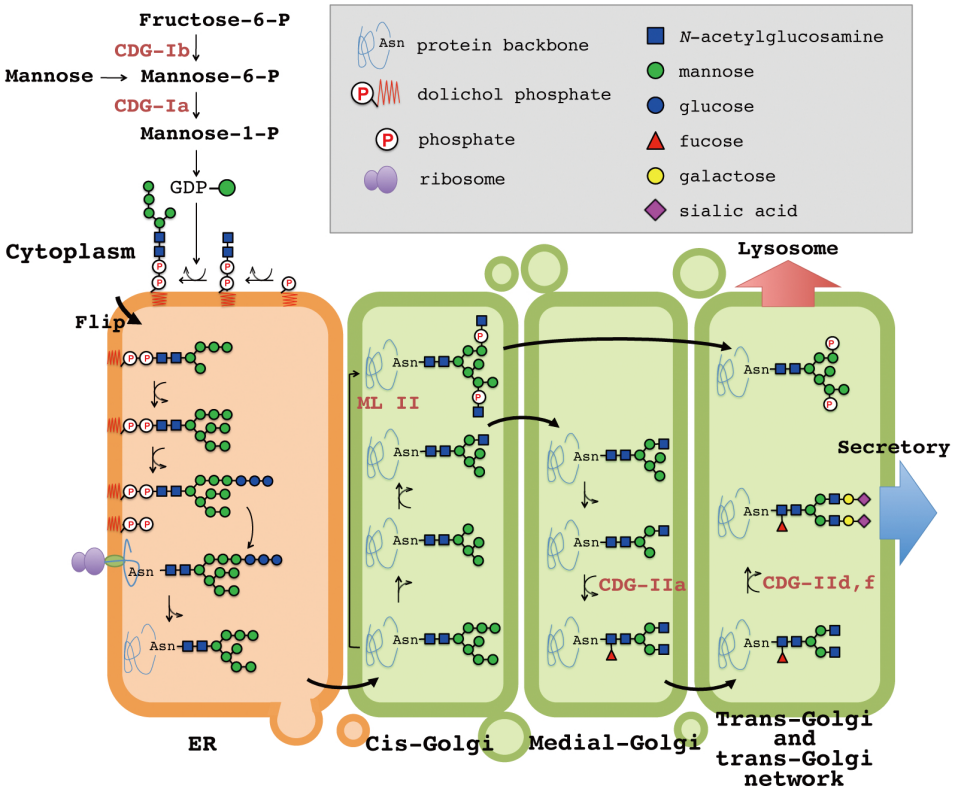

Figure 1.3: N-glycosylation begins in the endoplasmic reticulum and continues in the golgi apparatus. Image from Nakayama et al. (2013).

Proteins that are incorrectly folded or glycosylated are degraded via an ER associated degradation pathway. The proteins are also deglycosylated by a peptide N-glycanase (PNGase) (Tanabe et al., 2006; Stanley et al., 2009) that allows recovery of the glycans independant of the peptide. The removal of the glycan by PNGase leaves a negative charge on the amino acid, resulting in a change from an asparagine to an asparate residue. This is useful for identification of N-glycan sites by mass spectrometry (subsection 1.3.1).

For a summary of the process of N-glycosylation and how its enzymes have been conserved and diversified through evolution, refer to Schwarz & Aebi (2011). N-glycosylation has been observed in bacteria and lower eukaryotes, but it is not a primary method of glycosylation for them.

1.1.1.3 O-Glycosylation

O-glycans are defined by the core sugar that forms the foundation of the chain, with N-acetyl galactosamine (GalNAc) being the most common initiating sugar unit of O-glycans. They can be attached to a number of amino acids, with the most common being serine, threonine, tyrosine and hydroxyproline.

The most common type of O-glycan are the mucins, whose primary role is in retaining water at epithelia and repelling microorganisms. Mucins are initiated as a GalNAc on a serine or threonine and extended with a selection of GlcNAc, fucose, galactose or sialic acids, which may later be acetylated or sulphated (Brockhausen et al., 2009). Mucins often form a bottle brush style conformation, where the mucins branch and can block exposure of the protein epitopes. This has functions in resisting protease degradation, which can help to maintain the mucosal barrier. Mucins bind water and salts, and come in a soluble or gel format, with the gel form being more complex with surface-exposed, crosslinkable cysteines on the ends of the proteins.

The truncated O-glycan known as the Tn antigen is formed when the initiator GalNAc is not extended, and is highly antigenic. Both it and its sialyated form are known tumour markers.

O-glycosylation commencing with other sugars than GalNAc is less common. O-fucosylation and O-glucosylation of the EGF-like notch receptor appears to be critical in its function, with incorrect glycosylation causing abberrant cell signalling (Freeze & Haltiwanger, 2009). O-mannosylation of α-dystroglycan is critical for its correct function, with dysregulation leading to muscular dystrophy (Yoshida et al., 2001).

1.1.1.4 Cell surface glycosylation

The final capping of N- and O- glycans and of glycolipids in mammalian cells is generally with an α 2-3 sialic acid, with galactose or α 2-6 sialic acids being less common (Stanley & Cummings, 2009). It is rare to see the final sugar on N- and O- glycans being mannose or GlcNAc in mammalian cells, although these are common on yeasts and some microorganisms, allowing these sugars to be an immune signal for foreign antigen.

The glycosylated proteins protrude from the exterior of the cell, acting as signalling molecules and adhesion molecules. It is estimated that some 80

% of membrane proteins are glycosylated (Apweiler et al., 1999). Dube et al. (2006) used a small molecule to modify golgi functions in order to alter cell surface glycans and observe the effects dysregulation of glycosylation had on cell function.

Cell surface carbohydrates interact with a variety of carbohydrate binding proteins, or lectins, in the body. These lectins can have specific glycans that they can recognise, often in clusters. Some are soluble, such as the galectin family, and others are bound to the surface of cells. Lectin proteins are also critical for cell attachment to the extracelluar matrix and to other cells, where the cell-based lectin can interact with the glycans on cells or in the matrix (Varki & Lowe, 2009).

The selectins recognise sialyl Lewis^x antigen and a number of mucins and are critical for the functioning of the immune system (Cummings & McEver, 2009). P-selectin (platelet) is exposed on activated platelets and induces its binding to vessel walls. E-selectin (endothelial) is an inducible lectin on the walls of the endothelium of blood vessels that encourages the capture of leukocytes and platelets to an inflamed area. L-selectin (leukocyte) helps white blood cells to localise to areas of inflammation and to the lymph nodes and Peyer's patches (Collins & Paulson, 2004).

Neural cell adhesion molecule (NCAM) is a surface protein on neurons that binds with NCAM on neighbouring neurons to signal. It has been shown to be polysialylated in the embryonic form, which physically reduces binding through steric hindrance and repulsion by the negatively charged sialic acids (Varki & Lowe, 2009).

The sialylation of CD22 causes homo-oligermisation of the CD22 on B-cells, as CD22 itself has a binding affinity for α2-6 sialic acid (Barnes et al., 1999). This modulates the threshhold of B-cell activation, decreasing activation. The homo-oligmers can be disrupted by CD22 binding from another cell surface, thus permitting B-cell activation by an antigen presenting cell (Marth & Grewal, 2008).

Many immune cells recognise foreign sugars or changes in the glycans of tumours or dying cells (Marth & Grewal, 2008), for example, the removal of the capping sugar is a known eat-me signal for macrophages to remove a dying cell (see subsection 1.2.1).

1.1.2 Glycosylation is critical for multicellular organisms

Cell-surface glycosylation plays a number of roles. Cell-surface glycans can mediate cell-cell interactions such as differentiation, cell signalling, contact inhibition, immune recognition of apoptosis and non-self cells, in addition, glycosylation is important for both cell-cell adhesion and cell adhesion to basement membranes, host-pathogen reactions, metastasis and disease development (Varki et al., 2009a).

When major glycan classes are knocked out in mice, the phenotype is lethal during early embryogenesis (Freeze & Schachter, 2009; Furukawa et al., 2001). In order to overcome embryonic lethality, many research groups have turned to the Cre-Lox system to selectively knockout glycosyltransferases in model organisms. The Marth group have used Cre-Lox mice to demonstrate the requirement for hybrid N-glycans, but not complex N-glycans in neuronal development (Ye & Marth, 2004); and the importance of GlcNAc transferase II on bone, intestinal, neuronal and muscular health (Wang et al., 2001). O'Donnell et al. (2004) demonstrated the necessity for OGT for cell function and embryonic development, also using Cre-Lox mice.

1.1.3 Role of glycosylation in disease

Congenital defects of glycosylation (CDGs) result in a number of syndromes with severe phenotypes that manifest in early childhood affecting nearly every organ system (Ungar, 2009; Freeze & Aebi, 2005; Ohtsubo & Marth, 2006). Changes in glycosylation are a common phenotypic alteration found in cancer cells. In particular the Tn antigen is associated with certain types of metastatic breast and colon cancers (Ghazarian et al., 2011; Rillahan & Paulson, 2011; Häuselmann & Borsig, 2014). Increased levels of N-acetylglucosamine (GlcNAc) found in type II diabetes can lead to elevated levels of proteins with O-GlcNAc attached to them and can cause cardiac dysfunction (Zachara & Hart, 2006; Vosseller et al., 2002).

Mutations in glycosyltransferases may lead to metabolic disorders associated with inappropriate glycosylation. Not all glycosyltransferases are seen with mutations, as some are so critical to the organism that the mutations are embryonic lethal. CDGs that relate to N-glycans are divided into two major classes, Class I where the precursor oligosaccharide is inappropriately constructed and not transferred to the glycoprotein, and Class

II where the mutations are in downstream glycosyltransferases that mature the N-glycan in the golgi apparatus (Freeze & Aebi, 2005). Class I patients still have some residual N-glycosylation that may be due to a leaky pathway, but a complete absence of N-glycosylation is not seen and is hypothesised to be embryonic lethal. Mutations in N- and O- glycans and glycolipids are strongly associated with neurological disorders, with defects seen in developmental pathways leading to an altered brain structure (Freeze et al., 2015).

α dystroglycan is a glycoprotein responsible for the attachment of the cytoskeleton to extracellular laminin in basal membranes. It has been observed that defective glycosylation of dystroglycan can cause muscular dystrophies, and mutations in certain glycosyltransferases have been associated with muscular dystrophy (Yoshida et al., 2001). Under mannosylation of α dystroglycan destabilises the cell's interaction with the extracellular matrix, altered neuronal migration, and reduced stability of muscle fibres (Moremen et al., 2012).

Cystic fibrosis is characterised by dysregulation in chloride ion channels, resulting in mucins that contain insufficient salt and are excessively viscous. In addition, it has been identified that abnormal fucosylation in the mucins produced by cystic fibrosis patients may cause the increased susceptibility to airway pathogens (Lazatin et al., 1994; Stoykova et al., 2003). The fucose is an attractive binding site for many pathogens such as *Pseudomona aeruginosa* and *Burkholderia cepacia*, which, combined with the reduced clearance of mucus, results in increased morbidity for cystic fibrosis patients.

The terminal α 2-6 sialic acids on the surface of cells are recognised by the haemagglutinin protein on the surface of influenza viruses and are released by the viruses neuraminidase on infection (Stanley & Cummings, 2009; Gamblin & Skehel, 2010). Many viruses, bacteria and parasites can recognise sugars on human cell surfaces, Imberty & Varrot (2008) review the range of sugar structures they can adhere to and the adhesins they use.

Hyper-O-GlcNAcylation of the neuronal tau protein has been implicated in the development of Alzheimer's disease and subsequent hyperphosphorylation (Kanninen et al., 2004; Liu et al., 2002; Wells et al., 2002). Adult tau protein is generally phosphorylated, with O-GlcNAcylation associated with infant tau protein and with Alzheimer's disease. Indeed, the region of the genome that encodes OGT has been implicated in Alzheimer's

disease and other neurological disorders (Wells et al., 2002).

Diabetes is associated with increased O-GlcNAcylation due to excess formation of UPD-GlcNAc as excess glucose is fed into the hexoamine signalling pathway. UDP-GlcNAc is then used by OGT to O-GlcNAcylate certain proteins, resulting in their downregulation (Vosseller et al., 2002). Overexpression of OGT and consequent hyper-O-GlcNAcylation has been shown to induce insulin-resistant diabetes in mice (McClain et al., 2002). The increased O-GlcNAcylation associated with diabetes has also been demonstrated to damage the mitochondria of heart muscle cells (Hu et al., 2009) and alter the calcium cycling of heart cells (Clark et al., 2003).

Cancers have been associated with a variety of changes in cell glycosylation, including increased, decreased, truncated, embryonic and generally aberrant surface glycans. For a review of the effects of altered glycosylation on tumour metastasis, refer to Häuselmann & Borsig (2014) . Work is ongoing to develop glycoprotein biomarkers for cancer diagnostics and prognostics, and to identify drug targets based on cell surface glycans or modulation of glycosyltransferases (Dube & Bertozzi, 2005; Ghazarian et al., 2011; Vasconcelos-dos Santos et al., 2015). Although there is a general trend towards identifying glycosylation markers for cancer, the often conflicting studies may mean that this may be ultimately futile as a general cancer marker (An et al., 2009).

Gene expression of glycosyltransferases in breast cancers was analysed by Potapenko et al. (2010), who noted that there was great variance in the mRNA levels. Some glycosyltransferases were up regulated and others down, altering the cell surface and how it interacts with the tumour microenvironment and immune cells. Malignant and non-malignant tumours could be clustered, with a small subcluster from normal biopsies was observed that had upregulation of lectin genes and down regulation of initiators of O- and N- glycosylation.

Prostate specific antigen is used as a screening marker for prostate cancer but is also associated with non malignant disease such as benign prostate hyperplasia. It has been observed that PSA in malignant cases has a higher rate of fucosylation, and so there is work ongoing to develop this as an improved diagnostic marker (Dwek et al., 2010).

1.1.4 Protective functions of glycosylation

Appropriate glycosylation of proteins increases the stability and solubility of secreted glycoproteins. Glycoproteins that are missing their sialic acid cap are rapidly sequestered by the liver, thanks to clatherin mediated uptake initiated by the asialoglycoprotein receptor on hepatocytes (Rigopoulou et al., 2012). Asialyoglycoprotein receptor is also responsible for the clearance of activated platelets and vonWillibrand factor in the blood. Insufficiently sialyated therapeutics such as erythropoietin (EPO) and monoclonal antibodies are also rapidly cleared by this receptor (Liu, 2015; Lee et al., 2012; Sethuraman & Stadheim, 2006).

Glycosylation is important for host-pathogen interactions. Many microorganisms use host glycans as anchors. Human milk is abundant in oligosaccharides, many of which are not digested by the infant gut. Such oligosaccharides appear to act as decoy molecules, encouraging pathogenic microorganisms to bind to them instead of the infant's gut. It has been demonstrated that human milk oligosaccharides inhibit rotavirus binding to human cells and porcine guts (Hester et al., 2013); and are effective at preventing colonisation by *Campylobacter jejuni* (Sharon, 2006).

Gastric mucins protect against *Helicobactor pylori*. α 1-4 GlcNAc forms part of the mucin MUC6 in the deep gastric mucosa, and is taken up by the *H. pylori* as if it were glucose. *H. pylori* then substitutes the glucose in cholesterol-α-D-glucopyranoside for α1-4 GlcNAc, which, when incorporated into the cell wall destabilises it and causes the death of the bacterium. It has also been observed that porcine milk also acts as a therapeutic against *H. pylori* due to α1-4 GlcNAc it contains (Gustafsson et al., 2006).

Carbohydrate based vaccines are a possible way to encourage the body to resist microorganisms, however the low response that is generally acquired requires the use of adjuvants and peptide backbones in order to generate sufficient immune response (Sharon, 2006; Ghazarian et al., 2011). In principle vaccinating against the sugars that are specific to bacterial walls or viral capsids should encourage an immune response that recognises and clears the microorganisms more rapidly than waiting for a primary response.

Sialyation of the glycans found at the core of the immunoglobulin IgG is proven to have anti-inflammatory effects (Anthony & Ravetch, 2010). When large volumes of α 2-6 sialyated IgG were infused, they were found to have protective effects, although therapeutic infusions of proteins rarely reach

such volumes.

1.1.5 Glycosylation and therapeutics

Many modern pharmaceutical products are biologics, proteins that are recombinantly produced by large volumes of cells in culture. Antibodies in particular represent a large part of the biologics market, with targets including receptors on cancer cells and inflammatory proteins such as TNF-α. The pharmacodynamics of such drugs is of great interest to the pharmaceutical industry and to regulators. Of particular note is the influence of protein glycosylation on the serum half life of such drugs in the body (Li & d'Anjou, 2009; Liu, 2015). There is noted heterogeneity in the glycoforms of the produced proteins (Butler, 2005) and there has been attempts at understanding how to control glycosylation to maximise production of the best glycoform (St. Amand et al., 2014). The glycosylation of other proteins such as EPO also has a very significant effect on their serum half life, with researchers attempting to select for production cells that produce the glycoform of interest (Park et al., 2010; Lee et al., 2012). Hyperglycosylated EPOs have been devised with additional glycosylation sites in order to increase the molecule's longevity in the blood (Egrie & Browne, 2001).

Indeed, the necessity to be able to correctly assess glycosylation at all stages of biologics production is driving glyco-analytical tools (Higgins, 2010; Wacker et al., 2011). Variations on mass spectrometric techniques (Wagner-Rousset et al., 2008), including native mass spectrometry (Thompson et al., 2013), and use of lectins to detect desired end products (Xu et al., 2010). Lectin affinity chromatography may also play a role in enriching for desired glycoforms in the final therapeutic product (Keogh et al., 2014).

Cell therapies, including bone marrow transplants, pancreatic islet cell transplants and red blood cell transfusions require matching of donor and recipient cell antigens to ensure there is no rejection of the implanted cells. The ABO blood group glycans are highly antigenic, and much work is focussed on removing or hiding these antigens.

A number of groups have attempted to use glycosidases to remove the ABO antigens (Olsson & Clausen, 2008), with Liu et al. (2007) specifically using bacterial glycosidases. Nacharaju et al. (2005) used PEGylation to hide the ABO antigens. Although the use of stem cells is at present prohibitively costly and unreliable at producing large quanities of mature red

blood cells (Douay & Andreu, 2007), Seifinejad et al. (2010) have generated red blood cells from induced pluripotent stem cells derived from a Bombay phenotype individual. The Bombay phenotype features a truncated glycan, where even the base O blood group is not present, and is potentially a useful starting point for ABO-free red blood cell production.

Platelets are similarly matched for transfusion as red blood cells, but are more challenging to store. During cold storage β O-GlcNAc is exposed on the platelet surface, resulting in their rapid clearance after transfusion, thanks to the asialyoglycoprotein receptor on hepatocytes (Ohto & Nollet, 2011). Attempts have been made to reduce the appearance of β O-GlcNAc on the platelet surface after cold storage by galactosylating the platelets (Wandall et al., 2008). Unfortunately, although galactosylation has been successful in murine models, it does not improve cold storage of human platelets.

As human sugars can be so different from animal sugars, a major challenge in xenografts is altering the donor animal so that it does not display foreign glycans. It was recently published that a pig kidney with an α galactose knockout was successfully grafted into a baboon for 136 days (Iwase et al., 2015). The ability to modify pig organs for xenotransplantation would greatly alleviate the pressures on organ transplantation lists, whether they could be used long term or as bridging organs until a human organ could become available.

Indeed, the difference in human glycosylation from many animal glycosylations has permitted the development of a test for recombinant human EPO used as a doping agent in horse racing (Hardy et al., 2010). As the sialyated human form lasts longer in the blood, it has extended the window for testing also.

1.2 Apoptosis

Apoptosis is the controlled death of a cell brought about through a number of proteolytic pathways. It is an important cellular process that is of great interest to cell biologists. Dysregulation of apoptosis can lead to a number of diseases. Inhibition of apoptosis is a hallmark of cancer, whereby aberrant cells do not undergo programmed cell death as they normally do and instead continue to proliferate. Increased apoptosis can lead to atrophy

and various wasting diseases including neurodegenerative disorders (Elliott & Ravichandran, 2010).

Apoptosis is a form of programmed cell death (PCD) that permits cells to be degraded and cleared by the immune system in a fashion that does not disturb neighbouring cells. Early apoptotic cells dampen the inflammatory effect in the nearby area but late apoptotic cells that have not yet been cleared are pro-inflammatory. The proteins involved in apoptosis have been long studied, however there has been much less research into the study of glycosylation changes during apoptosis, some examples include Meesmann et al. (2010) and Franz et al. (2006).

Apoptosis is characterised by cell shrinkage, blebbing of the cell membrane, exposure of phosphatidyl serine (PS), fragmentation of the nuclear DNA, and general degradation of the cell contents. The cell is in a perpetual balance between pro-apoptotic factors and anti-apoptotic factors. When there is a shift towards an excess of pro-apoptotic factors, apoptosis is initiated. Extrinsic (activated by the death-induced signalling cascade) and intrinsic (mediated by the mitochondria) pathways share many common factors, most of which lead to a cascade of proteases called caspases activating further caspases to degrade the cellular components. Caspases are abundant in the cell, but are inactive until they are enzymatically cleaved. Fuchs & Steller (2015) have a comprehensive of review the various modes of programmed cell death, including apoptosis, and the signals the dying cells release.

The activation of glycoproteins on the surface of cells by lectins can induce apoptosis. For example, galectin-1 and galectin-3 binding of the O- and N-linked glycans on CD45 on T-cells induces apoptosis (Xue et al., 2013), and jacalin also induces apoptosis in B-cells by binding the glycans on CD45 (Ma et al., 2009).

Measurement of apoptosis can be carried out by flow cytometry, detecting the appearance of fluorophore labelled PS, often with the pentameric protein - Annexin-V, and the uptake nuclear stains that are generally excluded by an intact membrane. Identification of activated caspases can be performed by western blot or on a microtitre plate using caspase cleavable substrates. Destabilisation of the mitochondrial membrane is another sign of apoptosis that can be investigated in the laboratory.

1.2.1 Glycosylation changes in apoptosis

It has been demonstrated that during late apoptosis, enzymes on the cell surface such as neuraminidase are activated and cleave the terminal sialic acid caps of membrane bound glycans (Meesmann et al., 2010; Franz et al., 2006). The removal of the sialic acid caps by cellular sialidases or by treatment with exogenous neuraminidase exposes sugars such as N-Acetylglucosamine (GlcNAc) which can then be recognised by macrophages and phagocytosed (Meesmann et al., 2010).

There are no changes seen in lectin binding in early apoptosis (Franz et al., 2006) and a decrease in mitochondrial membrane potential precedes the change in GSL II binding.

An increase in mannose binding, such as with NPL, seems to indicate the transfer of immature glycans in the ER and Golgi bodies to cell surface. The transfer endoplasmic reticulum to the cell surface was demonstrated by Franz et al. (2007) using a dysfunctional immunoglobulin chain that could not transfer to the cell surface under normal conditions, but was observed on the cell surface after induction of apoptosis.

1.2.2 Apoptotic bodies have a role in autoimmune disease

Microparticles derived from activated cells and apoptosing cells appear to have a role in the pathogenesis of autoimmune disease such as Systemic Lupus Erythamatosus (Pisetsky et al., 2012; Dye et al., 2013; Bilyy et al., 2012). The microparticles contain nucleic acids and epitopes that are not normally accessible to the immune system and can stimulate the generation of autoantibodies. Display of ribosomal and endoplasmic reticulum proteins on the surface of late apoptotic cells have also been implicated as a cause of autoimmune disease such as SLE (Sun et al., 1996) and appear to form sub-populations of apoptotic bodies.

It may be possible to identify late apoptotic bodies and microparticles in the blood based on their glycosylation pattern using new tools, as it is known that late apoptotic cells and blebs display desialylated and immature glycans (Bilyy et al., 2012). By developing better techniques to detect desialyated blebs, it may be possible to improve the diagnostics of certain autoimmune diseases.

1.2.3 B-lymphocytes are a convenient cell for studying apoptosis *in vitro*

B-lymphocytes or B-cells are the cells of the immune system that produce antibodies. They are produced from haematopoetic stem cells in the bone marrow, and remain in the marrow to mature. Mature lymphocytes then migrate to the lymph nodes where they wait until they are activated by antigen presenting cells. When they are so activated, they clonally expand and begin to produce antibodies to the antigen that was presented. A small proportion of the activated B-cells then become long lived memory cells so they can be reactivated quickly if another encounter with that antigen happens.

The B-cell receptor (BCR) consists of a heavy chain immunoglobulin paired with a light chain. The structure of the BCR is very similar to the antibody that the B-cell will produce if stimulated appropriately. When B-cells are produced, the gene coding for the BCR binding site is shuffled to produce a range of binding sites across the range of B-cells. The binding site of the BCR recognises antigen and when it binds the matching antigen, if given the correct co stimulus, causes the B cell to clonally expand and produce antibody. In addition, the B-cells will undergo some shuffling of the DNA coding for the binding site of the BCR and undergoes affinity maturation, whereby a better binding antibody may be produced. (Lebien & Tedder, 2008)

As the range of antigens the BCR can recognise includes some self-antigens, mechanisms are required to prevent the B-cells from producing antigens against the body. Indeed, when such antibodies are produced, the result is auto-immune disease, where the body's own tissues are targeted by the immune system. When antigen is presented by antigen-presenting cells (APC's) or presented bound to complement, a co-stimulus of nearby receptors to the BCR enhances the binding signal for the B-cells to activate. In the absence of the co-stimulus, the B-cells undergo apoptosis to remove the self-recognising B-cell from the immune system's repertoire. As an alternative to apoptosis, some B-cells undergo annergy, where they no longer can clonally expand but the cell is not induced to die.

The cross-linking of the BCR in the absence of a co-stimulus is therefore a biologically relevant method of activating apoptosis in B-cells *in vitro*. As

the BCR is identical to the IgM immunoglobulin, saving that it has a transmembrane domain, anti-IgM antibody can be used to bind and activate the BCR. As this does not activate the co-receptors on binding the BCR, the cell undergoes apoptosis. B-cells at different stages of maturation appear to undergo apoptosis and anergy through various mechanisms (Eeva & Pelkonen, 2004; Lebien & Tedder, 2008).

Ramos is a Burkitt's lymphoma cell line that undergoes apoptosis after anti-IgM cross-linking of the BCR. The cross-linking of the BCR initiates the intrinsic apoptotic pathway by causing mitochondrial destabilisation through the incorporation of excess ceramide in the mitochondrial membrane, and thus activating downstream effector caspases (Eeva & Pelkonen, 2004; Kroesen et al., 2001).

1.3 Current methods for the detection of glycosylation

Detection, localisation and understanding the structure of glycans is crucial to understanding the role of glycans in cellular pathways. Due to the possible combinations of sugars in multiple orientations that can make up glycan structures, the glycome is massively more complex than the genome or proteome, where the respective subunits can only be joined up in a linear fashion (Bertozzi & Sasisekharan, 2009). Furthermore, the glycome appears to be even more dynamic than genome or proteome, with multiple isoforms of glycans found within apparently homogeneous cell populations. As the predictive power of computational glycomics is limited, it is crucial that accurate measurements of glycosylation are carried out in order to build databases that allow scientists to understand the role of glycosylation in relation to the proteome and genome.

Crude identification of glycosylation can be carried out using Periodic Acid Schiff (PAS) labelling of SDS-PAGE gels or tissue samples. The stain does not provide information on the nature of the glycosylation, but does allow general detection of glycans and localisation on gels and tissue sections.

Lectins are carbohydrate binding proteins that recognise specific sugar groups, but have no enzymatic activity. Commercially available lectins are generally derived from plants, where they act as toxins to deter predators (Vandenborre et al., 2011). Proteins with carbohydrate binding proper-

ties are also found in mammals, including selectins, galectins and mannose binding lectin and have roles in cell adhesion and immune recognition (Varki et al., 2009a). Proteins such as HSP-70 have lectin-like properties as they can detect glycosylation changes on other proteins (Guinez et al., 2004). Prokaryotes also have carbohydrate binding proteins that are important pathogenic mechanisms for attaching to host cells. The Irish Separation Science Cluster has taken advantage of such proteins to create novel tools for probing glycans.

Identifying key groups on a glycoprotein using lectins can offer a simpler method than using mass spectrometry to identify the glycans as the specificities of commercial lectins are well characterised. Labelled lectins have been used to stain cells for microscopy and flow cytometry (Varki et al., 2009a; Roth, 2011; Wang et al., 2008) or to detect glycosylation on glycoproteins by enzyme linked lectin assay (ELLA) (Gornik & Lauc, 2007; Thompson et al., 2011). Lectins can also be used to create microarrays for detection of glycoproteins in solution or on cells (Li et al., 2011; Rillahan & Paulson, 2011).

Although not as straightforward to study as glycoproteins, glycolipids are also analysed for their glycan structures. It is possible to separate lipids using thin layer chromatography and to blot these onto a membrane to probe with lectins in the same fashion as western blotted proteins (Taki et al., 1994).

Metabolic labelling with radio-labelled sugars may be performed, to identify where sugars are incorporated into glycan structures, their turn over, and localisation in the cell (Mulloy et al., 2009). Fluorescence Assisted Carbohydrate Electrophoresis is an alternative to radio labelling, where easily tagged sugars are given to the cells to metabolise and are then fluorescently labelled after extraction prior to electrophoresis (Gao & Lehrman, 2006).

1.3.1 Mass spectrometry

Mass spectrometry can provide a great deal of information about protein and peptide sequences, and can also be used to identify glycan structures. The challenge, however, is performing both of these analyses, allowing information about the peptide to be tied with its related glycan (Nilsson et al., 2013). Mass spectrometry requires specialist training, access to equipment, and requires very careful sample preparation.

There are a number of strategies employed to study the glycoproteome using mass spectrometry. Generally an enrichment is performed, by chemical or lectin chromatography, followed by mass spectrometric analysis. Enrichment by lectin pull-down columns relies on lectin affinity for the glycoproteins of interest, and can be problematic where lectins have multiple binding specificities and can bind a non carbohydrate ligand (Nilsson et al., 2013), for example, Annexin V is a known binder of phophatidyl serine but also recognises bisecting GlcNAc (Gao et al., 2005). Chemical methods rely on binding specific glycans, in particular, a lot of work has been carried out on the chemical capture of sialic acid bearing glycans. These glycans are held covalently to beads, and can be washed well and digested prior to elution by means of a mild acid wash to break the sialic acid from the rest of the glycopeptide. The released glycopeptides can be analysed by standard mass spectrometric methods.

It is preferable to use Electron Transfer Dissociation (ETD) or Fast Atom Bombardment (FAB) methods to ionise the glycopeptides for mass spectrometric analysis, as the more common method of Collision Induced Dissociation (CID) breaks the bond between glycan and peptide, losing localisation data (Mulloy et al., 2009; Nilsson et al., 2013). ETD and FAB are regarded as "soft" fragmentation methods that leave the peptides in relatively intact charged chunks, and so post translational modifications are more likely to remain intact. However, ETD and FAB are usually upgrade ionisation methods for standard mass spectrometers, and are so not always available.

PNGase-F is an enzyme that cleaves N-glycans from their peptide backbone, and permits separation of glycan and peptide for analysis. Unfortunately, although N-glycans and their originating peptides can be easily identified with various LC-MS protocols, it is challenging to associate the specific glycans with their location on the glycoprotein itself (Nilsson et al., 2013).

Localisation of O-linked glycans can be performed through beta-elimination followed by Michael addition of DTT (BEMAD). The DTT link to the peptide backbone is stable, and the added DTT is of known mass, allowing relatively straight forward identification of the sites of O-linked glycan binding. Although BEMAD offers localisation data, the glycan is lost during sample preparation and its structure cannot be correlated with its site on the peptide (Banerjee et al., 2013; Mulloy et al., 2009).

Furthermore, mass spectrometry techniques are primarily performed on purified proteins or bulk lysates, offering no resolution at the single cell level. Although a number of single cell mass spectrometry techniques are being developed, thanks to advances in capillary electrophoresis and microfluidics, they are not yet suitable for such complex samples and analyses as glycobiology requires (Mellors et al., 2010; Yin & Marshall, 2012; Simone, 2014).

1.3.2 Currently available carbohydrate binding proteins

Although lectins were first identified in 1888, there was no great interest in them until their usefulness in ABO blood typing was realised in the early 20th Century (Varki et al., 2009b). Lectin is derived from "legere" meaning "to select", and lectins are very selective in their binding of carbohydrates. Lectins are defined by their carbohydrate binding activity, and it is possible to inhibit the binding of lectins with sugars. Enzymes with carbohydrate binding abilities are not lectins. Many lectins appear to have defence functions in plants, discouraging animals from grazing on them.

The availability of pure, reliable plant lectins has catapulted the field of glycobiology into the modern era (Cummings & Etzler, 2009). This enabled a range of techniques, from agglutination assays to western blot style detections to be performed to identify the presence of particular glycans on a protein or cell. Lectins are largely classed based on their origins and the familys of sugars they bind.

At present, the majority of commercially available carbohydrate binding proteins are lectins that are purified from plant sources. This process is time consuming and expensive. Thanks to modern manufacturing methods, batch to batch variation is rarely an issue, and many lectins can be purchased with useful modifications such as biotin or dye labels, or conjugated to agarose beads for purification purposes.

Lectins are usually low affinity binders with their dissociation rate constants (Kd) ranging from 10^{-4} to 10^{-7} mol^{-1} s^{-1}. However, lectins are generally multimeric, with multiple glycan binding sites, and it is this avidity that gives lectins their binding strength. It is this avidity that also makes lectins better at binding proteins and cells than free sugars, in particular on cell surfaces where glycoproteins are often found in clusters (Varki et al., 2009b). When a lectin has bound to a glycoprotein on a cell or blot, it

can have multiple binding partners, requiring a high concentration of free sugars to overcome mass transport effects in order to compete at the binding sites that can be blocked by the lectin. Inhibition of lectins with free sugars before binding is a common way to demonstrate specificity, as this also shows that it is only the binding site of the lectin that is involved in the binding process and not affinity for other parts of the lectin structure. Use of larger haptens such as compound sugars or purified glycoproteins can help interfere with lectin binding at a lower concentration than that of the corresponding free sugar as they more closely represent the more complex ligands the lectin prefers to bind.

A number of anti-glycan antibodies are also available but rarely achieve the exquisite specificities of lectins. Anti-glycan antibodies have a high binding affinity compared with lectins (Gemeiner et al., 2009). Raising anti-glycan antibodies is challenging, and inoculating an animal with a glycoprotein generally causes antibodies to be produced against the protein epitopes or glycan-protein epitopes rather than the glycan itself. In addition, as glycosylation is so critical to all multi cellular organisms, it is difficult to get an animal to raise antibodies against self antigens, including common glycans. Examples of anti-glycan antibodies in humans include those against the ABO blood group, and α-galactose which causes a red meat allergy (Apostolovic et al., 2015).

Antibodies against glycans are often raised against a glycan-epitope and are often specific to a limited number of glycoproteins, missing other forms of the same glycan that are bound to a different protein.

In principle, where antibodies have been raised, it should be possible to mutate the antigen recognition site of the antibody and perform rounds of panning to find the optimum binder, however in practise this is a time consuming procedure that may not produce the desired results.

1.3.3 Current uses of carbohydrate binding proteins to detect cellular glycoproteins

Lectins are used for a range of methods for detecting glycoproteins both on cells and in lysates. Flow cytometry can be carried out on large populations of single cells using a fluorophore conjugated lectin to detect the presence of lectins on the cell surface (Varki et al., 2009a). Lectins can also be used for microscopy, whether fluorescence or immunohistochemical (Wang et al.,

2008). This permits visual localisation of the glycans that the lectin binds. Lectins are a useful tool in the histological identification of some cancers as changes in the display of certain glycans is associated with malignant change (Roth, 2011).

Micro arrays are useful for identifying glycoproteins in lysates or proteinaceous samples such as serum. The protein mixture is stained with a non-specific fluorescent protein dye, then flowed over the array, and detection of binding is carried out on a specialised reader(Zheng et al., 2005). Alternatively, the sample is adhered to the surface or otherwise captured, and fluorescently labelled lectin is used to bind the analyte (Zhao et al., 2007; Gemeiner et al., 2009). Antibody sandwich assays are a form of microarray where the glycoprotein is caputured on an antibody array and probed with a lectin (Yue & Haab, 2009). Further advances in microarray detection include the use of evanescent field fluorescence-assisted measurements that allow such sensitive measurements that on-off rates can be calculated on the arrays (Kuno et al., 2005). While microarray data has allowed great advances in the field of glycoproteomics (Hirabayashi et al., 2013; Rillahan & Paulson, 2011), it relies on the measurement of bulk lysates and does not have single cell resolution. Diffusion blotting against microarrays of lectins can allow high-throughput analysis of multiple glycoforms of range of proteins on an SDS-PAGE gel in a single assay (Etxebarria et al., 2012).

Cell capture with microarrays is challenging, as the shear force between the large cell and the small capture area of the lectin array makes it difficult to retain the cells at the spot for measurement (Li et al., 2011). Cell capture with microarrays is possible (Zheng et al., 2005), but due to the nature of microarrays, only a small number of cells can be interrogated at any time for a particular glycan.

The Enzyme Linked ImmunoSorbent Assay (ELISA) is a common tool for quantification of proteins, and the lectin equivalent, the enzyme linked lectin assay (ELLA) is a useful way to quantify glycoproteins (Gornik & Lauc, 2007; Thompson et al., 2011). The ELLA, like the ELISA, can be performed in a variety of modes, from competitive inhibition to sandwich style assay. The sample can be adsorbed to a microtitre plate, probed with lectin and an enzyme labelled secondary antibody with matching substrate used to generate signal. Likewise, where a lectin is bound to the surface, an antibody against the glycoprotein of interest can be used to detect if the

lectin has captured the glycoprotein.

By mounting lectins on beads or similar surfaces, lectins can be used to separate out particular glycoproteins which can then be eluted and analysed further (Alwael et al., 2011; Hirabayashi, 2008).

Lectins have been used as a probe for western blots (Freeze, 2001), whereby the lectin takes the place of a primary antibody. Blotting is a common technique in biology laboratories, and blotting with lectins is a straightforward way to begin glycobiological analysis of proteins of interest. By combining a variety of lectins with various enzymatic digestions of the glycans being probed, a great deal of information on the likely structure of a glycoprotein can be elucidated, which can further guide the choice of mass spectrometry technique for complete identification. Furthermore, changes of lectin binding between samples can give insights into the impact glycosylation may have on the pathway under investigation. Like traditional blotting, blocking of the membrane must be considered, the use of glycan free blocking solutions is critical, with the polymer polyvinylalcohol (PVA) and gelatine being useful agents.

1.4 Recombinant lectins as novel carbohydrate binding probes

Lectins are ubiquitous in nature and have been identified in all kingdoms of organisms. Traditionally plant lectins have been the most widely studied and by far the most common type of lectin used commercially. However, plant lectins are, for the most part, not amenable to recombinant production as they are often multimeric and glycosylated. More recent research into lectins from non-plant sources, such as prokaryotic, fungal and animal lectins, has yielded new lectin sources that are amenable to being recombinantly produced as alternative carbohydrate binding proteins (Oliveira et al., 2012; Lam & Ng, 2011).

The production of recombinant lectins serves a number of functions. Mutations of the binding site can allow identification of key amino acid residues for ligand recognition, expression in non-plant vectors can be used to see what post translational modifications are critical for lectin activity, and purification of protein for crystallography can be performed (Streicher & Sharon, 2003). As yields of plant lectins can be quite high from the amount

of source material, purification is the primary method of production rather than using recombinant sources (Lam & Ng, 2011).

The yields from non-plant sources of lectins can be quite poor when directly purified, and so cloning into an alternative expression vector should allow for production of useful amounts of protein (Lam & Ng, 2011; Gemeiner et al., 2009). Furthermore, as many plant lectins are glycosylated, they can interfere with the detection of the sample glycosylation by giving high background due to self recongition, it is hoped that non glycosylated prokaryotic proteins could be a useful alternative for glycoanalysis (Arnaud et al., 2013; Keogh et al., 2014; Vanderschaeghe et al., 2010).

GafD is a prokaryotic carbohydrate binding protein from *E. coli*'s fimbrial adhesin complex that recognises β terminal N-Acetylglucosamine (GlcNAc) (Saarela et al., 1996; Merckel et al., 2003). GafD is part of a larger fimbrial complex that contains other carbohydrate binding proteins that are important for bacterial attachment to a host's surfaces. In particular, GafD was isolated from pyelonephritogenic *E. coli* that causes rare urinary tract infections. GafD permits the *E. coli* to bind to the basement membrane protein laminin, which has many GlcNAc units exposed.

The isolation of the GlcNAc specific AAL-2 protein from the dried fruiting bodies of the mushroom *Agrocybe aegerita* was first reported by Jiang et al. (2012). It has terminal non-reducing GlcNAc specificity, similar to that of the plant lectin GSL II, and has been demonstrated to have a higher binding affinity than GSL II and has the advantage of being metal-ion independent (Jiang et al., 2012).

1.4.1 Advantage of recombinant lectins over commercially available lectins

Production of recombinant lectins has many benefits over purification from plant sources (Gemeiner et al., 2009). Purification of plant lectins , using conventional purification protocols, has also yielded significant batch-to-batch variation in the performance of the commercial plant lectins. Recombinant production of lectins yields consistent batches of proteins thus eliminating the batch to batch variation that has limited the use of commercial plant lectins to date. Recombinant lectins can be further refined through directed mutagenesis of the binding site and general lectin structure. This gives the potential to generate a library or array of related lectins

with slightly altered affinities or even specificities. It is possible to engineer in multivalency to recombinant lectins to improve binding through increased avidity (Arnaud et al., 2013).

The addition of linkers permits further labelling methods such as the addition of lysine groups for conjugation of small molecules such as biotin using N-Hydroxysuccinimide (NHS) chemistry, or the direct attachment of fluorescent proteins such as GFP, RFP or dsRed. Furthermore, the purification tag of the protein can also be targeted with, for example, anti-his antibodies, allowing detection without the need for direct labelling. The process of purification from plant extracts can be much more complex and time consuming than than using affinity purifications such as nickel-NTA (Lam & Ng, 2011; Keogh et al., 2014).

As prokaryotic lectins tend to be smaller and monomeric, some can be less toxic than the larger multi-meric plant lectins which can cross-link cell surface receptors and induce cellular change (Data not published, O'Connor lab). Their smaller size can allow multiple binding sites across a cell surface with no steric hindrance, and as each individual prokaryotic lectin is labelled, can give an increased signal across the cell.

Due to their low affinity, generating lectins through phage-display is challenging as the displaying-bacteria do not bind strongly to the substrate (Streicher & Sharon, 2003).

1.5 Isolation of cell surface proteins

A number of methods exist for the fractionation of cells for further analysis (Smith, 2011). Of particular interest is the plasma membrane, as this is the main point of interaction of a cell with its surroundings. Mature N- and O-glycans are found predominantly on the outer cell membrane, while O-GlcNAc is found interior to the cell. Fractionation permits the removal of cytosolic proteins and organelles that may display immature glycans or that might mask an investigation into surface proteins. It may be more worthwhile to examine outer membrane proteins when investigating findings from flow cytometry, as this is generally all that is labelled in such experiments. It is estimated that more than 30 % of expressed human proteins are membrane bound, however only 1 in 100 of the structures deposited in the Protein Data Bank are membrane proteins (Walian et al., 2004).

Fractionation by ultracentrifugation is a common method. Cells are mechanically lysed through a narrow gap, whether by the tiny bore of a high gauge needle or by a Dounce homogeniser. The organelles and unlysed cells are pelleted, and the finely shredded plasma membrane should exist as micelles in the supernatant. The supernatant is then ultracentrifuged to pellet the plasma membrane micelles which can be disrupted with detergent to release the plasma membrane proteins. The fractionation can also take place using discrete sucrose concentrations to collect the membrane micelles at the interface.

Solvent isolation of the plasma membrane proteins can be carried out after crude separation of the membrane from the cytoplasm and organelles (Smith, 2011). Such extraction, using butanol for example, relies on the hydrophobic solvent dispersing the lipids of the plasma membrane and the released protein moving to the polar phase. Phase extraction can also be carried out using detergents with cloud points at low temperatures such as Triton-X114 (Arnold & Linke, 2008).

Kits based on surface biotinylation also allow membrane isolation without complex equipment (Jang & Hanash, 2003; DeBlaquiere & Burgess, 1999). A sulfo-NHS-biotin is used to label exposed lysines from the surface of live cells as it is not water soluble and cannot enter the intracellular compartment through the intact cell membrane. The biotin can then be pulled down by a streptavidin bound to beads, and after washing the protein can be cleaved from the linker and examined. This method relies on the surface proteins having labellable side groups that are exposed to the environment and may not label all surface proteins.

Another common method relies on WGA affinity columns (Ghosh et al., 2004; Lin & Guidotti, 2009). As glycans are generally a feature of extracellular proteins, the WGA affinity column pulls out any GlcNAc bearing proteins which can then be eluted for analysis. Drawbacks of this approach include missing any proteins that do not contain GlcNAc and possible collection of immature proteins that have been glycosylated but not yet transported to the cell surface. Furthermore, enrichment of GlcNAc bearing proteins can influence later analysis of glycosylation to be biased towards GlcNAcylated proteins.

1.6 Flow cytometry for single cell interrogation

Flow cytometry is a powerful technique capable of analysing thousands of cells per second. Cells are hydrodynamically focussed to pass through an optical detection system in single file. Lasers excite any fluorescent stains in or on the cells and this fluorescent signal is captured per cell. In addition, the amount of laser light that passes around the cell is collected as "forward scatter" and is roughly correlated with cell size. Light scattering at 90 °is collected as "side scatter" and this refraction roughly correlated to the internal complexity of the cell. By collecting fluorophore, forward and side scatter data on each cell, a large volume of data about cell populations can be gathered rapidly. By collecting sufficient cell numbers, rare events can be studied with necessary statistical power. Many flow cytometers are also cell sorters and can electrostatically sort hundreds of cells per second into collection tubes or well plates. Flow cytometry is used in a range of research and clinical applications, from identifying apoptotic cells to monitoring residual disease in leukaemia. (

1.6.1 Principles of flow cytometry

Flow cytometry is used to measure populations of particles in suspension, generally mammalian cells, but sometimes micro-vesicles, bacteria or viruses. Samples can be stained with fluorophore labelled antibodies or lectins, stained with DNA dyes that fluoresce on intercalation between base pairs, can contain native pigments such as chlorophyll (Dubelaar et al., 1999) or recombinant fluorescent proteins such as green fluorescent protein (GFP), or be unstained and rely on the autofluorescence and scattering properties of the cell.

Samples are aspirated by direct pumping or by increasing the air pressure above the sample and therefore pushing it up a loading capillary. Direct pumping allows volumetric measurements to be made and along with cell count, cell concentration can be calculated. Air pressure driven flow does not have accurate volumetric information, but cell concentration can be calculated by adding a known volume of calibrated counting beads to the sample.

The sample is focussed into the centre of the fluidic channels by hydrodynamic focussing. Sheath fluid is injected at high speed into a channel and

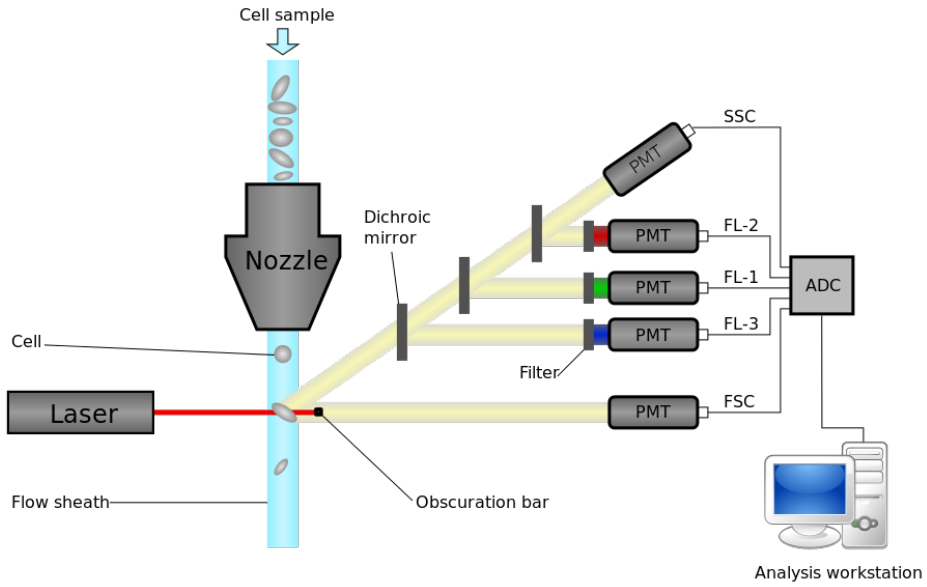

Figure 1.4: Schematic of a flow cytometer. Cells are focused in a sheath fluid and pass a laser, one by one. Each cell has its fluorescent signal and optical properties measured. The light emitted and refracted by the cell passes through a series of dichroic mirrors and band pass filters to be detected by photo multiplier tubes. Image "Flow cytometer" by Kierano, downloaded from WikiMedia.org 26/11/2015

the sample is injected into the core of this stream at a lower flow rate. The particles in the sample tend towards the centre of the stream, and the distance between the particles increases, such that the particles are travelling in single file at the core of the fluidics. There is little mixing between the sheath fluid and the sample. Generally much larger volumes of sheath fluid in relation to sample volume are required (Austin Suthanthiraraj & Graves, 2013).

Alternatives to hydrodynamic focussing allow the user to reduce fluid waste. Acoustic focussing can be used instead of or in addition to hydrodynamic focussing (Ward et al., 2009). Acoustic focussing uses sound-waves to centre the particles in the fluid stream. Some systems, such as the Millipore Guava are sheathless, where the sample is focussed through the fluidics having a very narrow diameter. The Guava also has the possibility to magnetically focus cells where they have been stained with a magnetic dye (Huh et al., 2005).

Excitation of fluorophores is carried out by lasers, with cytometers hav-

ing from one to four lasers on board. Many instruments, especially older instruments, have air-cooled gas lasers whereas newer instruments use solid state lasers that permit a smaller footprint and lower energy usage (Shapiro & Telford, 2009). Some older instruments may be retrofitted with solid state lasers as their gas lasers need replacing.

Laser light is directed at the centre of the focussed stream of particles travelling through the flow cell and the emitted light is collected and diverted to the detector array via fibre optic cables. Optical detection is generally carried out by passing the emitted light through a series of dichroic mirrors and filters to separate the light into discrete bands on to photomultiplier tubes (PMT). The collected light can be fluorescent emissions or light that is scattered due to the optical properties of the cell. The voltage across the PMTs can be adjusted to change their sensitivity, but there is always background noise at the low end of the signal (Wood, 2009). As there is often spectral bleed-over between dyes used, it is usual to perform compensation to remove the contribution of dyes into neighbouring channels.

Sony, in their SP-6800 spectral cytometer, use a series of prisms to direct the captured light on to a series of 32 PMTs, collecting the entire spectral emission rather than discrete bands as obtained with filters. They then perform spectral deconvolution to identify the signal contributed by individual fluorophores. Although this technology is not yet able to process signals fast enough for cell sorting, it provides a lot more spectral information for autofluorescence than traditional filter based cytometers.

Removing the need for discrimination of fluorophores, mass cytometry relies on heavy metal isotopes as antibody labels and uses time of flight mass spectrometry to detect the tags (Bandura, 2009). Fluidigm's Helios CyToF has the capability of measuring in 135 channels and requires new ways to analyse such potentially large datasets. As the cells are atomised to release the heavy metal tags, it is not possible to recover the cells after analysis.

Image cytometry permits micrographs of cells to be taken instead of simply measuring fluorescence signal of the cells. Examples include the Fluid-SPIM (Gualda et al., 2015), an open source single plane illumination microscope with a flow-cell for imaging cell clusters and zebrafish embryos; and Millipore's ImageStream which takes high-speed images of thousands of cells per minute at a moderate magnification. Image analysis coupled with fluidics can permit high throughput screening of cell populations and

provides a great deal of data for analysis. Such high throughput techniques requires robust software capable of unsupervised analysis of the images obtained.

Microfluidics for cytometry is an emerging field, using miniaturised fluidics and detection systems while attempting to approach the high throughput of typical flow cytometry. Few are in current commercial use, with the Sony SH800 being a notable example as it features a disposable microfluidic cuvette that can be easily replaced after clogs or dirty samples (Piyasena & Graves, 2014), although the analyser itself occupies a similar footprint to other cell sorters. For a review of microfluidics in flow cytometry, Piyasena & Graves (2014) focus on the emerging applications of microfluidics to modern flow cytometry, where Huh et al. (2005) review microfluidics are they are currently integrated into flow cytometry devices.

1.6.2 Analysis of flow cytometric data

The power of flow cytometry lies in its ability to generate large amounts of data rapidly. The bare minimum data set contains 10,000 events with at least two parameters of forward and side scatter each, but often they can be hundreds of thousands of events with multiple fluorescent parameters in addition to the scatter measurements. Although a sample may contain thousands of data points, it is but a single replicate, and care must be taken not to overinterpret single results. Indeed, the International Society for the Advancement of Cytometry recommends minimum information that should be deposited with flow cytometry publications to ensure the data is robust and appropriately interpreted (Lee et al., 2008)

Samples are generally analysed as single parameters or on bivariate plots. Fluorescence signal is compared to the unstained levels to identify background from signal. Forward scatter against side scatter can be used to screen out debris and as a crude way to identify populations. Populations can be selected on histograms or scatter plots and analysed as a subpopulation. This generation of subpopulations based on relationships between parameters is called gating, and is usually performed in a sequential manner until the population of interest is fully characterised and identified. Removal of debris, doublet cells and, in many cases, dead cells is an important part of the data refinement and should be a clear part of the gating strategy.

As the number of measurable parameters is increasing, new techniques

to handle the data are required. A variety of supervised and unsupervised multivariate analyses have been devised in recent years. Lugli et al. (2010) present a review covering the pro's and con's of SPICE (Simplified Presentation of Incredibly Complex Evaluations) and principal component analysis, which are two of the most used methods in use for multivariate flow cytometry analysis.

1.6.3 Applications of flow cytometry

Flow cytometry has made a major impact in clinical haematology laboratories where it is used for diagnosis and monitoring of haematological diseases such a leukaemias and paroxysmal nocturnal haemoglobinuria, monitoring CD4+ count of HIV positive patients, identification of foetal-maternal haemorrhage, and enumerating CD34+ stem cells in stem cell transplants. Standardisation of measurements on the flow cytometers of haematology labs is led by the EuroFlow consortium and various EQA labs such as UK-NEQAS. In the research laboratory, flow cytometry is used for characterisation of cells, bacteria and microvesicles. Immunophenotyping, investigation of cell death, cell cycle analysis, and sorting of cell subsets are but a few examples of the application of flow cytometry in the research laboratory. western blot for example. Many flow cytometers are also cell sorters and can be used to isolate cells for subculturing, or selecting subpopulations for further analysis by western blot for example.

Apoptotic cells are characterised by a decreasing forward scatter due to cell shrinkage, increasing side scatter due to condensation of cellular organelles, and the binding of fluorophore labelled annexin-V which binds the phosphotidyl serine that becomes exposed on the apoptotic cells (van Engeland et al., 1998). Late apoptosis is characterised by also taking up a fluorescent nuclear stain that should be excluded by an intact membrane. An increase in debris is also usually observed.

Surface glycosylation may also be measured using flow cytometry. Using fluorophore labelled lectins, it is possible to probe the cell surface for the presence of particular glycan structures. By selecting an appropriate fluorophore, labelled lectins can be combined with a range of other cytometric stains. Lectins have been used with cytometry to investigate apoptosis (Batisse et al., 2004; Meesmann et al., 2010; Heyder et al., 2003; Franz et al., 2006) and cancer (Bergmann et al., 1998; Arndt et al., 2011; Wang et al.,

2009).

1.7 Microfluidic platforms for single cell interrogation

Microfluidic devices typically have at least one dimension in the sub-100 μm range. This allows close control over the system as the liquid flow is predictably laminar. In addition, the small size of microfluidic systems allows scale down of reagents used in experiments, greatly reducing costs. Devices can be made optically transparent with structures to mix, measure, and meter liquids as well as trap particles such as cells. Microfluidic devices generally have scope for parallelisation for multiplexing and high throughput analyses.

Liquid handling for microfluidics requires control over the flow rate through passive or active pumping, and direction of the fluid through channel geometries and valving. Pumping can be carried out directly using syringe pumps, by relying on centrifugal force or by relying on the liquid height in a reservoir to form a pressure head. Valving can present a challenge, whether to use passive single use valves or active valves that can be actuated again and again, although some devices for single cell analysis use valving many use unvalved systems (Roman et al., 2006; Huh et al., 2005). Further considerations include the materials for manufacturing the device, the fluid itself and how it interacts with the cells and the device surfaces, how long the assay will be carried out, and how the cells will be studied.

For single cell analysis, the geometries used to capture the cells are of particular interest. Some geometries allow detailed probing of large numbers of cells while other systems are limited in cell number or in how they can be assayed. A variety of geometries are discussed here, with Lab in a Trench specifically expanded on in section 3.1.

Rowat et al. (2009) presented a device that allows for the trapping of single cells in a linear channel designed to monitor single cells as they divide and multiply. The device allows for medium term culture and monitoring of cells, and later staining of the cells for analysis.

An elegant design to capture two different cell types for fusion studies was devised by Skelley et al. (2009) based on flowing cell into cup shaped traps. By capturing the cells in a shallow trap, then reversing the flow, the

cells are transferred into a deeper trap, ensuring a single cell per deep trap. The secondary cells are then flowed into the system to fall into the deep traps directly and allowed to fuse with the cells for production of hybridomas.

Another cup based method for single cell capture is the centrifugal V-cup array presented by Burger et al. (2015, 2012). The advantages of centrifugal microfluidics is that all fluidic flow is controlled by the rotation of the disc, and therefore requires no intervention beyond changing spin speeds. The cups are oriented axially, so the settling force on the cells is due to the centrifugal force of the spinning disc. As the capture chamber is primed with fluid before cell capture, shear forces on the cells can be better controlled. The cups are scaled to fit single cells, to reduce the capture of multiple cells in the cups. A further addition of optical tweezers (Burger et al., 2015) increases the flexibility of this device by allowing selective manipulation of cells, and their transfer to a side chamber for potential downstream analysis.

Lin et al. (2013) present a system based on sieve traps with side pillars to maximise trapping of cells in the sieves. Not only are the cells trapped in the sieve, but one side of the device is micropatterned with adhesive patches for the cells to adhere to and grow. As the spaces between the micropatterning are made of non-fouling materials, stray cells cannot adhere outside of the defined micropatterns. The microfluidic traps can be removed, leaving the cells growing on their designated patches. This system allows for tracking of cells that are grown on specifically defined adherent patches.

Microwell traps for single cells come in a variety of formats. Kobel et al. (2010) trap cells in microwell divots in the sidewall of long channels, where the cells are retained by the pressure differential between the fluid flow on either side of the divot. A limitation with Kobel's device is that the area required to capture a single cell means that it is not possible to have many cells located under the microscope objective at the same time. Carlo et al. (2006) captured HeLa cells in an array of microwells, and observed their growth in relation to the shear stress on the system, noting that when the cells divided, the daughter cells also remained trapped in the wells. Cao et al. (Cao et al., 2015) use microarrays of wells for single cell trapping of cells, where the cells flowed into the device and allowed to settle into the microwells. The trapped cells can be further probed, for example for their extracellular glycans. Park et al. (2010) employ settling to fill their microarrays also, but their system is open, so the cells are allowed to settle

from a droplet on top. The open array allows probing of the cell supernatent with an antibody-conjugated membrane, which can then be used to identify cells to pick out and subculture.

Pillar arrays have been used to capture cells with antibodies (Nagrath et al., 2007; Vickers et al., 2011) and with lectins (Vickers et al., 2011). The cells are forces through convoluted paths and interact with the pillars, binding where the cell has the appropriate ligand for the capture molecule. As lectins have poor affinity, the lectin capture pillars were demonstrated to be not as effective as the antibody pillars.

Using an acoustic field with a wavelength on the same order as the cell size, Collins et al. (2015) were able to distribute single cells across a plane, with the ability to keep cells in position while media is exchanged or the cells are washed. The single cell array can thus be stained and analysed, and the device is reusable, which is unusual for many lab on a chip devices.

Droplet microfluidics involves encapsulating cells or reagents in aqueous droplets and transporting them in an oil-based carrier liquid. Single cells can be trapped in the droplets and merged with droplets containing reagents to study them. Droplet microfluidics enables relatively easy sorting of the droplets for recovery afterwards. A summary of the state of droplet microfluidics by Guo et al. (2012) covers a number of high throughput applications, including drug screening, antibody generation and virally infecting cells.

These various microfluidic devices for single cell analysis have advantages and disadvantages. Recovery of cells of interest is not practical from the acoustic set-up or linear traps, and can be challenging from cup based systems. Droplet microfluidics allows cell recovery, but as a population of droplets. Most microfluidic set ups are based on light and epi-fluorescent microscopy, which for some geometries limits the high throughput capabilities that are often portrayed as a benefit of microfluidics. Microwells and cup arrays generally allow multiple cells in the field of view of microscopes at low to moderate magnifications. Microwell arrays and some cup-based arrays are well suited to multiply probing cells with a variety of probes, whereas droplet fluidics only permit the summed addition of reagents.

Microfluidic devices are often designed as disposable, made from relatively cheap materials. PDMS is a common material for making microfluidic devices in an academic setting as it is easy to use for rapid prototyping purposes and for casting devices with high aspect ratios. PDMS is how-

ever, impractical for scaled-up production, not ideal for cell culture, and hydrophobic (Berthier et al., 2012). In some cases, it may be possible to manufacture the devices by hot embossing or injection moulding thermoplastics such as PMMA, techniques which allow for scale up but can be beyond the scope of the academic laboratory. Other devices that are made from materials such as SU-8 on silicon are generally reusable, as the cost of manufacture is quite high.

All devices also require consideration of sterility for cell work. Some materials are suitable for autoclaving, such as PDMS, other sterilisation options include running 70 % alcohol through the system for a time followed by rinsing with sterile buffer (Lu et al., 2004), gamma irradiation, or low-pressure plasma treatment (Meyvantsson & Beebe, 2008). Open systems require the use of antibiotics, and, where possible, carrying out the work in a sterile environment such as a biological safety cabinet.

Another consideration is the shear force on the captured cells. It is known that shear forces can influence the physiology of cells (Meyvantsson & Beebe, 2008; Christophis et al., 2010). For some microfluidic geometries, such as droplet microfluidics, the cells can be maintained in shear free environments, whereas other geometries such as shallow cups and microwells, there is a shear force over the top of the cells at all times there is flow in the system. Depending on the nature of the cell and the magnitude of the shear force, shear should be taken into account when observing cells in microfluidic devices.

1.8 Current use of microfluidics for glycosylation studies

Microfluidic applications in glycobiology are primarily chromatographic in nature. For a comprehensive review on microfluidics in glycomics see Lazar et al. (2011). Microscale columns for liquid chromatography with integrated ionisation nozzles for direct injection on to mass spectrometers require tiny sample and reagent volumes and are easily replaced if the column becomes damaged (Lazar et al., 2011). Lectin affinity columns have also been scaled down for microfluidic chromatography, and multiple variations of capillary electrophoresis are well suited to microfluidic platforms. Lectin microarrays have also been scaled down for automated use in microfluidic channels (Roy

et al., 2014).

Lectin adhesion assays are another use for microfluidic devices. Lectins are used to coat microfluidic devices, for capture and elution of cells (Vickers et al., 2011; Zheng et al., 2007) or for observing the cell interaction with a lectin coated surface that can promote rolling or adherence (Vickers et al., 2012). Vickers et al. (2012) used strength of adhesion as a measure of glycosylation and compared it to the strength of signal in related flow cytometry assays. This sort of comparison relies on the integrity of the cell membrane under flow, as well as binding strengths that compare to the affinity seen under staining conditions.

Agglutination within droplets in microfluidic channels has been demonstrated for ABO blood typing, using the lectin DBA for group A sub-typing (Kline et al., 2008). Blood typing is traditionally carried out using agglutination assays, with multi-valent anti-A or anti-B antibodies and using DBA for the detection of "weak A's" that are not readily detected by anti-A. This platform permitted loading of droplets with blood cells and antibody or lectin, followed by mixing and automated detection at multiple time-points.

Fewer examples of labelling cells with lectins for live cell imaging can be found in the literature. Gossett et al. (2011) labels cells trapped in individual cups with a series of stains, including WGA. The fluorescence of the previous stain is used as the baseline for the next, and so the signal from a number of probes is summed over the experiment. This results in an upper limit of probes that can be used, but has the advantage of using a single channel in an epifluorescent microscope, thus keeping equipment costs low.

Cao et al. (2012b) describe a method for detecting cell surface glycans by capturing cells on lectin electro-sensors in a microfluidic device. On this system the cell suspension was divided to pass over four different sensors and the cells allowed to settle on the sensors for 20 minutes after which the sensors were washed and detection carried out. This device isn't suitable for multiplexed sensing of single cells, however it does have the advantage of being labelled free. Cao et al. also produced a microfluidic platform that captured single cells in an array and used it for lectin based labelling of cells (Cao et al., 2012a) and subsequently performed chemical labelling of quantum dot based dyes to investigate sialic acid expression in cells (Cao et al., 2015). While the quantum dots give a very bright signal, and the ability to see individual cells gives information on population heterogeneity,

the use of chemical labelling limits the possible glycan detection.

1.9 In summary

While great advances have been made in glycobiology thanks to improvements in mass spectrometry, there is room for more techniques based on lectins and recombinant carbohydrate binding proteins.

At present, it is challenging to probe a cell surface with multiple lectins due to the steric hindrance caused by lectins binding to adjacent sugars. The current state of the art is to label populations of cells with single lectins, and assume that the population is homogeneous, allowing assumptions about glycosylation to be drawn. Unfortunately, it is now understood, that even within apparently homogeneous cell lines, there can be vast heterogeneity within the population, especially in the glycome. Better understanding of the nature of cellular glycosylation will require further correlatable data generation, that allows relationships between the sugars of glycan structures be determined.

Another area that needs to be addressed is the use of novel carbohydrate binding proteins as probes for glycans on cells. Plant lectins continue to dominate the glyco-analytical landscape, with some anti-glycan antibodies used for specific cases. The adoption of novel carbohydrate proteins would allow the detection of glycans for which plant lectins have not been identified. The generation of libraries of CBP's with similar binding specificities would allow further confirmation of the specificity of binding, and so the generated data is controlled for by multiple proteins in the way alternative antibodies are sometimes used to confirm specificity of binding in immunology. As many plant lectins can have multiple specificities, and carbohydrate binding antibodies often show cross-reactivity, the availability of such a library could vastly improve investigations that use CBP's to detect glycans. The use of CBPs can give a great deal of preliminary data on the glycosylation status of glycoproteins and cells without incurring the costs associated with mass spectrometry.

1.9.1 Aims and objectives of this work

This work has two primary goals, to use microfluidics to permit sequential labelling of the cell surface with a number of lectins, and to use novel CBP's

to investigate cell surface glycosylation in relation to apoptosis.

The microfluidic lab in a trench platform allows cells to be captured in a shear-free environment, and to be monitored by microscopy. As the exchange of fluids in the system is straightforward, it is easy to flow in fluorophore-labelled lectins for cell labelling. We reasoned that the addition of free sugars should permit the elution of the lectins from the surface of the captured cells, and that once the fluorescence had returned to background levels, a different fluorophore-labelled lectin could be added to the system to label the same cell. This would remove the steric hindrance caused between lectin molecules and permit localisation data for multiple lectins binding to the cell surface, allowing them to be correlated on individual cells.

Chapter 3 describes the rationale and limitations of LiaT for this use, while chapter 4 describes how this will be achieved, through loading cells in to the LiaT, observing the cells by bright field and epifluorescent microscopy, labelling with fluorophore-conjugated lectins, removing the lectin with free sugar, and subsequent labelling with another lectin.

The Irish Separation Science Cluster has been generating novel carbohydrate proteins for a number of years. This project seeks to apply two of their GlcNAc binders to the study of apoptotic lymphocytes, as it is known that terminal GlcNAc is exposed during late apoptosis. As AAL-2 has very similar specificity to GSL II, they were compared to see if AAL-2 would make a good substitute probe, bringing with it the flexibility of recombinant probes and the added benefit of not requiring metal ions. GafD was also trialled as it is a GlcNAc binder, but as it is an O-GlcNAc binder rather than a general terminal GlcNAc binder, it was not known how or if it might bind to the apoptotic cells. The application of these CBPs to apoptotic studies, will further affirm the use of novel CBP's in the study of glycobiology.

Chapter 5 expands upon how this will be achieved by biotinylating and fluorophore-labelling GafD and AAL-2, and using them to stain apoptotic and non-apoptotic cells by flow cytometry that will be co-stained with apoptotic markers. In this instance, flow cytometry is a more suitable technique than LiaT due to time restraints (section 4.2) and the requirement for high data collection to identify rare cell events. They will be further tested as blotting probes, and any interesting changes will be further investigated by identification with mass spectrometry.

Chapter 2

Methods

2.1 Microfabrication

2.1.1 SU-8 Masters

SU-8 (MicroChem) masters were prepared by photolithography. The lids were prepared as single layer masters and the channels and trenches were formed by two layers. Feature heights were confirmed by profilometry, as it is critical that a ratio of 1:5 between channels and trench height is obtained.

2.1.1.1 Inlet lid

A 100mm silicon wafer was sprayed with nitrogen to ensure there was no dust on the surface. The wafer was loaded onto the spin coater and SU-8 3025 poured on to cover approximately one third of the disc. The disc was spun at 500 rpm for 10 seconds and ramped to 2500 rpm for 30 seconds. The disc was soft-baked at 95 °C for 15 minutes. The mask aligner (OAI) was loaded with the lid mask and the disc exposed for 14 seconds. The disc was baked, post exposure, for 3 minutes.

The disc was developed in 30 mL of EC solvent, rocking, for 7 minutes. The solvent was changed and the disc rocked for a further 7 minutes. The disc was then washed in isopropanol, dried with nitrogen and hard baked at 150 °C for 5 minutes.

2.1.1.2 Trenches and channels

A 100mm silicon wafer was sprayed with nitrogen to ensure there was no dust on the surface. The wafer was loaded onto the spin coater, and SU-8 3025 was poured on to cover approximately one third of the disc. The disc was spun at 500 rpm for 10 seconds and ramped to 2500 rpm for 30 seconds. The disc was soft-baked at 95 °C for 15 minutes. The mask aligner (OAI) was loaded with the channel mask and disc exposed for 14 seconds. The disc was baked, post exposure, for 3 minutes. The wafer was loaded onto the spin coater and SU-8 3050 poured on to cover approximately one third of the disc. The disc was spun at 500 rpm for 10 seconds and ramped to 1000 rpm for 30 seconds. The disc was then soft-baked as before for 20 minutes.

A second layer of 3050 was poured in the same fashion, and the disc soft-baked for 25 minutes. The trenches mask was loaded on to the mask aligner (OAI). The alignment marks on the disc and mask were used to adjust the position of the disc until they were aligned. The alignment was also confirmed by checking a sample of the features. The disc was exposed for 20 seconds. The disc was baked for 5 minutes post exposure.

The disc was developed in 30 mL of Microposit EC Solvent (Chestech Ltd., UK) , rocking, for 7 minutes. The solvent was changed and the disc rocked for a further 7 minutes. The disc was then washed in isopropanol. If there was any residue, the disc was given a further 7 minutes in EC solvent, before washing again with isopropanol. It was then dried with nitrogen and hard baked at 150 °C for 5 minutes.

2.1.1.3 Profilometry

Feature heights were measured on the Dektak profilometer. Lid features should be at least 20 μm in height. Channel features should be 25-40 μm and trenches should be 150-200 μm where the ratio of channel height to trench height is at least 1:5.

2.1.2 OTS coating of masters

OTS coating is performed to prevent the PDMS from bonding to the SU-8 masters during moulding.

Masters were stacked feature-side down in a glass dish, using pieces of glass to raise the discs from the dish and any underlying discs. 30 mL of

heptane per disc was added to the dish, with 4.7 μL OTS added per disc, yielding a final concentration of 400 μM OTS. The dish was sealed to prevent evaporation of the heptane. The discs were left submerged for 2 hours. The OTS was discarded and fresh heptane added. The discs were sonicated in a sonic bath in the fresh heptane for 1 minute. The discs were then washed in methanol, followed by isopropanol and dried with nitrogen gas. They were then baked on a hot plate at 100 °C for 30 minutes.

2.1.3 PDMS Casting (optimised method)

The lid was prepared with 45 g elastomer to 2 g of curing agent. The trenches were prepared with 5 g elastomer to 1 g of curing agent. Partial curing of the pieces ensured the completed chip had good bond strength between the layers and didn't burst when subjected to high pressures during the initial loading.

Elastomer and curing agent were mixed well and poured evenly over the masters. The masters were put under vacuum for 30 minutes. The masters were transferred to an oven at 70 °C for 90 minutes. The channel and trenches master was removed as it cures fully in this time. The lid master was returned to the oven for a further 30 minutes if the PDMS stuck to a glove when touched. The lid should be tacky but not elastic. Fully cured lids do not bond well.

The PDMS was cut, carefully peeled from the masters and placed feature side up on the cutting mat. A 2 mm punch was used to make inlet holes in the lid, aligning the punch with the feature markings. The channel PDMS was cut into sections of 3 to 6 trenches and excess PDMS trimmed away. Incisions were made into the waste chamber, and the trench pieces mounted feature side up on cover-slips. Matching sections were cut from the lid PDMS and the inlets cleared of any fragments of PDMS remaining after punching. The pieces were then placed feature side down on the channel sections. The pieces were pressed together to ensure no air gaps near the features.

Chips were placed in an oven at 70°C for 2 hours to overnight to ensure they were fully cured and bonded together.

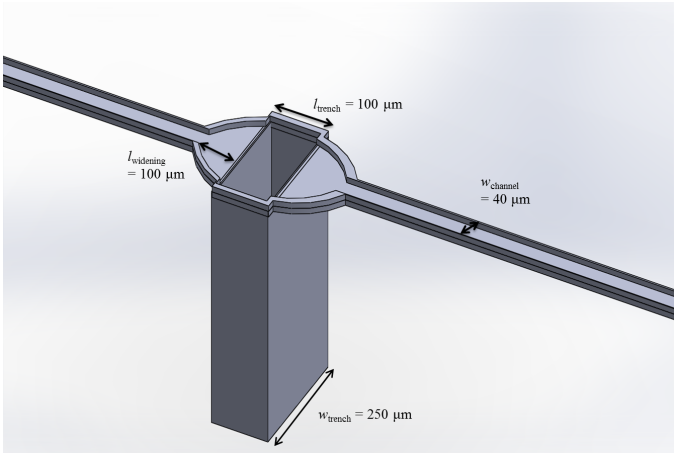

Figure 2.1: The main structure of the Lab in a Trench platform.

2.1.4 PDMS casting (original method)

Both layers were prepared with 10:1 ratio of elastomer to curing agent. The lids contain 40g elastomer to 4g curing agent, and the channels were cast from 10g of elastomer to 1g of curing agents. Plasma treatment of the surfaces increases the bond strength between the layers; however it was not always sufficient to prevent bursting of the chips during the initial high pressure of loading.

Elastomer and curing agent were mixed well and put under vacuum for 30 minutes. The PDMS was then poured onto the masters carefully to avoid air bubbles and transferred to an oven at 65 °C for 4 hours or overnight.

The PDMS was cut, carefully peeled from the masters and placed feature side up on the cutting mat. A 2 mm punch was used to make inlet holes in the lid, aligning the punch with the feature markings. The channel PDMS was cut into sections of 3 to 6 trenches and excess PDMS trimmed away. The trench pieces were mounted feature side up on cover-slips. Matching sections were cut from the lid PDMS and the inlets cleared of any fragments of PDMS remaining after punching.

The pieces were placed, feature side up, in a Harrick plasma cleaner, and subjected to 5 minutes of air plasma treatment at an RF setting of high at a pressure of approximately 1 Torr. The pieces were pressed together to ensure no air gaps near the features. Chips were placed in an oven at 70°C for 2 hours to overnight to ensure they were fully cured and bonded together.

2.2 Lab in a Trench experimental procedures

2.2.1 Preparation of Lab in a Trench chips for cell capture

Chips were plasma treated to hydrophillise the surface to ensure easy priming and reduce the occurrence of air bubbles.

LiaT chips were placed in a dish in the chamber of a Harrick plasma cleaner. A vacuum was applied to the chamber until the pressure reached 300 mTorr and air was metered into the chamber to give a pressure of approximately 1 Torr. The plasma cleaner was set to an RF setting of 'high' and the chips treated for 5 minutes.

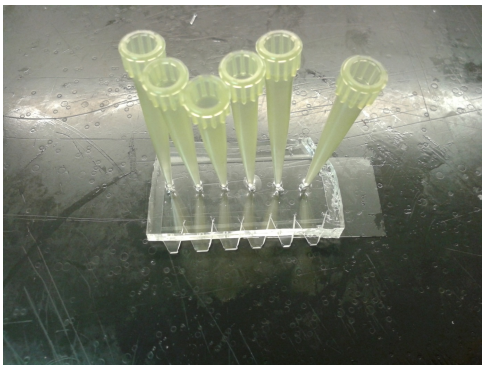

Figure 2.2: A completed LiaT chip with reservoirs in place.

Chips were removed from the vacuum and primed with 20 μL of appropriate buffer or media. Priming was performed immediately after removal from the plasma cleaner to take advantage of the temporarily hydrophillised surfaces. Pressure was maintained on the pipette until the refractive index of the channels matched that of the surrounding PDMS. The pipette tip is left in the inlet to serve as a reservoir.

Chips were examined under the microscope to ensure there was no debris or fragments of PDMS obstructing the trenches and that the system was free of air bubbles. Reservoir tips were removed from unsuitable channels to ensure they would not be used in error.

2.2.2 Cell capture using Lab in a Trench

Cell capture was observed using an Olympus IX81 motorized inverted microscope with an attached Hamamatsu ORCA - ER digital camera C4742-80, and stopped when sufficient cells were captured. Cell capture was halted

when up to two thirds of the trench area had been covered. Overfilling of the trenches is not advised as overlapping cells cause difficulty in subsequent image analysis.

When used at 37 °C, the chamber was humidified to reduce evaporation effects.

Most of the liquid from the reservoir was removed using a gel loading tip, until there was less than 1 μL of liquid remaining in the reservoir and it was below the height of the lid PDMS (but not lower than the tip in the inlet, so as to prevent bubbles). 0.5 μL of cells at a concentration of 5x10^{5}to 5x10 ^{6} cells / mL were added directly to the bottom of the reservoir using reverse mode pipetting to prevent air bubbles.

Cell capture was observed under the microscope. When cells appeared to be travelling too fast for capture, some liquid was removed from the reservoir to reduce the flow rate.

When sufficient cells were captured, 20 μL of appropriate buffer or media was added to the reservoir to increase the flow rate and flush remaining cells from the reservoir without any further capture.

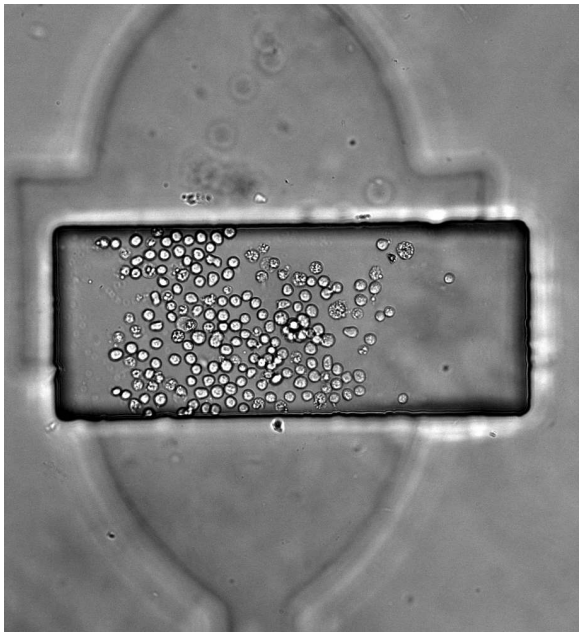

Figure 2.3: Ramos cells trapped in a trench. The optimal cell capture should have single cells that do not overlap, and occupy no more than 70 % of the trench floor.

2.2.3 Sequential lectin labelling of live cells using Lab in a Trench

Lectins can sterically interfere with one another, and so release of lectins by free sugars on captured cells allows localisation of multiple lectins across the surface of a single cell. This method is described in detail in O'Connell et al. (2014).

The experiment was carried out on an Olympus IX81 motorized inverted microscope with an attached Hamamatsu ORCA - ER digital camera C4742-80 using a 10× objective. The heated chamber was humidified and maintained at 37 °C . Images were captured every five minutes.

LiaT chips were primed with TBS with 1 mM $CaCl_2$ (as per section subsection 2.2.1) and 0.4 μL Ramos cells at a density of 10^5 cells/mL loaded (as per section 2.2.2.). After sufficient cells had been captured, 20 μL TBS with 1 mM $CaCl_2$was added to the reservoir.

Biotinylated lectins were mixed with a five molar excess of DyLight488 labelled streptavidin and diluted with TBS with 1 mM $CaCl_2$to a concentration of 0.1 mg/mL. 0.1 μL of this was added to the reservoir and allowed to flow into the channel.

Lectin binding was observed until saturation of binding was observed. Matching free sugar was added to the reservoir at a final concentration of 100 mM and elution of the lectin observed. Trenches were flushed with TBS with 1 mM $CaCl_2$to remove any free sugar that might interfere with lectin binding. These steps were repeated with other sugars to complete the sequential labelling of cell surface glycans.

Table 2.1: Sequence of lectin and free sugar for sequential glycoprofiling of live cells.

	Lectin 1	Free Sugar	Lectin 2	Free Sugar	Lectin 3	Free Sugar	Lectin 4	Free Sugar
Seq. 1	LCA	Manose	ECL	Lactose	-	-	-	-
Seq. 2*	LCA	Mannose	ConA	Mannose	NPL	Mannose	-	-
Seq. 3	LCA	Mannose	ECL	Lactose	ConA	Mannose	WGA	GlcNAc

*TBS wash strictly required between each step.

Analysis of images was carried out using ImageJ. Cells were selected and added to the ROI manager. The average pixel intensity for each cell was recorded in each image and plotted. Overlays of selected cells were also created using ImageJ.

2.3 Flow cytometry

Flow cytometry was mainly carried out on a BD FACS Aria, with some use of a BD FACS Calibur. Analysis was carried out using FlowJo.

Compensation controls were set up for every experiment, namely unstained controls and singly stained controls for every stain used, such that at least 20 % of the cells were highly stained and at least 20 % were unstained. Compensation was calculated using the built in tool in FACS Diva.

Forward scatter signal was collected in area and height to allow screening out of doublets. Fluorescence signal was generally collected in logarithmic format, using biexponential display of the axes. Voltages were set at the beginning of experiments and left unchanged between samples.

2.3.1 Measuring apoptosis with Annexin-V

Apoptosis was measured using the BD Bioscience Annexin-V kits for flow cytometry. Annexin-V PE and 7AAD kits were used when another probe was used with a FITC label. Where the other probe had a violet fluorophore, Annexin-V FITC and PI kits were used.

The kits were used in accordance with the manufacturer's instructions, with the exception that 3 μL of stain was used in place of 5 μL of stain.

2.3.2 Lectin staining

Biotinylated lectins were incubated with fluorophore labelled streptavidin to allow use of the lectins in flow cytometry. These lectins were bound to cells prior to annexin-V staining and running on the flow cytometer.

Biotinylated lectin was incubated with a 5 molar excess of fluorophore labelled streptavidin for five minutes at room temperature. This was then made up to a final concentration of 10 μg/mL of lectin in 10 mM HEPES with 1 mM $CaCl_2$.

Cells were washed twice in PBS before incubation with the labelled lectin for one hour at 4 °C . Cells were then centrifuged and the supernatant discarded. Cells were resuspended in 10 mM HEPES with 1 mM $CaCl_2$ before further staining and running on the cytometer.

Confirmation of the specificity of binding was carried out using fluorophore labelled streptavidin only and labelled lectin with its specific free sugar as controls.

2.3.3 Analysis of Flow Cytometry results using FlowJo

Flow cytometry results were analysed using FlowJo. All data was exported as ungated FCS 3.0 files.

Samples were first gated on FSC-A / FSC-H to exclude debris and doublets. Cells that did not fall close to the diagonal or that had very small FSC were discarded. Fluorescence gating was carried out against FMO's or unstained samples. Where fluorescence signal was reported, median intensity was the preferred descriptor.

2.3.4 Cell sorting

Cell sorting was carried out on a BD FACS Aria equipped with a 100 μm nozzle. A long clean with ethanol was performed prior to sorting. Stream stabilisation and setting of the drop delay was carried out prior to cell staining.

2.3.4.1 Sorting for GafD labelling

Cells were induced to apoptose (see subsection 2.9.6.) in a 50 mL volume for four days to maximise yield. The entire volume was collected for cytometry and sorting along with a sample of untreated cells.

Cells were washed twice with PBS. Some of the cells were sampled for setting up compensation controls. Treated and untreated cells were labelled with GafD and with the Annexin-V FITC / PI kit (see subsection 2.3.1) alongside singly stained and unstained compensation controls.

The bulk cells for sorting were labelled with 10 μg/mL GafD with a Dylight 405 fluorophore and incubated on ice for one hour. Cells were then spun down and resuspended in 10 mL of 10 mM HEPES with 1 mM calcium

and 50 μL of propidium iodide from the BD Annexin-V FITC kit added. These bulk cells were kept on ice during the sort.

Cytometry was carried out on the treated and untreated samples and controls. Polygon gates were drawn on the GafD/PI plots to allow isolation of the GafD+/PI+ and GafD-/PI+ populations. Two-way sorting was carried out using a 16-16-0 mask to optimise purity without drastically reducing yield.

Cells were transferred from the bulk tube on ice to the sampling tube on the cytometer, 1 mL at a time. Cells were sorted into 15 mL tubes containing 1 mL PBS and 10X HALT protease inhibitor without EDTA. When the volume in the tubes reached approximately 10 mL, the tubes were swapped out and stored on ice.

Collected cells were stored at -20 °C until required. Pelleting of the cells was not carried out, as the apoptotic cells largely burst during the sorting procedure.

2.4 Purification of apoptotic cells using AAL-2 bound to magnetic beads

Biotinylated AAL-2 was bound to 10 μm streptavidin coated magnetic beads (New England Biosciences). These beads were used to bind to late apoptotic cells in culture and a magnet used to pull down the beads and attached cells.

Streptavidin coated magnetic beads were mixed with a 10 molar excess of biotinylated AAL-2. The beads were then washed twice in PBS, using a neodymium magnet to pull the beads out of solution for washing. The beads were resuspended in cell culture medium supplemented with 1 % pennicillin / streptomycin and left for 24 hours in order to reduce any microbial load.

Ramos cells were induced to apoptose (see subsection 2.9.6) for 24 hours. The AAL-2 beads were mixed with the cells (allowing 0.5 mg beads per mL) and mixed for ten minutes. The beads were captured at the side of the tube with a neodymium magnet and the cell suspension swirled past the magnet five times. The cell suspension was then transferred to a fresh tube and the level of apoptotic cells remaining determined by flow cytometry (see subsection 2.3.1).

2.5 Microscopy

Cells were labelled with lectins and nuclear stain, then imaged using a Nikon Eclipse Ti-E.

Cells were centrifuged at 210 g for 5 minutes and the supernatant discarded. The cells were washed twice in PBS to remove background glycans from the media. Cells were resuspended in 1 - 10 μg/mL of lectin labelled with Dylight-488 conjugated streptavidin. Cells were incubated in the dark for 1 hour at 4 °C. Samples were centrifuged and the cells resuspended in 10 μL of NucBlue Hoescht stain (Life Technologies). Samples were kept in the dark, on ice, until their turn for imaging. 5 μL of cells was placed on a clean glass slide and a cover-slip placed on top. Cells were imaged using a Nikon Eclipse Ti-E in the centre of the coverslip. Edges of sample where evaporation was occurring were avoided.

Unstained controls were run in each microscopy session.

2.6 Western and lectin blotting

2.6.1 Preparation of Cell Lysates for SDS-PAGE

Cells can be lysed mechanically or chemically using detergent. Mechanical lysis is appropriate where proteins embedded in lipid membranes are to be isolated. Detergent lysis is rapid and suitable when whole cell lysates are to be run on SDS-PAGE gels.

2.6.1.1 Mechanical Lysis (30G needle)

Cells were aspirated through a needle to form a single cell suspension, and then aspirated through a fine gauge needle to mechanically disrupt the cells. This rapid method is suitable for applications where the membrane will be separated, and also where whole cell lysates are required.

Cells were washed twice with PBS and the pellet resuspended at a concentration of 10^8 cells / mL in PBS with protease inhibitors. Where cells were acquired through sorting and a pellet could not be isolated, the complete contents of the sorting tube were lysed and the entire volume brought for ultracentrifugation.

Cells were passed three times through a 20G needle to disrupt any cell clumps and then mechanically lysed by passing them three times through a

30G needle. Lysates were centrifuged at 14,000 g for 20 minutes to pellet unlysed cells and organelles. The lysate was then be used for further purification of membrane proteins or prepared directly for SDS-PAGE in Laemelli buffer (see subsection C.2.3).

2.6.1.2 Mechanical Lysis (Dounce homogeniser)

Cells were aspirated through a needle to form a single cell suspension, and then disrupted in a Dounce homogeniser. This method is suitable for applications where membranes will be isolated, and also where whole cell lysates are required.

1 x 10^7 cells were centrifuged at 210 g for 5 minutes and washed twice in PBS. The cells were then resuspended in 3 mL of buffer containing protease inhibitors and passed through a 20G needle. This was then transferred to a Dounce homogeniser. The cells were lysed with 20 strokes of the homogeniser. The lysate was transferred to a fresh centrifuge tube for further purification or prepared directly for SDS-PAGE in Laemelli buffer (see subsection C.2.3).

2.6.1.3 Detergent Lysis (Laemelli buffer)

Cells can be lysed in Laemelli buffer to allow rapid preparation of samples for SDS-PAGE.

Laemelli buffer was prepared with fresh reducing agent. Laemelli buffer was added to the washed cells, allowing 100 μL for every 1-2 x 10^6 cells. The cells were mixed well with the buffer and incubated on ice for one hour, with occasional vortexing.

Samples are centrifuged at 100 g in a benchtop microfuge for 20 minutes at 4 °C to separate the insoluble fraction. The samples are then heated to 101 °C for 10 minutes. The sample was loaded directly onto an SDS-PAGE gel.

Where required, the protein concentration of the sample was measured directly by the 660 nm method using the ionic detergent compatibility kit.

2.6.2 SDS-PAGE

SDS-PAGE gels were run for Western and lectin blotting and also to prepare samples for mass spectrometry.

2.6.2.1 Precast gels

4-20 % Precise Tris-Glycine gels from Thermo Scientific were used according to the manufacturer's instructions with the standard SDS-PAGE Tris-Glycine buffer (see subsection C.2.4). PageRuler Plus (Thermo Scientific) prestained ladder was used as a molecular weight marker and gels were run until the green (10 kDa) marker neared the end of the gel. Empty wells were loaded with Laemelli buffer to ensure a constant resistance across the gel and to reduce the effect of smiling.

2.6.2.2 In-house poured gels

Gels were cast using the ATTO mini gel rig. APS was made fresh on the day the gel was to be poured. APS and TEMED were added at the last moment before mixing well and pouring each gel.

Table 2.2: Volumes for SDS PAGE gels

Per 1 minigel	10 %	12.5 %	Stacking
dH_2O	3.0 mL	2.4 mL	1.54 mL
Acrylamide/bis acrylamide (Sigma)	2.5 mL	3.1 mL	325 μL
0.5 M Tris (pH 6.8)	-	-	625 μL
1.5 M Tris (pH 8.3)	1.88 mL	1.88 mL	-
10 % SDS	75 μL	75 μL	25 μL
10 % APS	37.5 μL	37.5 μL	12.5 μL
TEMED	3.75 μL	3.75 μL	2.5 μL

Any empty wells were filled with loading buffer to ensure a constant resistance across the gel and to reduce the effect of smiling. PageRuler Plus (Thermo Scientific) prestained ladder was used as a molecular weight marker, and gels were run until the green (10 kDa) marker neared the end of the gel.

2.6.3 Coomassie staining of SDS-PAGE gels

2.6.3.1 Standard Coomassie staining

Standard Coomassie staining is suitable for most gels. It can detect between 0.3-1 μg of protein per band.

The gel is placed in a designated staining box and covered with Coomassie stain (see subsection C.2.5) to a depth of 1 cm. The gel is allowed to

stain at room temperature on a rocker for at least 20 minutes to overnight. Coomassie stain is poured off and collected in a bottle for reuse.

Coomassie destain (see subsection C.2.6) is added to a depth of 2 cm. A piece of paper towel that has been rolled and tied in a knot was placed in the container with the gel and destain to capture Coomassie dye. The container is placed on a rocker at room temperature and allowed to destain overnight and up to two days if background is high.

The destain and paper towel were discarded and the gel placed in water.

The stained gel was imaged, and where required was stored in distilled water at 4 °C in a labelled zip lock bag.

2.6.3.2 Colloidal Coomassie staining

Colloidal Coomassie staining is more sensitive than standard Coomassie staining. It is less sensitive than silver staining, but it is more appropriate for samples that will go for mass spectrometry as it does not reduce the proteins. Colloidal Coomassie staining can be used to detect as little as 8 - 10 ng of protein per band.

The gel was fixed in 40 % v/v ethanol with 10 % v/v acetic acid for a minimum of 60 minutes. The gel was then washed in two changes of dH_2O for ten minutes. The gel was flooded with colloidal Coomassie working solution (C.2.7) for a minimum of two days.

The gel was transferred to a new container and washed with several changes of 1 % v/v acetic acid until there was minimal background staining of the gel.

2.6.4 Silver staining of SDS-PAGE gels

When protein yields are low, silver staining helps visualise the proteins on the gel. It is not ideal for staining proteins that are intended to be used on mass spectrometry. Silver staining is sensitive down to 2 ng of protein.

The gel was fixed for at least 1 hour in 30 % ethanol with 10 % acetic acid. It was then washed for 15 minutes in 20 % ethanol, followed by 15 minutes in water. The gel was sensitised for 1 minute in 0.1 % sodium thiosulphate and rinsed twice with water for 20 seconds. Staining is carried out for 30 minutes in 0.1 % silver nitrate with 0.026 % formaldehyde followed by further rinsing of the gel, twice for 20 seconds in water.

The gel was developed in 3 % sodium carbonate with 0.019 % formaldehyde and 0.000198 % sodium thiosulphate until there was satisfactory visualisation of the bands. Bands with high concentration of protein develop rapidly. Development of the bands was halted with 5 % Tris base with 2.5 % acetic acid for 1 minute. The gel was then transferred to water and imaged.

Over-development of the molecular weight marker was common, and overdevelopment of some lanes of proteins occurred while trying to develop lanes with low protein content.

2.6.5 Transfer of gels to blots

2.6.5.1 Semi-dry transfer

Semi-dry transfer can be used with nitrocellulose or PVDF membranes.

The gel was soaked for 30 minutes in semi-dry transfer buffer (see subsection C.3.1) at 4 °C. Pieces of nitrocellulose membrane were cu to size, and soaked in the semi-dry transfer buffer with four blotting filter papers per membrane for fifteen minutes. When PVDF was used in place of nitrocellulose, it was soaked for 30 seconds in methanol before continuing as for the nitrocellulose.

The blotting sandwich was assembled in the blotter (2 x filter paper, membrane, gel, 2 x filter paper), ensuring there were no air bubbles. The transfer was run at 10 V for 30 minutes to transfer a wide range of proteins. After transfer was complete, the ladder was checked to see if it had transferred fully before disassembling the blot sandwich. If it had not transferred satisfactorily, the blot sandwich was not disassembled and was transferred for a further 10 minutes at 10 V.

The membrane was then placed in fresh PBS or TBS to remove any transfer buffer. The membrane was then stained for protein and blocked.

The gel was also Coomassie stained to confirm protein loading and transfer.

2.6.5.2 Thermo G2 fast blotter

The G2 fast blotter is used for rapid transfer of proteins from SDS-PAGE gels to membranes.

The gels were soaked in the rapid transfer buffer (Thermo Pierce). Nitrocellulose membrane was cut to size, and soaked with four blotting filter

papers per membrane for 5 minutes. Where PVDF was used in place of nitrocellulose, it was soaked for 30 seconds in methanol before continuing as for nitrocellulose.

The blotting sandwich was assembled in the blotter (2 x filter paper, membrane, gel, 2 x filter paper), ensuring there were no air bubbles. The blotter cartridge was assembled and placed in the control unit. The "Mixed Range Proteins" setting was used for transferring a range of glycoproteins for lectin blotting, as a particular size of protein was not expected.

Satisfactory transfer of the prestained ladder was checked before disassembling the blot sandwich. The blot was then transferred to fresh TBS or PBS for protein staining and blocking.

The gel was Coomassie stained after blotting to check protein loading and transfer.

2.6.6 Ponceau total protein staining

Ponceau is a rapid total protein stain that is used for visual confirmation of the quality of transfer.

The transferred blot was washed and covered with Ponceau stain. The Ponceau was washed off with distilled water until the background is reduced. The blot was then imaged, while taking care not to let the blot dry out. The blot was further washed with water to reduce the amount of Ponceau. Any remaining Ponceau was flushed from the blot during the blocking process.

2.6.7 MemCode total protein staining

MemCode is a reversible stain that allows for stable imaging of total protein on the transferred blot. It can be used to check the quality of transfer and also as a total protein loading control. The MemCode reversible protein stain for nitrocellulose membranes was purchased from Thermo Scientific.

The MemCode was applied as per manufacturer's instructions, with the exception that the volumes were reduced such that the liquid just covered the blot rather than filled the tray.

2.6.8 Probing of blots

PVA gives a carbohydrate free blocking solution. Milk and BSA are traditional for antibody probed blots.

2.6.8.1 Lectin blots

Lectin blots use lectins as a primary probe, antibodies as a secondary probe, and PVA as a carbohydrate-free blocking agent.

Blots were blocked with 0.5 % PVA in TBS for at least 2 hours or overnight at room temperature on a rocking platform. The blot was then incubated with lectin in TBST at a concentration recommended in table 2.3 for 2 hours at room temperature, rocking. The blot is then washed twice in TBST for five minutes. Secondary antibody (anti-his / anti-biotin) at a concentration of 1:10,000 in TBST is incubated with the blot for 1-2 hours. The blot is then washed three times in TBST for 10 minutes and imaged according to section 2.6.9..

2.6.8.2 Antibody blots

Antibody blotting uses antibodies for both primary and secondary probes, with BSA and/or non-fat milk used as a blocking agent.

Blots were blocked with 5 % BSA or 2.5 % BSA with 2.5 % non-fat milk powder in PBS for two hours at room temperature or overnight at 4 °C . The blot was then incubated with appropriate antibody in TBST at a concentration recommended in 2.3, rocking, for two hours at room temperature or overnight at 4 °C . The blot is washed twice with TBST for five minutes. The blot is then incubated with appropriate secondary antibody (according to Table 2.3) for 1 hour, rocking at room temperature. The blot is washed three times for 10 minutes in TBST and imaged according to subsection 2.6.9..

Table 2.3: Lectins, primary and secondary antibodies used for Western Blotting.

Probe	Binds to	Optimal conc.	Manufacturer	Product Code	Notes
GSL II	Terminal GlcNAc	1-10 μg/mL	Vector Laboratories		Requires Ca^{++}, biotinylated
ConA	Core Mannose	1-10 ug/mL	Vector Laboratories		Requires Ca^{++}, biotinylated
WGA	GlcNAc	1-5 ug/mL	Vector Laboratories		Requires Ca^{++}, biotinylated
GafD	Terminal O-GlcNAc	1-10 ug/mL	Recombinantly produced in-house	-	Biotinylated, his-tagged
AAL-2	Terminal GlcNAc	1-10 ug/mL	Recombinantly produced in-house	-	Biotinylated, his-tagged
Anti-beta Actin	Beta Actin	1:30,000	Sigma	A5316	Monoclonal produced in mouse ascites
Anti-GAPDH	GAPDH	1:10,000			Produced in rabbit
Anti-biotin HRP	Biotinylated proteins	1:10,000	Sigma		
Anti-mouse IgG (Fab specific) HRP		1:10,000	Sigma	A9917	Produced in goat
Anti-His HRP		1:10,000	Sigma		
Anti-Rabbit AP		1:10,000			
Dylight 488					
V450 streptavidin			BD	560797	0.5 mg/mL

2.6.9 Imaging of Blots

2.6.9.1 Imaging of blots using colourimetric substrate

Where a 2 °antibody with HRP was used, the Sigma TMB for membranes was the substrate used. For alkaline phosphatase labelled antibodies, NCBIP liquid substrate for membranes was used. The blot was drained of buffer, but not allowed to dry. The blot was covered with up to 5 mL of colourimetric substrate and allowed to develop on the bench at room temperature. Once the blot had sufficiently developed, the substrate was washed off with appropriate buffer and blot imaged. With slow development of substrate, the blots were left at 4 °C overnight to develop.

2.6.9.2 Imaging of blots using chemiluminescent substrate

Thermo-Pierce Femto reagent gives good signal even when there is low initial loading of protein. It is used with HRP labelled secondary antibodies.

The Femto reagent was made up as per manufacturer's instructions. The blot was removed from the buffer and placed in a plastic sleeve. The Femto reagent mix was evenly pipetted over the blot and the plastic sleeve closed. This was then placed in the imager (Syngene GelDoc).

White light images were taken to allow alignment of the ladder with the chemiluminescent blot. A series of 30 s exposures of the blot were taken, with the imager set to sum the previous exposures for each image.

Where insufficient signal was achieved, 5 minute exposures were taken for up to 30 minutes.

The blot was returned to buffer solution and stripped and re-probed where required.

2.6.10 Stripping of blots

Antibody blots in particular can be reliably stripped and re-probed to save running valuable samples on multiple blots. It also permits the use of loading control antibody stains on lectin blots where all protein bands are of interest.

The membrane was washed in TBST, and covered with just enough stripping buffer (Thermo) to cover the entire blot. The blot was then shaken by hand for 10 minutes at room temperature. The blot was then transferred to a new container and washed with TBST.

The blots were then re-blocked with appropriate blocking buffer for at least 30 minutes. Chemiluminescent substrate was added and imaged to confirm stripping was sufficient. Where stripping was insufficient, the blot was stripped for a further 10 minutes and blocking and stripping confirmation repeated.

Blotting then continued for the next antigen of interest.

2.6.11 2DE of membrane preps

7cm Immobiline DryStrip IPG strips (GE Healthcare) with a linear pH gradient of 3 -10 were rehydrated with rehydration buffer (see subsection C.2.8) containing 20 μg of the protein sample. The strips were rehydrated overnight in a rehydration chamber at room temperature.

The strips were run on an Ettan IPGphor (GE Healthcare) under the following conditions:

- Step and hold (300 V) 150 minutes
- Gradient (1000 V) 30 minutes
- Gradient (5000 V) 80 minutes
- Step and hold (5000 V) 25 minutes.

Strips were placed in the equilibration buffer (see subsection C.2.9) for 30 minutes at room temperature. The ends of the strip were trimmed to fit the width of the SDS-PAGE rig and the strip placed on the surface of a 15 % SDS-PAGE gel. The strip was then covered with a 4 % stacking gel. A comb with a single tooth was used to prepare a lane in the stacking gel, so molecular weight marker could be run alongside.

The gels were run at 30 mA / gel until the bromophenol blue ran off the end of the gel. The gels were blotted, stained or imaged as appropriate.

2.7 Membrane protein isolation

2.7.1 Isolation of plasma membrane by ultracentrifugation

As cytosolic proteins are often O-GlcNAcylated, it was necessary to fractionate the cell lysates to obtain proteins only from the outer membrane of

the cells. Ultracentrifugation was the method of choice, as the use of membrane extraction kits gave low protein yields or enriched for glycoproteins in a way that might bias further experiments.

Lysates were obtained by mechanical lysis, whether by 30G needle or Dounce homogeniser (2.6.1.). Lysates were spun at 14,000g for 20 minutes at 4 °C to pellet organelles and undisrupted cells. The supernatant was retained and spun at 90,000g for 90 minutes at 4 °C . The supernatant was discarded and the membrane pellet resuspended in PBS with protease inhibitors and 100 mM NaCl to wash cytosolic proteins that may have been non-specifically bound to the membrane. This was then spun at 90,000g for 90 minutes at 4 °C . The supernatant was discarded and the membrane pellet resuspended in 50 - 100 μL PBS with protease inhibitors and 0.5 % Triton-X100. The resuspended pellet was be stored at -20 °C until required.

2.7.2 Membrane isolation by solvent extraction

Solvent extraction allows for enrichment of membrane bound proteins without the use of an ultracentrifuge and without biasing the sample toward particular glycoproteins as with a WGA pull-down column. The method is described in Methods in Protein Chromatography (Walls & Loughran 2011)

Lysates were obtained by mechanical lysis, whether by 30G needle or Dounce homogeniser (2.6.1). Lysates were then spun at 25,000 g for 60 minutes at 4 °C . The supernatant was discarded and the pellet resuspended in TE buffer. The resuspended pellet was mixed with an equal quantity of 1-butanol. The suspension was centrifuged at 500 g for 10 minutes to improve phase separation. The aqueous phase should then contain solubilised membrane proteins.

The interphase and butanol were back extracted by mixing with an equal volume of TE buffer and the separation repeated. The initial aqueous phase was combined with the back extract and concentrated using a Vivaspin 500 ultrafilter with a molecular weight cut off of 10 kDa.

The concentrated protein was then quantified and used for further investigations.

2.7.3 Confirmation of membrane isolation quality by blotting

Western blot was performed on membrane isolates to confirm the removal of cytosolic proteins. GAPDH was used as a marker of cytosolic proteins as beta-actin is a cytoskeletal protein with anchorage to the membrane. Blotting was carried out as per section 2.6).

2.8 Mass spectrometry identification of proteins

2.8.1 In-gel trypsin digestion

Bands are cut from Coomassie stained gel and destained. Proteins are then digested in the gel and collected for MS. The method is based on (Shevchenko et al. 2006)

The gel was rinsed in distilled water for at least 2 hours or overnight. The bands / spots were cut into 1 mm x 1mm cubes by pressing a scalpel or cut pipette tip into the gel. Care was taken to not drag the blade but press it so as not to tear the gel.

Fresh 100 mM ammonium bicarbonate was made up daily. 100 μL of a 1:1 mix of ammonium bicarbonate and acetonitrile was added to the gel pieces. The gel pieces were incubated at room temperature for 30 minutes, vortexing every 10 minutes.

The liquid was removed from the tube and 100 μL of acetonitrile added. The gel pieces shrank and turned white as they were dehydrated. The acetonitrile was discarded. At this point the gel pieces could be frozen.

A 1:10 dilution of the 1:1 mix of ammonium bicarbonate and acetonitrile was made up and 1500 μL used to resuspend a vial of trypsin. [volume] was added to the gel pieces and allowed to rehydrate on ice for two hours. If the pieces had absorbed all the buffer, more was added to ensure excess. After two hours incubation, the gel pieces were transferred to 37 °C overnight for the digestion to take place.

The gel pieces were sonicated on 'high' for 10 minutes. The pieces were then centrifuged at 20,000 g for 10 minutes and the supernatant removed to a fresh tube. The gel pieces were stored at -20 °C in case they were required for further extraction. The supernatant was dried on medium in a speedy-vac for 2 hours. The dried peptides were stored at -20 °C until it

was time for sample clean up.

2.8.2 Sample clean-up for MS

C18 zip tips (Millipore) were used to desalt the peptides for mass spectrometry.

Samples were resuspended (no more than seven at a time) in 20 μL 0.5 % TFA. Samples were then sonicated for 2 minutes to resuspend the peptides and centrifuged briefly. Samples were kept on ice during clean up.

A zip tip was wetted by aspirating and dispensing 10 μL of 0.1 % TFA in 80 % acetonitrile five times. The tip was then equilibrated by aspirating and dispensing 10 μL of 0.1 % TFA five times. The sample was aspirated and dispensed 15 times to bind the peptides to the C18. The sample was washed by aspirating and dispensing 10 μL of 0.1 % TFA into a waste container five times. Elution was carried out by aspirating and dispensing 10 μL of 0.1 % TFA in 60 % acetonitrile into a fresh tube five times. Samples were dried down in a speedy-vac set to medium for two hours. Samples were stored at -20 °C until required.

2.8.3 Mass spectrometry of trypsinised peptides

Peptides were resuspended in 20 μL of 2 % (v/v) Acetonitrile, 0.5 % (v/v) TFA and sonicated for 2 minutes. The samples were then centrifuged briefly and 19 μL transferred to a vial for loading on the mass spectrometer, ensuring there were no bubbles in the vial.

The peptide mixtures were analysed via a Thermo ScientificQ-Exactive mass spectrometer coupled to a Dionex RSLCnano using an EASY-Spray column 75 μm ID x 50 cm Pepmap RSLC C18 2 μm.. The LC gradient ran from 3-40 %B (A: 0.1 % (v/v) formic acid, B: 80 % (v/v) acetonitrile, 0.1 % (v/v) formic acid) over 65 min, and data was collected using a Top15 method for MS/MS scans. The LC gradient in more detail is as follows; 0-10 min 3 % B, 10-40 min increase from 10 % to 40 % B, 40-45 min increase to 90 % B, hold at 90 % B for 4 min before returning to 3 % B for 15 min.

Samples were analysed using Proteome Discoverer (Thermo) with Sequest against the Uniprot human database followed by Percolator to reduce false negatives.

Results were filtered to ensure only proteins with at least two unique peptides of high confidence were included.

2.9 Cell culture

Ramos cells (ATCC no. CRL-1596), a B cell line of Burkitt's lymphoma origin, was used as the model cell for apoptosis induction.

2.9.1 Maintenance of suspension cultures

Ramos were cultured in suspension flasks which are treated with a hydrophobic coating to reduce cell adherence. They were seeded at a density of 2.5-5 x 10^5 cells / mL and subcultured every two to three days to ensure they did not reach densities that are too high.

Ramos were maintained at 37°C in a humidified incubator at 5 % CO_2 in RPMI-1640 medium supplemented with 10 % heat inactivated foetal calf serum and 2 mM L-glutamine. Addition of 1 % penicillin/streptomycin is optional. Medium was warmed at 37 °C prior to subculturing cells.

The cell suspension was drawn up through a pipette a number of times and washed along the lower face of the flask. A sample of the cells were taken for cell viability measurements and counted (Section 2.9.2.). Based on the viable cell count, and desired culture volume, enough cells to reseed the flask were taken and centrifuged, with the remaining cell suspension discarded appropriately.

Where cell viability was good, cells were spun at 210 g for 5 minutes and the supernatant discarded. If cell viability was poor, cells were spun at 90g for 10 minutes to enrich for viable cells and the supernatant carefully discarded.

The cells were then resuspended in the desired volume of warmed fresh media and returned to the original flask or a differently sized fresh flask.

2.9.2 Measurement of cell viability using Trypan Blue

Cell viability was measured routinely using Trypan Blue and occasionally using Annexin-V staining and flow cytometry (section 2.3.1.).

An aliquot of cell suspension was removed from the culture flask and transferred to a centrifuge tube. 100 μL of this was added to a fresh tube

with 10 μL of Trypan Blue solution (Sigma) and mixed well. 10 μL of stained cells were loaded onto a haemocytometer. The cells in a 1mm x 1mm square were counted, with counts of multiple 1x1mm squares averaged. Cells lying on or touching the top and left borders were included and cells lying on or touching the bottom and right borders are excluded from the count.

Viable cells appeared clear, while non-viable cells took up the blue stain. Percentage viability is calculated from the number of viable cells as a proportion of total cells counted.

Cell count per mL was calculated by multiplying the average number of cells in a 1mm x 1mm square by 1.1 (dilution factor) and 1 x 10^4 (accounting for the volume of the square). For most purposes, only viable cells were counted.

2.9.3 Measurement of cell viability using MTS assays

Cell metabolism was measured using the Promega one-step MTS assay. This assay can be roughly correlated to cell numbers. A triplicate standard curve was run with every assay. Optimum cell concentration was identified by selecting a midpoint from the linear portion of the sigmoid standard curve. The standard curve was set up such that the highest point on the curve was higher than the concentration used for the toxicity assays.

A concentration of [cells/mL] was used for assays in which reduced viability was expected. The reagent was used according to the manufacturer's instructions and readings were referenced to the standard curve that was run with each experiment.

2.9.4 Cryogenic storage of cultures

Cells are frozen at peak growth. For suspension cultures this is the point where the cells have just doubled.

Cells were seeded in 50 mL at 5 x 10^5 cells / mL. The cells were then counted after seeding to confirm their starting density. After 26 hours, the cells were counted again. When the cell count had doubled that of the previous day, the cells were collected and centrifuged at 210 g for 5 minutes. The supernatant was discarded and the cells resuspended in freezing stock solution (C.4.2) at a concentration of 1 x 10^7cells / mL. This was then added to cryovials in 1mL aliquots.

The vials were transferred to a Mr. Frosty and stored at -80 °C overnight. Vials were then transferred to liquid nitrogen for long term storage. After a number of days, cells were recovered and grown for one week to determine the viability of the stored cells.

2.9.5 Recovery of cell stocks from cryogenic storage

Media was warmed to 37 °C before the cells were retrieved from storage. The cryovial was then defrosted at 37 °C and the entire contents of the vial added to 9 mL of warmed media. Cells were spun at 210 g for 5 minutes and resuspended in 7 mL of warm media and transferred to a T25 suspension flask.

An aliquot was taken for counting and viability measurement. After two days, the cells were counted and reseeded in fresh media.

2.9.6 Induction of apoptosis in B-lymphocytes

Activation of the B-cell receptor (BCR) in the absence of a co-stimulus induces apoptosis in B-lymphocytes. Anti-IgM binds the BCR *in vitro* and initiates apoptosis.

Cells were counted and sufficient cells to seed the experimental volumes at a concentration of 5 x 10^{5} cells / mL were measured out. The cells are spun down at 210g for 5 minutes and the supernatant discarded. Cells are re-suspended in media that has been mixed with anti-human IgM (Biosciences) at a final concentration of 1μg / mL. Cells were returned to the incubator under normal conditions, and were be collected as usual for experiments.

Anti-human IgM was not be added directly to the cells in suspension as it caused rapid clumping and necrosis in some of the population.

2.10 Preparation of Lectins for experiments

2.10.1 Biotinylation of lectins

Lectins were biotinylated with the NHS-sulfo linker kit from Thermo Fisher.

Lectin concentration was carried out by BCA assay or 660nm assay. Biotinylation was carried out as per manufacturer's instructions.

Molecular mass of GafD : 21 kDa

Molecular mass of AAL2 : 45 kDa

2.10.2 ELLA to confirm lectin activity

Enzyme-linked lectin assay was used to confirm the specificity and activity of the lectins, whether after long storage or after biotinylation.

200 μL of relevant control glycoprotein or sample at a concentration of 10 μg / mL was added to the wells of 96 well microtitre plate and allowed to adsorb for at least two hours at room temperature. The plate was washed with TBST and 250 μL of 0.5 % polyvinylalchohol in TBS was added to the wells for blocking. The wells were blocked for a minimum of one hour at room temperature. The plate was washed with TBST and 200 μL of lectin at a concentration between 1-10 μg / mL in TBST added and incubated for 2 hours. The plate was washed twice with TBST and 200 μL of secondary antibody at is added and incubated for 1 hour.

The plate was washed three times with TBST and developed with the relevant substrate. The plate was then measured on a Tecan Saffire II to determine the binding of the lectins.

2.10.3 Protein measurement assays

2.10.3.1 BCA Assay

The Thermo-Pierce BCA kit is used for all BCA assays. The assay is sensitive from 20 μg / mL to 2000 μg / mL. The BCA assay is compatible with Triton-X100 up to 1 % and is not compatible with reducing agents or urea. Standard curves were prepared in the same background as the samples.

The kit was used according to the manufacturer's instructions for the microtitre plate version of the assay

2.10.3.2 Pierce 660 nm protein assay

The Pierce 660 nm protein is a rapid assay that is compatible with Triton-X100, and compatible with SDS when using the ionic compatibility reagent. A standard curve from 1 mg/mL to 18 μg/mL was prepared in the same buffer as the sample. Buffer is used for the blank.

Assays were carried out according to the manufacturer's instructions for the microtitre plate version of the assay.

2.10.3.3 Bradford assay

The Bradford assay is used when there are reducing agents in the sample buffer. The standard curve should be prepared in the same buffers as the sample. A standard curve from 1 mg/mL to 18 μg/mL is prepared in the same buffer as the sample. Sample buffer is used for to blank. Where samples are made up in IEF buffer, prepare the standards in IEF buffer. Then dilute both the samples and standards 1:9 in PBS to reduce the interference of urea.

Bradford reagent was diluted 1:4 with dH_2O. This working reagent is stable at 4 °C for up to two weeks and was be brought to room temperature before use.

980 μL of Bradford working reagent is added to a cuvette. 20 μL of sample or standard is added to this and the cuvette mixed well.

The cuvettes were incubated at room temperature for 5 minutes and read at 595 nm on a UV-vis spectrophotometer

Chapter 3

Lab in a Trench: design and manufacturing considerations

3.1 Lab in a Trench

Lab-in-a-Trench (LiaT) is a microfluidic platform developed by Dimov et al. (Dimov, 2010; Dimov et al., 2011; Kijanka et al., 2011) in which cells are contained and analysed in a shear-free environment. The platform relies on gravity-driven flow and gravity-based capture of particles that are too heavy or slow moving to pass over a trench. The sudden widening of the channel near the trench allows for a reduction in flow rate and therefore the speed of the cells travelling in the system. It is known that hydrodynamic forces can alter cell morphology and physiology (Elliott, 2009), and so LiaT removes this possibility from interfering.

The Lab in a Trench system relies on capturing cells as they fall into a trench by gravity. When the cells are trapped, we can exchange the buffers and media by diffusion. As the cells remain *in situ*, it is possible to track cells after the addition (or elution) of probes.

LiaT has been used to observed the effect of LPS on the appearance of CD86 on the surface of murine macrophages by adding labelled anti-CD86 antibody and watching its binding (Dimov et al., 2010; Kijanka et al., 2014). Kijanka et al. (2014) further used it to observe macrophages phagocytosing *Escherichia coli* that express green fluorescent protein, using time lapse microscopy and tracking the increasing fluorescence of the macrophages as they accumulated the green bacteria.

As reagent delivery is diffusion based, the Stokes radius of the probes and sugars determines their diffusion rate. The diffusion of the lectins is correspondingly longer than the diffusion of the free sugars.

Although the depth of the trench allows it to hold an volume of free fluorophore that is much larger than the cells, the bulk signal is much less than that of the concentrated fluorophore near the cells surface.

Table 3.1: Requirements for Lab in a Trench

Biological requirements	
Ability to track cells	Cells trapped in the trench remain in place.
Ability to exchange reagents	For sequential labelling in particular, it must be possible to completely replace fluids within the system.
Compatible with cells	PDMS is not an ideal material for this, so the time live cells can usefully be monitored in the system is on the order of hours.
Optically clear with no fluorescent signal	The device is intended for use with microscopy imaging.
Can be used at 37 °C	This is a physiological requirement for working with live cells.
No glycans on the device surfaces	This could cause background signal with lectins. PDMS is a glycan free polymer.
Engineering requirements	
Ease of prototyping and manufacture	PDMS cast from SU-8 masters meets both of these requirements.
Strong bonding of surfaces	The small channels necessitate high pressures for initial loading.
Compatible with aqueous buffers	Plasma treatment of the surfaces makes the PDMS hydrophilic, permitting flow of aqueous solutions in the channels.
Micro-scale features	Permits rapid diffusion of reagents within the system. Reduces reagent cost.
Adjustable flow rates	Flow rates can be adjusted to improve or prevent capture by varying the height of fluid in the reservoir.

3.1.1 Lab in a Trench - Microfluidic Theory

The LiaT platform contains a deep, micron-scale indentation within a continuous channel that enables the capture and retention of cells purely based on gravity (Dimov et al., 2011; Kijanka et al., 2011) (Figure 3.1). LiaT follows a well-known working principle that is based on the Camp-Hazen model of a settling basin (Saady, 2011). In this model, the velocity of cells over the trench is the most critical parameter for ensuring their gravity-driven capture.

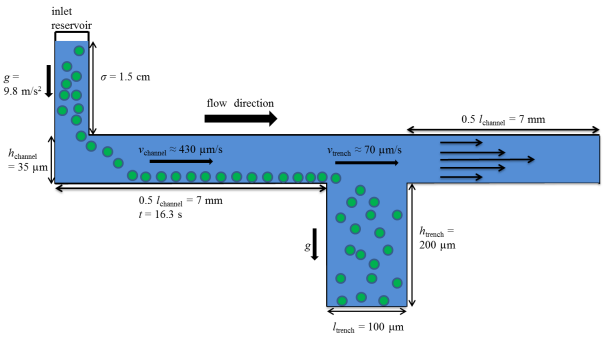

(a)

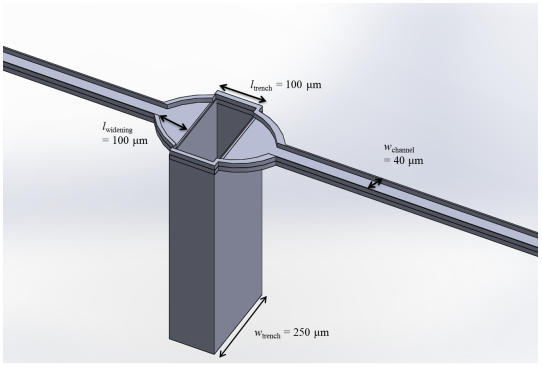

(b)

Figure 3.1: Overview of the Lab in a Trench microfluidic platform. (a)Cells of the Lab in a Trench platform. Fluid exchange is performed by diffusion permitting a shear free environment at the bottom of the trench structure. (b) 3D schematic of the Lab in a Trench Platform.

Cells are suspended in a flow of PBS buffer of density $\rho = 1.0 \times 10^3\,\mathrm{kg\,m^{-3}}$ and viscosity $\eta = 1.09 \times 10^{-3}\,\mathrm{Pa\,s}$ under the influence of gravitational acceleration $g = 9.81\,\mathrm{m\,s^{-2}}$. A pressure head $\Delta p = 1.5\,\mathrm{hPa}$ built up by a pipette

filled to a liquid level $\sigma = 1.5\,\mathrm{mm}$ applies across the main channel which has total length $l_{channel} = 14\,\mathrm{mm}$, constant height $h_{channel} = 35\,\mu\mathrm{m}$ and width $w_{channel} = 40\,\mu\mathrm{m}$ which broadens to $w_{trench} = 250\,\mu\mathrm{m}$ above the trench of stream-wise length $l_{trench} = 100\,\mu\mathrm{m}$ (Figure 3.1 (b) & (c)). Neglecting the trench section, the (average) flow of velocity then amounts to

$$v_{channel} = \frac{h_{channel} w_{channel} \Delta p}{C_{nc} \eta l_{channel}} \approx 430\,\mu\mathrm{m\,s^{-1}}$$

with the numerical coefficient for the rectangular channel $C_{nc} \approx 32.14$. The (average) flow velocity even reduces to

$$v_{trench} = \frac{w_{channel}}{w_{trench}} \cdot v_{channel} \approx 70\,\mu\mathrm{m\,s^{-1}}$$

within the sector above the trench. The resulting Reynolds numbers

$$Re = \frac{\rho v w}{\eta} \ll 1$$

indicates that flow conditions are strictly laminar within the channel as well as in the trench for typical flow speeds v and widths w. Hence, streamlines will only penetrate into the uppermost region of the trench and molecular (reagent) transport across streamlines into the trench occurs solely through diffusion (Dimov et al., 2011) (Figure 3.1).

With the speed of sedimentation

$$v_{sed} = \frac{g d^2}{18\eta}(\rho_{cell} - \rho)$$

for cells of density ρ_{cell} and diameter d we can determine the ratio

$$\frac{t_{sed}}{t_{in}} = \frac{18\eta h_{channel}}{g d^2 (\rho_{cell} - \rho)} \cdot \frac{v_{channel}}{l_{channel}/2}$$

between the sedimentation time

$$t_{sed}(h) = h_{channel}/v_{sed}$$

across the entire channel height $h_{channel}$ and the (minimum) residence time of the cells in the incoming segment $t_{in} = 0.5 l_{channel}/v_{channel}$ located at about $0.5 l_{channel}$ after the inlet. For Ramos cells with a density of $\rho_{cell} =$

$1.02 \times 10^3\,\mathrm{kg\,m^{-3}}$ and a typical diameter $d = 10\,\mu\mathrm{m}$ suspended in PBS buffer, this ratio is much smaller than unity so that the entire population of Ramos cells will have settled to the bottom of the channel way before reaching the downstream trench (Figure 3.1).

Due to the parabolic flow profile, their speed of cell migration will hence be significantly reduced with respect to the above calculated (average) flow velocity v_{trench}. The cell velocity in the trench region

$$v_{cell} \approx 2v_{trench}\left(\frac{h_{cell}}{h_{channel}/2}\right)^2 = 8v_{channel}\frac{w_{channel}}{w_{trench}}\left(\frac{h_{cell}}{h_{channel}}\right)^2$$

depends on the distance of the cell from the bottom of the channel h_{cell}. If, for instance, a cell was touching the bottom of the channel (Figure 3.1 (b)), i.e. $h_{cell} = d/2$, their speed of horizontal migration would amount to $v_{cell} 10\,\mu\mathrm{m\,s^{-1}}$, only.

For efficient trapping, the ratio

$$\frac{t_{sed}}{t_{res}} = \frac{18\eta h}{gd^2(\rho_{cell}-\rho)}\cdot\frac{v_{cell}}{l_{trench}} \approx \frac{18\eta h}{gd^2(\rho_{cell}-\rho)}\cdot\frac{2v_{channel}w_{channel}}{w_{trench}l_{trench}}\left(\frac{d}{h_{trench}}\right)^2 < 1$$

of the cell sedimentation time (to a depth d into the trench) and the cell residence time in the trench region needs to be lower than unity. This implies an upper limit

$$v^*_{channel} = \frac{g(\rho_{cell}-\rho)w_{trench}l_{trench}h^2_{trench}}{36\eta h w_{channel}}$$

for the flow speed in the (main) channel. Assuming that the cell will be irreversibly trapped after penetrating a distance corresponding to the channel height into the trench, i.e. $h = h_{channel}$, we obtain a speed limit of $v^*_{channel} = 545\,\mu\mathrm{m\,s^{-1}} > v_{channel} = 430\,\mu\mathrm{m\,s^{-1}}$ as calculated above.

3.1.2 Forces on particles in the system

All cells in the LiaT system experience gravity, and also experience buoyancy. Cells travelling in the channel experience wall lift, which drives the cell away from the wall towards the centre of fluid flow (**?**). This tendency towards the centre of fluid flow is countered by a shear effect from the parabolic flow profile of the fluid in the channel. As the channel widens at the trench, fluid flow rate drops and the walls of the device are further

from the cell. At the point where the fluid flow rate drops, the cell travels forward with the inertia that is countered by the Stoke's drag, causing the cell to decelerate with the liquid. In the trench itself, wall lift and shear are no longer significant forces acting on the cell. Gravity pulls the cell towards the bottom of the trench, with buoyancy and Stokes drag slowing the cells descent.

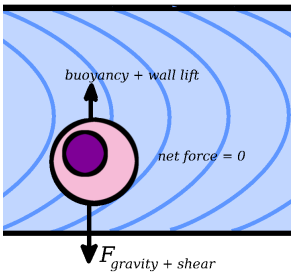

(a)

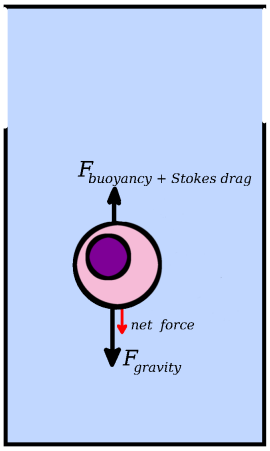

(b)

Figure 3.2: Cells in Lab in a Trench experience a variety of forces. (a) When the cell is in the channel, the cell experiences wall lift, which drives the cell away from the wall, and shear force away from the centre of fluid flow (**?**). In addition, the cell experiences the forces of gravity and buoyancy. These forces balance to produce zero net lift at an equilibrium location. This location is is a function of channel geometry, carrier fluid properties, flow velocity, cell density and morphology. As the cell does not move laterally in the flow it is not subject to Stokes drag. (b) When the cell reaches the channel expansion (trench), the fluid flow is much reduced and so the shear force becomes negligible. The distance from the bottom of the trench ensures the wall lift is similarly negligible. The combined forces of buoyancy and the weight of the cell results in a nett downward motion of the cell across streamlines as it sinks. This downward motion is retarded by an additional drag force, caused by the cell motion through the carrier fluid, called the Stokes drag.

3.2 Rationale for the use of Lab in a Trench

Lab in a Trench offers some advantages over many of the microfluidic methods described in section 1.7 and section 1.8. In particular it permits the exchange of fluids over the cells, the possiblity to track individual cells through the experiment, and ease of manufacture.

The small volumes in LiaT allow reduction in reagent costs, and in particular, allow rapid diffusion of reagents in the system. The diffusion times of the reagents in the system relates to their molecular mass, with larger molecules taking longer to diffuse than smaller molecules. A system that was larger in scale would necessitate longer analysis times.

As the system fits on a microscope slide, it can be easily used with existing equipment. The small volumes leads to increased pressure in the system, in particular with respect to the initial loading of the chip, but optimised assembly of the chips reduces the stress that this can put on the chip (subsection 3.3.1).

As LiaT is an open system, fluids can be easily removed and exchanged from the system without introducing air bubbles or introducing valving. By the use of a narrow pipette, the reservoir can be emptied and refilled as required. The disadvantage of this open system is that it renders the device non-sterile, and the use of antibiotics is required to reduce bacterial contamination of experiments.

Operating LiaT at 37 °C lowers the viscosity in the system and thus raises the Reynolds number of the system slightly. However, operation at 37 °is required for work with live cells.

The LiaT system is ideal for working with cultured suspension cell lines or with blood cells, as the cells can be added to the system in their physiologically relevant state and measured. Adherent cell lines can be loaded into the system after resuspension, however, they are not left in the system for long enough that they can adhere to the base of the trench. PDMS is not an ideal material for manufacturing devices used for medium to long term culturing of cells, as unpolymerised molecules can diffuse in to the system and distress the cells (as discussed in section 1.7).

PDMS is an ideal material for rapid prototyping, but it is not a preferred material for cell culture work. The high aspect ratios of the trench to channel makes hot-embossing of the channels challenging without specialised moulds.

Milling of the device removes the optical clarity of the trench and makes it unsuitable for microscopy. Further, manufacture in a elastic material such as PDMS makes the addition of reservoirs at the inlets as easy as sticking a pipette into the device. Inelastic materials would require sealing of the reservoirs to the device, with the risk that the sealant might block the channels. As PDMS does not contain any glycans, it is a suitable material for glycoanalysis applications.

3.3 Preparation of chips

Chips were manufactured in PDMS cast from SU-8 masters as described in subsection 2.1.3. Multiple revisions of the chip manufacturing process were required to address issues during sample loading. The assembly of the PDMS was optimised to reduce bursting of the chips during loading (see subsection 2.1.3). Hydrophilisation of PDMS surfaces is also required to permit fluid flow and reduce the occurrence of bubbles within the system.

Despite the improved manufacturing process, there is some variability in the chip assembly process, which can lead to differing distances from the inlet to the trench itself. This reduces the predicted control over the system somewhat, but can be countered by experience using LiaT with a range of distances from the inlet. The velocity of the cells appears to vary with the distance of the inlet to the trench, and this may be due to the cells not having time to reach an equilibrium state in the fluid flow.

3.3.1 The move to partial curing

In initial experiments, the PDMS had been fully cured and plasma treated before bonding the lid and channel segments together (as described in subsection 2.1.4). The bond between the surfaces was of variable quality and the upper and lower parts of the chips regularly separated on loading.

Partial curing of the PDMS before assembly eliminated bursting of chips. The PDMS was more difficult to manipulate, and more prone to collecting debris during assembly, but these issues were offset by the improved loading. Partial curing gives a high bond strength between the layers without resorting to adhesive (Eddings et al., 2008). Punching inlet holes in the partially cured PDMS also gave cleaner inlet walls and made them less inclined to

leak around the reservoirs. The fully cured PDMS tended to crumble on punching, and could leave fractures around the inlet that leaked on loading.

In addition, the chips were assembled in groups of 3 to 6 trenches, rather than attempting to align the entire disc as was initially performed. This improves alignment, and is also much easier to manipulate, especially when working with the partially cured polymer.

3.3.2 Hydrophilisation of channel surfaces

The hydrophobic nature of the PDMS surface made loading with aqueous solutions challenging. When loading the plasma bonded chips, loading was easiest when the chips had been bonded on the same day as the assay was to be performed. However, small air bubbles often accumulated and expanded as the surface wetting was not always complete.

The chips assembled from partially cured PDMS were particularly difficult to fill if they were not treated for hydrophilisation. The use of proteinaceous buffers, such as 5 % BSA in TBS, improved loading but was not always desirable as it can interfere with upstream applications that require low protein background.

Plasma treatment of the channels in the completed chip was impossible using a corona plasma probe (Electro-Technic Products, Chicago), as it could not reach internal surfaces. The probe tip could be inserted into the inlet hole and plasma treat the channels in a localised fashion, however the plasma treatment did not extend for enough of the channel to provide adequate hydrophillicity, and in addition, prolonged plasma treatment caused damage to the surfaces of the chip.

It was decided to trial plasma treatment in a plasma cleaning chamber (Harrick Plasma, Ithaca) under reduced air pressure. The resulting hydrophilisation is successful but short lived, requiring that the chips are loaded immediately after removal from the plasma chamber (see subsection 2.2.1).

3.3.3 Lab in a Trench in use

The manufacturability of the platform was improved by assembling the chips using partially cured PDMS instead of fully cured. Furthermore, loading was improved through the use of plasma hydrophilisation of the channel

surfaces. Loss of liquid from the reservoir and through evaporation through the PDMS was reduced by humidifying the microscope chamber.

Loading the chips with cell media containing 10 % serum also improved loading. In addition, it was noted that the cells were less inclined to stick to the channel surfaces, possibly due to blocking of the surface by the proteins. For glycosylation studies however, it is preferred to minimise the amount of protein loaded into the system as it may contain glycoproteins that could give a background signal during imaging.

Managing the flow rate is challenging using the current system. As flow rate is regulated by the height in the channel, it is necessary to adjust the rate by adding or removing microlitre volumes of liquid. This can be tricky when working with the small volumes that are required for the slow flow rates during cell capture. The liquid meniscus is often below the height of the PDMS, making it hard to see. Moreover, as the reservoir tips are not always at the exact depth in the PDMS, finding the right liquid height can often be a case of trial and error.

Sterility of the platform was not considered during testing, as the platform is used as an open system, with the potential for bacteria and yeasts to fall from the air and the operator into the reservoir. It is possible to autoclave PDMS chips, but it is uncertain if it would be necessary, as the present system requires plasma treatment of the device surfaces. Precautions to reduce contamination that were taken include, wearing gloves and clean labcoats, and using antibiotics in the media to ensure bacteriostatic conditions.

Optimisation of the system manufacture and loading conditions has improved the robustness of the device for use in the laboratories, although some further refinements are still required.

Chapter 4

Sequential glycoprofiling of single cells using Lab in a Trench

The Lab in a Trench (LiaT) platform was used to investigate cell surface glycosylation on Ramos B-lymphocytes. It was demonstrated that it is possible to label cells with lectins and to elute the lectin with free sugar, allowing, for the first time, sequential glycoprofiling of the cell surface (O'Connell et al., 2014). The method for sequentially glycoprofiling live cells was further expanded for other uses including investigation of fixation on lectin binding.

4.1 Sequential glycoprofiling of live cells

The LiaT platform was employed to examine the surface glycosylation of Ramos B lymphoma cells. Ramos cell surface glycans were sequentially probed using a panel of two and subsequently four fluorescently-labelled lectins, as described in subsection 2.2.3. The interference of free sugar from previous lectins was assessed with three mannose-binding lectins, LCA, ConA and NPL. An additional wash step was incorporated between sugar elution and addition of the next lectin in the probing sequence.

The sugar elution steps were rapid (in the order of minutes), thus minimising any potential physiological impact on the cells in the trenches.

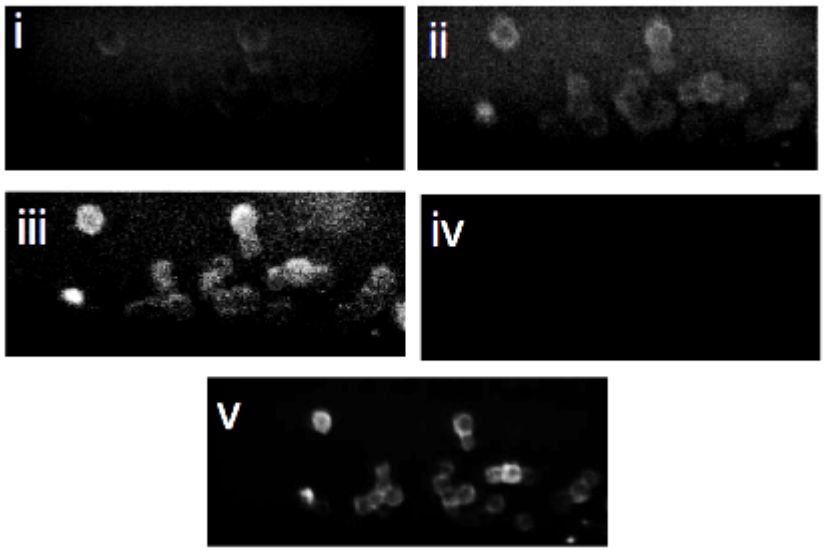

Figure 4.1: Series of images of sequential elution of fluorophore labelled LCA off Ramos cells. Images i, ii, iii show diffusion of LCA into the channel and staining of the cells after 0, 5, 10 minutes. Image iv shows the cells after free mannose had been diffused into the system. Image v was taken after ECL had been added to the system.

4.1.1 Glycoprofiling with LCA and ECL

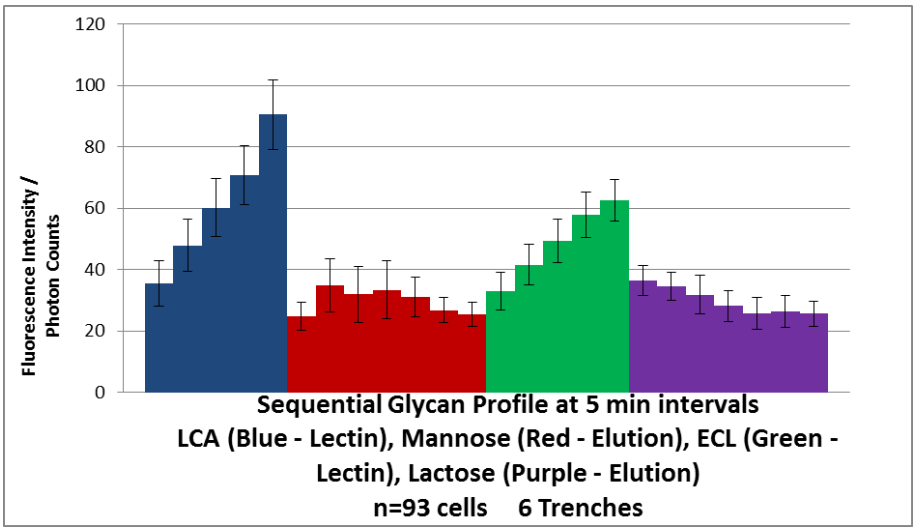

(a)

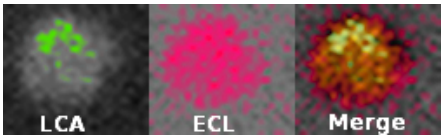

(b)

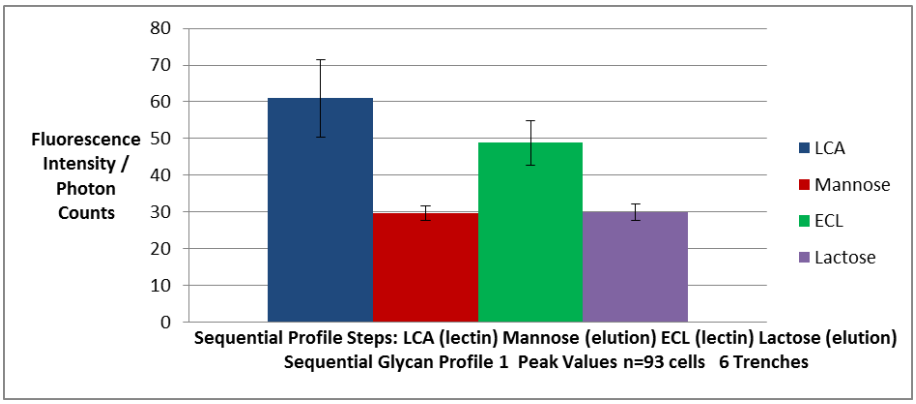

(c)

Figure 4.2: Sequential labelling of Ramos cells with LCA and ECL. (a) Average intensity of individual cell staining as calculated by ImageJ. Images collected at five minute intervals after addition of LCA (Blue), mannose (red), ECL (green) and lactose (purple). (b) An example of a cell stained sequentially with LCA and ECL, and resulting overlay. (c) Average peak intensity values of individual cell staining. Standard deviation is noted by the bars on each graph.

In the first experiment, the two lectins LCA and ECL were used. Stronger signals were detected with LCA indicating a denser mannose distribution at the cell surface when compared with ECL, which has an affinity for galactose residues (Figure 4.2). This is in agreement with general cell surface glycan structures because galactose is known to be either protected or partially exposed on live healthy cells which results in poor ECL binding and hence lower equilibrium concentrations and reduced signals (Tateno et al., 2007).

4.1.2 Glycoprofiling with three mannose binding lectins

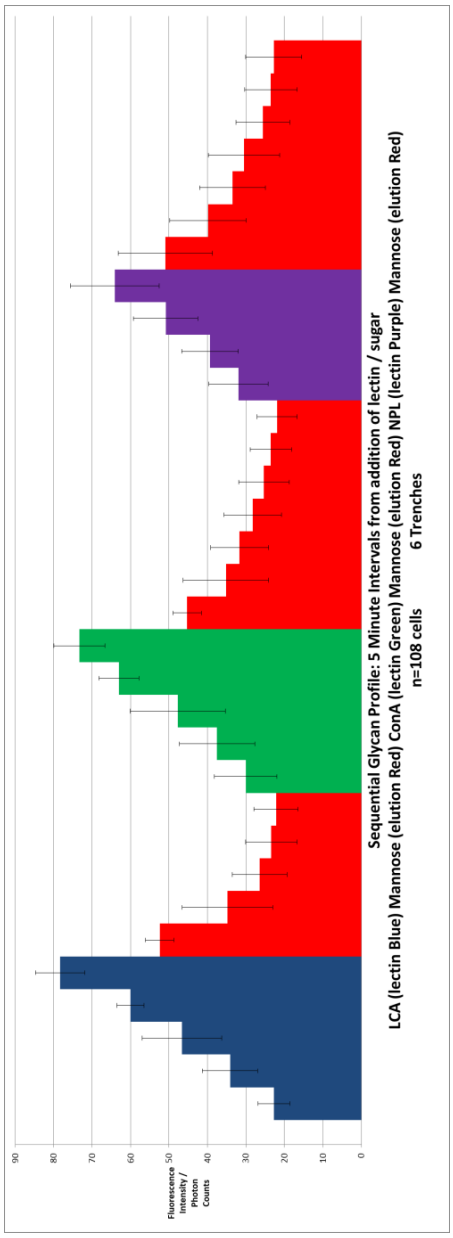

(a)

Figure 4.3: Sequential elution of three mannose binders.(a) Average intensity of individual cell staining as calculated by ImageJ. Images collected at five minute intervals after addition of LCA (Blue), mannose (red), ConA (green) and NPL (purple). (b) An example of a cell stained sequentially with LCA, ConA and NPL, and resulting overlay. (c) Average peak intensity values of individual cell staining. Standard deviation is noted by the bars on each graph.

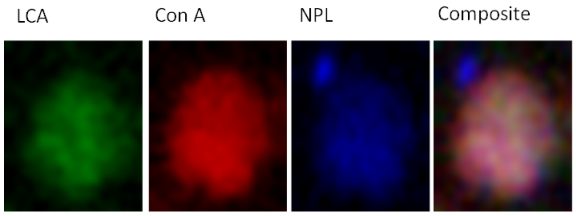

(b)

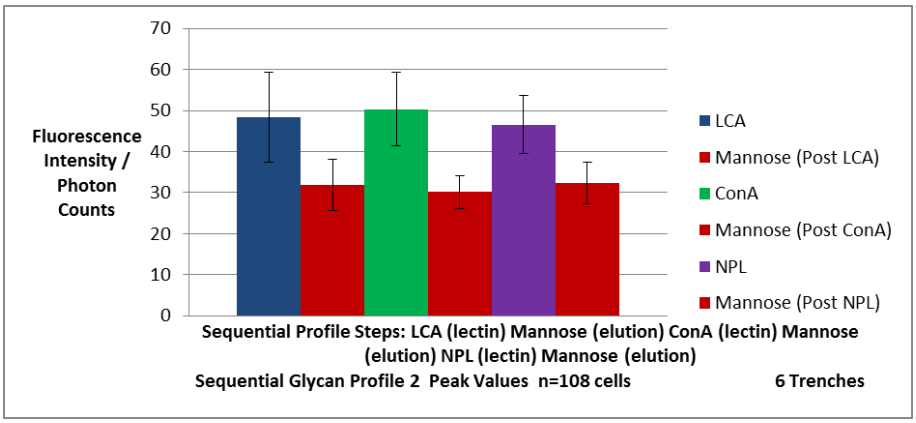

(c)

Figure 4.3 :Sequential elution of three mannose binders (cont'd).

In a second experiment, three mannose-binding lectins were sequentially used. The binding of the second and third lectins was not affected by the presence of mannose during earlier steps in the probing sequence indicating the effectiveness of the preceding wash step (Figure 4.3). The peak fluorescence of LCA and ConA was comparable to those achieved in a four-lectin experiment (Figure 4.5). In that experiment wherein the repertoire of probes was extended to four lectins, to include ConA and WGA, a higher signal was obtained with the latter and an intermediate signal with the former (Figure 4.5). When mannose binders (LCA and ConA) were compared, fluorescent signal of bound LCA was found to be lower than that of bound ConA. This is likely to reflect the known difference in affinity between LCA and ConA, where the former only recognises α-linked fucosylated mannose.

We have confirmed that the free sugars can be washed from the system such that they do not interfere with the following lectin. This has been demonstrated by targeting a common carbohydrate (mannose in this case) with three different lectins (LCA, ConA and NPL) that probe mannose

and exhibit similar specificities. We found binding of all lectins to similar positions on the cell surface but with varying intensities (Figure 4.4b).

4.1.3 Glycoprofiling with four lectins

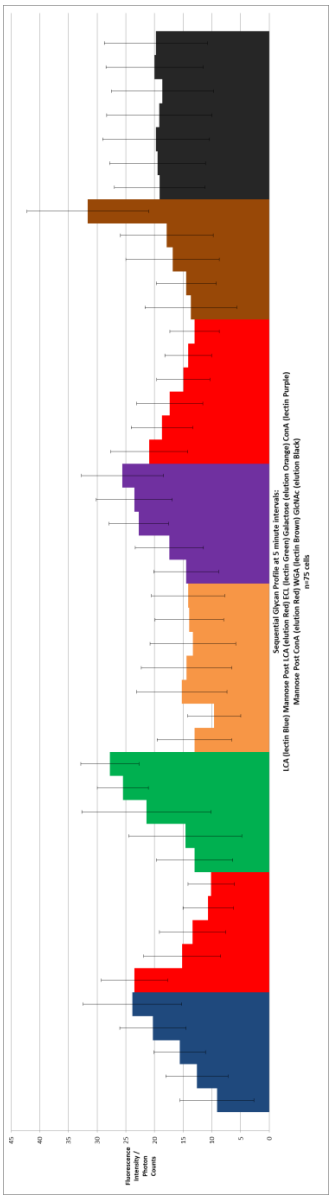

(a)

Figure 4.5: Sequential glycoprofiling with LCA, ECL, ConA and WGA.(a) Sequential Profile Steps (5 Minute Intervals): LCA (lectin-Blue), mannose (elution-Red), ECL (lectin-Green), galactose (elution-Orange), ConA (lectin-Purple), mannose (elution-Red), WGA (lectin-Brown), GlcNAc (elution-Black). (b) An example of a cell sequentially stained with LCA, ECL, ConA and WGA and resulting images overlaid. (c) Average peak intensity values of individual cell staining. Standard deviation is noted by the bars on each graph.

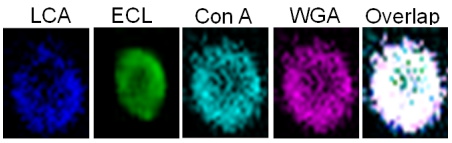

(b)

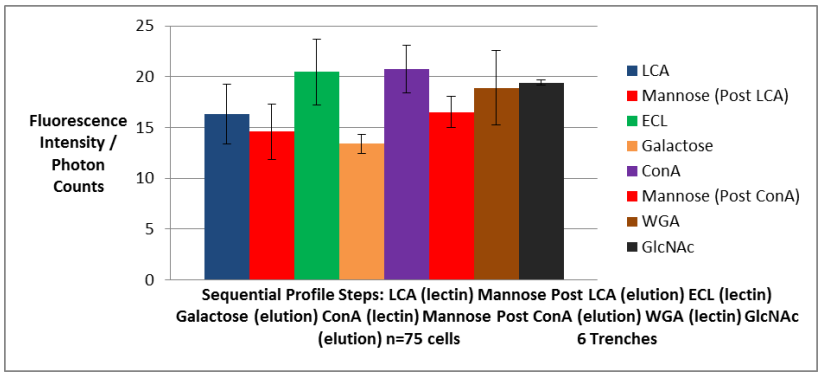

(c)

Figure 4.5 : Sequential glycoprofiling with LCA, ECL, ConA and WGA (cont'd.).

This experiment confirmed high GlcNAc and core mannose levels on the cell surface. GlcNAc was found to have the highest density among all the extracellular glycans that were probed.

As the lectins were added in an order such that sugar elution would not interfere with the following lectin, it was possible to image individual cells without the requirement for wash steps. It was therefore possible to create glycan density profiles of the cell surface through image overlays with ImageJ. In addition, the order of lectins was selected so as to minimise impact on the cells, based on the changes observed when using each lectin in flow cytometry (Figure D.1). It can be noted that in the three lectin (mannose binders) sequence and four lectin sequence, LCA was followed directly or indirectly by ConA (Figure 4.3,4.5). Similar observations were made in both experiments, indicating that the fucose elution of ECL in the four lectin experiment had not interfered with the cells' binding of ConA.

4.1.4 A summary of sequential glycoprofiling

The results generated were analysed with a view to understanding glycan heterogeneity at the single cell level. An observable difference was obtained

at the inter-cellular level in the glycan-probing behaviour of lectins on individual cells. This further confirms the wide range of glycoforms that can be displayed on apparently heterogeneous cell populations.

The sequential lectin-elution method has enabled us to detect multiple sugars on a given live cell, and that is a considerable technical advancement over current state-of-the-art methods. At present, cell surface labelling is limited to a single lectin probe, as multiple probes can interfere with each others binding through steric hindrance as they attempt to interact with adjacent sugars.

It has been shown here that the LiaT platform also permits the differential characterisation of diverse glycosylation features at the single cell as well as at a population level. By overlaying the images of different lectin probes on can observe glycan distribution profiles over the cell surface. This allows a map of glycan localisation to be generated, and for the first time, allow relative distributions of glycans to be observed on the same cell.

Due to the high avidity of many lectins, the sugar concentrations used to elute the lectins are relatively high. This is necessary in order to overcome the multiple binding partners of the lectins on the cell surface, and also to ensure it is at a high enough concentration in the vicinity of the lectin binding site to have the opportunity to compete with the cell glycan. The use of disaccharide haptens in place of the free sugars might enable a reduction in this concentration. The change in local osmolarity caused by high sugar concentrations may have an adverse effect on the cells, despite only being under this osmotic pressure for short times.

Priming of the trenches must be carried out immediately after plasma treatment as the hydrophillicity of plasma-treated PDMS is short lived. PDMS is not an ideal substrate for this system between its hydrophobicity and deformability, although it is a popular choice for rapid prototyping and allows a good seal between the reservoir tips and the LiaT platform.

4.2 Monitoring apoptosis in trench

Attempts were made to monitor apoptosis in trench, with induction of apoptosis carried out both in trench and before loading. Unfortunately, due to the time taken to observe apoptotic changes, coupled with the PDMS environment being unsuitable, at present, for long term observations of apoptotic

changes. Furthermore, as only small numbers of cells can be examined at a given time, it is unsuitable for identifying rare events, as this requires large numbers of cells to be analysed. For these reasons, it was chosen to move forward using flow cytometry for subsequent investigations of the surface glycosylation of apoptotic cells.

4.3 Future work

Better management of the flow rate is required. The reservoir tips, while simple, do not allow for tight control of the flow rate. It may be possible to control the flow rate using syringe pumps, but a great deal of optimisation will be required to allow easy loading of cells into the system and the substitution of buffers that is currently facile with the reservoir tips.

In addition, further manufacturing refinements to the platform are desirable. Polystyrene is the traditional plastic used by biologists when performing cell culture work and is more bio-compatible than PDMS (Berthier et al., 2012). Polystyrene also lends itself to manufacturing scale-up in a way that PDMS does not (Becker & Gärtner, 2008; Berthier et al., 2012). Unfortunately, the high aspect ratios of the features limits production to PDMS in the academic lab. Hot embossing is not possible as the features may snap off during demoulding, and production of masters for injection moulding is beyond the scope of rapid prototyping.

Furthermore, work should be carried out to reduce the optical depth of the base of the trench. At present, the channels are fabricated by spreading a very thin amount of PDMS on the SU-8 masters by tilting the disc until the PDMS had covered the area. Spin coating the PDMS onto the master could allow even thinner bases to the trench, allowing higher resolution microscopy. If the trench base could be eliminated altogether and the chip mounted on a coverslip, this would allow optical depths comparable to slide-based microscopy and would offer the biocompatible surface of the glass for cell adhesion.

Future experiments might also incorporate dimeric sugars and glycans bound to proteins as haptens for release of the lectin probes. Using more complex molecules for elution of the lectin probes may overcome the weak release seen with some free sugars without the present requirement to use very high concentrations of free monomeric sugar which may cause inad-

vertent changes to the cell state. Repeated measurements with the same lectin may help identify if the high sugar causes changes of the cell surface glycosylation.

Performing cell synchronisation may also reduce the observed heterogeneity in the cells, and it may be a worthwhile step to improve homogeneity as well as permitting glycosylation changes in the cell cycle to be analysed. Furthermore, staining to identify cell features may allow one to understand if the cells adopt a particular orientation when they settle in the trench, or if differing cell faces are seen, further accounting for heterogeneity.

4.4 Possible applications

The possibility of sequential glycoprofiling with the Lab in a Trench platform opens up many new routes of investigation of cell surface glycosylation in the laboratory. With improved manufacturing and shorter optical distances, LiaT could allow any laboratory to perform sequential interrogation of live cells with lectins.

It may be feasible to glycoprofile the surfaces of cells that are being subjected to drug treatments or other stresses *in vitro*. It would also be useful to label a cell with a single lectin, elute the lectin and subject the cell to a particular condition or stress followed by relabelling of the same cell with the lectin to show any changes in binding that may have been caused. An example of such an application would be demonstrating potential differences in lectin binding between cells before and after fixation with a variety of fixatives. It may be necessary, however, to change the materials that the system is made from in order to fully realise its potential for long experiments involving live cells.

Chapter 5

Labelling late apoptotic cells with novel carbohydrate binding proteins

The appearance of terminal GlcNAc (N-acetyl-glucosamine) in late apoptosis has been previously characterised by GSL II binding (Meesmann et al., 2010; Franz et al., 2006). GafD and AAL-2 are recombinant lectins that bind terminal GlcNAc. They were produced recombinantly and selected for testing against late apoptotic cells based on the reported binding of GSL II to such cells.

Testing is primarily carried out using flow cytometry as it is a high throughput technique that permits analysis of large numbers of cells to identify rare events. As Lab in a Trench does not meet these criteria (section 4.2), flow cytometry was deemed to be the more useful technique in this instance, with western blot and mass spectrometry used as confirmatory techniques.

GafD is specific for binding to O-GlcNAc (Saarela et al., 1996; Merckel et al., 2003) , whereas AAL-2 binds to both N- and O- linked terminal GlcNAc in a similar fashion to GSL II (Jiang et al., 2012).

5.1 GafD and AAL-2 do not induce apoptosis in Ramos cells

As may be seen in Figure 5.1, triply stained cells for flow cytometry (AAL-2/GafD, Annexin V, PI) show no increased apoptosis over doubly stained

cells (Annexin V, PI) treated with the same conditions (Figure 5.1) (staining process described in subsection 2.3.2).

This would indicate that terminal GlcNAc is only exposed on the cell surface after the cell has entered the late apoptotic phase. Prior to desialyation, the terminal GlcNAc is effectively covered by the sialic acid 'cap' and is therefore not exposed for GafD or AAL-2 binding. Any receptor this glycan may be on will not be activated by lectin binding and therefore, GafD and AAL-2 may be used for staining cells without inducing apoptotic death.

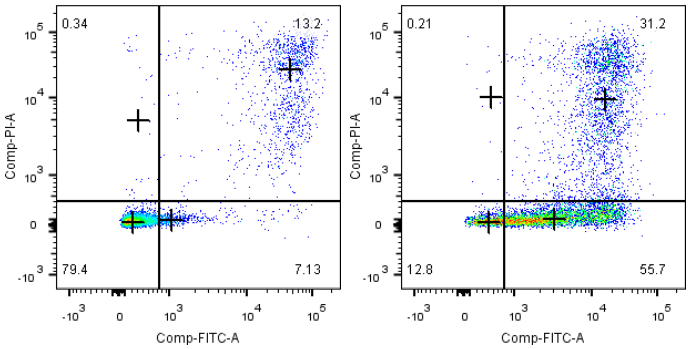

(a) Double Stained untreated

(b) Double Stained anti-IgM treated

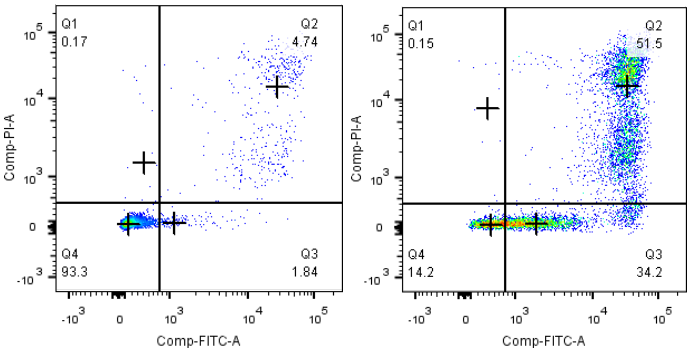

(c) Triple Stained untreated (GafD)

(d) Triple Stained anti-IgM treated (GafD)

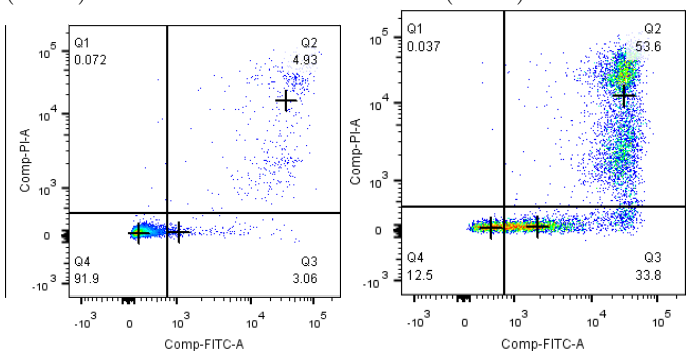

(e) Triple Stained untreated (AAL-2)

(f) Triple Stained anti-IgM treated (AAL-2)

Figure 5.1: Staining with GafD and AAL-2 does not induce apoptosis in Ramos B-cells under staining conditions for flow cytometry. All measurements were taken on the same day. All samples were stained with Annexin-V FITC and PI, with triple staining incorporating V450-labelled GafD or AAL-2. Compensation causes some adjustment of FITC and PI channels where staining is seen on the V450 channel.

5.2 Flow cytometry of apoptotic cells using GafD

5.2.1 GafD binds late apoptotic Ramos B-cells

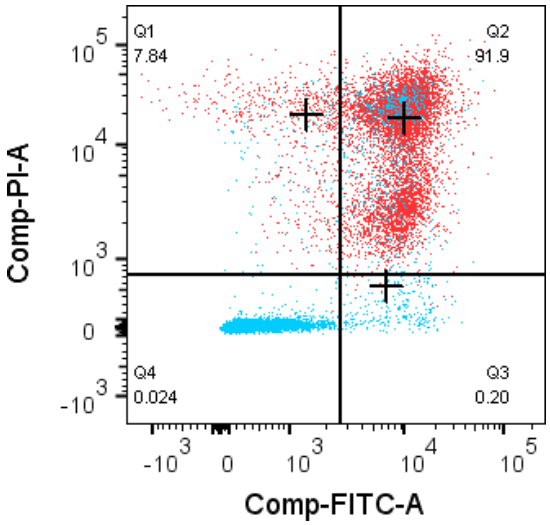

(a) GafD binds late apoptotic cells

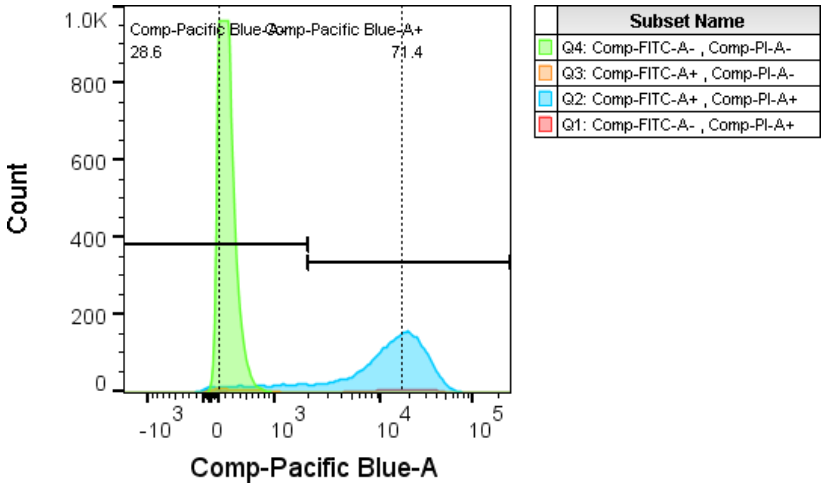

(b) GafD binding is strongest in late apoptotic cells

Figure 5.2: Detection of GafD binding to late apoptotic Ramos B-cells cells by flow cytometry. Apoptotic Ramos cells were labelled with Annexin-V FITC, PI and V450 GafD. Cells were measured on the BD FACS Aria and analysed with FlowJo. Quadrants and histogram gating was set using unstained samples. In (a) red cells are GafD positive and blue cells are GafD negative based on histogram gating. In (b) the non apoptotic cells (green) and early apoptotic (orange) show no GafD staining, where the late apoptotic cells (blue) show strong staining.

As may be seen in Figure 5.2, apoptotic cells are identified using Annexin-V and uptake of a nuclear stain that is excluded by the membranes of healthy cells. In this case, the Annexin-V is FITC labelled and the nuclear stain is propidium iodide (PI; as described in subsection 2.3.1). Gates are set against unstained samples. The Annexin-V negative / PI negative quadrant (Q4) contains healthy cells. The Annexin-V positive / PI negative quadrant (Q3) contains early apoptotic cells that have flipped phosphotidyl serine (PS) to the outer membrane of the cell but whose membranes have not lost integrity. PI positive quadrants (Q2 and Q1) represent dead and late apoptotic cells, most cells in late apoptosis exhibit Annexin-V binding (Q2) although some cells are dead without PS expression (Q1).

GafD gating is set on a histogram against the unstained sample. By gating on Annexin-V/PI and comparing the GafD signal, it can be seen that the highest signal is found in the Annexin-V positive/PI positive (Q2) quadrant. Little binding is seen in Annexin-V negative PI positive (Q1), with no staining seen in the PI negative quadrants (Q3/4).

Changes in display of terminal GlcNAc are known to occur in late apoptosis, when desialyation exposes previously hidden GlcNAc. Display of O-GlcNAc is unexpected as O-GlcNAc is exclusively a nucleo-cytoplasmic protein (Hart & Akimoto, 2009). Further investigation was carried out to identify the O-GlcNAc bearing proteins in order to identify whether nucleo-cytoplasmic proteins were migrated to the cell surface or the exposure was due to removal of much of the glycan structure of an O-linked glycan (see section 5.4).

5.2.2 GafD binding to cells can be inhibited with free GlcNAc

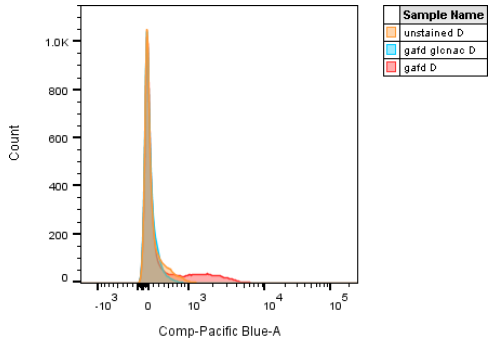

Figure 5.3: GlcNAc inhibits GafD binding to late apoptotic Ramos B-cells, as observed by flow cytometry. Apoptotic Ramos cells were labelled with V450 GafD (red); V450 GafD and 10 mM GlcNAc (blue); and left unstained (orange). Cells were measured on a BD FACS Aria and analysed with FlowJo.

As may be seen in Figure 5.3, when pre-incubated with GlcNAc, GafD binding to cells was inhibited. This demonstrates that binding of the GafD to the cells is mediated through the glycan binding site and not by uptake via an alternative mechanism, nor is this specificity of binding affected by the damaged membrane of the apoptotic cells.

5.3 GafD as a probe for Western Blotting

Western blotting with GafD was carried out to begin to clarify the changes in GafD binding observed on the surface of Ramos B-cells using flow cytometry. Initially it was carried out using whole cell lysates and later using membrane enriched-fractions that better represented the binding in a flow cytometric context.

5.3.1 GafD binds to many intracellular components of whole cell lysates

It is known that O-GlcNAc is found in high abundance in nucleo-cytoplasmic fractions, and it would therefore be expected to find many bands on blots of whole cell lysates, as was indeed the case Figure 5.4. Differential binding between untreated and apoptotic cells was not apparent Figure 5.4. The abundance of nucleo-cytoplasmic binding may have masked any small

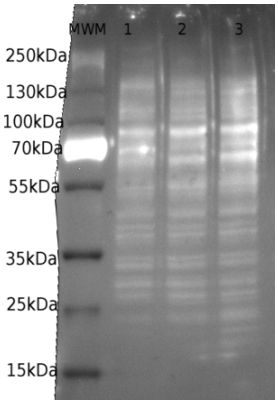

Figure 5.4: GafD binds nucleo-cytosolic proteins in whole cell lysates of Ramos B-lymphocytes. Ramos lysates were run on a 4-20 % SDS-PAGE gel with PageRuler Plus as the molecular weight marker (MWM) and transferred to 0.45 μm nitrocellulose using the Thermo Fisher G2 fast blotter (as per subsection 2.6.2 and subsection 2.6.5). Blots were probed with GafD / anti-his. Lanes 1 to 3 contain lysates of cells induced to apoptose for 0, 24, and 48 hours. Lanes 1 to 3 were equally loaded.

differences in O-GlcNAc in cell surface proteins. In addition to which, if the O-GlcNAc change seen on flow cytometry is due to the migration of nucleo-cytosolic proteins to the surface, the change in localisation will not be demonstrated on a blot of the whole-cell lysate.

As differential binding is observed on the flow cytometer, where GafD would have access only to the cell surface, it was decided to enrich the lysates for plasma membrane proteins.

5.3.2 Plasma membrane enrichment of Ramos B-cell lysates

5.3.2.1 Solvent extract of plasma membrane proteins

As described in subsection 2.7.2, it was attempted to purify membrane proteins by butanol extraction. Butanol extraction relies on the hydrophobic properties of the trans-membrane domains of proteins embedded in the membrane. It also does not require specialised equipment and may be carried out on the benchtop. Yields were low, with only 40 μg of protein recovered from 10 million cells. As may be seen in Figure 5.5, 2D-electrophoresis was performed on the extracted sample with band visualisation being achieved following silver staining (see subsection 2.6.4).

Figure 5.5: Silver stained 2D-electrophoresis of butanol-extracted plasma membrane proteins from Ramos B-lymphocytes. 50 million Ramos B-lymphocytes were apoptosed for 24h and butanol extracted as per subsection 2.7.2. The extracts were run on 2D-electrophoresis and stained as per sections 2.6.11 and 2.6.4.

5.3.2.2 Ultracentrifugal enrichment of plasma membrane proteins

Ultracentrifugation to enrich for plasma membrane proteins gave much better yields than the butanol extraction, with 80 μg per 10 million cells. The membrane enrichment is described in section 2.7.

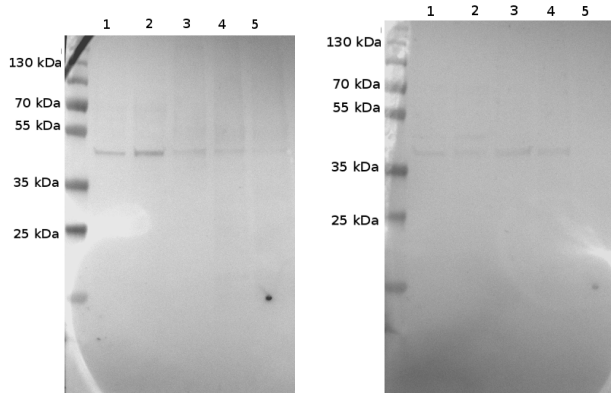

(a) β-actin **(b)** GAPDH

Figure 5.6: GafD blotted against the membranes of late apoptotic and untreated Ramos B-cells. Ultracentrifuged fractions of Ramos lysates were equally loaded run on a 4-20 % Tris-glycine gel followed by transfer to 0.45 μm nitrocellulose using the G2 fast-blotter (see sections 2.6.2, 2.6.5 and 2.6.8.2). Blot (a) was probed with anti-human β actin and blot (b) probed with anti-human GAPDH. Lanes contain: 1 - whole cell lysate, 2 - supernatant from 1st ultracentrifugation, 3 - supernatant from salt wash step, 4 - membrane pellet without salt wash, 5 - membrane pellet after salt washing.

Ultracentrifugation of whole cell lysates allows for depletion of the nucleo-cytosolic fraction. A salt wash (100 mM NaCl) was incorporated to further reduce non-specific binding that may cause cytosolic proteins to be pulled down with the membranes. As β -actin is a cytoskeletal protein, it is still seen with the membrane fraction after the salt wash (Figure 5.6). GAPDH is exclusively cytosolic and is fully depleted.

Depletion of the nucleo-cytosolic fraction reduces its interference in blotting with GafD. This allows investigation of the GafD binding to the cell membrane as was observed during flow cytometry.

5.3.3 Probing of membrane enriched samples with GafD

GafD was used to probe blots of membrane enriched apoptotic and non-apoptotic Ramos B-cells (methods described in sections 2.9.6, 2.7, 2.6.2, 2.6.5, 2.6.8.1 and 2.6.9.

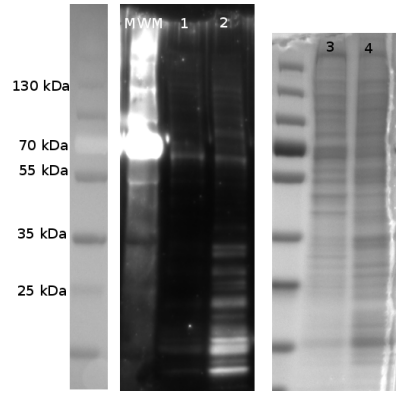

Figure 5.7: GafD blotted against the membranes of apoptotic and untreated Ramos B-cells. MWM is PageRuler plus. Lane 1 and 2 contain Ramos membrane fractions enriched by ultracentrifugation. Lane 1 cells were untreated and lane 2 cells were treated with anti-IgM for three days. Lanes 3 and 4 are the colloidal coomassie stained gels after transfer. The proteins were electrophoresed on 4-20 % Tris-Glycine gels and transferred to 0.45 μm nitrocellulose. The blots were probed with GafD and anti-biotin antibody, followed by imaging with Sure Signal Femto (Fisher). White light image of the MWM included for alignment as the chemiluminescent reagent resulted in a strong signal with the ladder.

GafD binds more strongly to the glycosylated proteins of the membrane-enriched extracts of apoptotic Ramos B-cells than to those of non apoptotic cells Figure 5.7. There is a change in the distribution of protein sizes seen, with more small proteins apparent in the apoptotic sample.

Some binding is seen in non-apoptotic cells. This may be due to contamination by the nucleo-cytosolic fractions or by the presence of a small number of apoptotic cells in the apparently non-apoptotic sample.

Some of the binding in the apoptotic fraction may be attributable to low level contamination by the nucleo-cytoplasmic fraction . However, as the apoptotic and non-apoptotic fractions were prepared in the same fashion, it is likely that such a contribution would be similar to the binding shown in the non-apoptotic fraction which is much lower than the overall binding observed in the apoptotic fraction (Figure 5.7).

This further confirms that increased O-GlcNAc is displayed on the membrane of Ramos B-cells during late apoptosis.

5.4 Proteomic analysis of membrane enriched GafD binding cells

5.4.1 Sorting of GafD + cells

Enrichment of the GafD binding cells was carried out by flow cytometric cell sorting (as described in subsection 2.3.4). Cells labelled with GafD were collected for further analysis by SDS-PAGE and mass spectrometry.

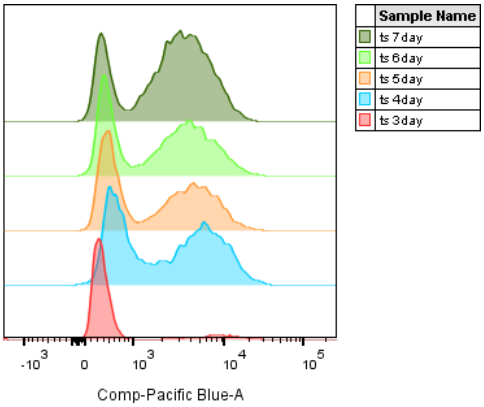

Figure 5.8: GafD binding is strong four days after initiation of apoptosis in Ramos B-lymphocytes. Cells were incubated with anti-IgM for up to seven days to determine maximum binding of GafD in order to increase yield for cell sorting. Cells were labelled with 1 μg/mL GafD with V450 and measured on a BD FACS Aria.

In order to maximise yield during sorting against sample preparation time, it was chosen to incubate cells with anti-IgM for four days.

Calculated sort efficiency was approximately 87 % with approximately 10 million cells collected from the GafD positive / PI positive gate.

Sorting of cells was carried out directly into PBS with protease inhibitors. It was observed that cell pellets could not be obtained after centrifugation of the sort collection tubes. It is likely that the already fragile late-apoptotic cells burst on impact with the sort tubes and buffers.

5.4.2 Selection of bands to prepared for analysis by mass spectrometry

Ramos cells were induced to apoptose for four days and sorted with a BD FACS Aria to produce GafD positive / PI positive subpopulation (as per sections 2.9.6 and 2.3.4). The plasma membranes of these samples were enriched by ultracentrifugation (as described in section 2.7). In addition, plasma membrane enrichments were carried out for untreated cells and for a bulk population of unsorted cells that had been induced to apoptose for four days.

These membrane-enriched protein extracts were run on a 4-20 % Tris-glycine SDS-PAGE and blotted on to 0.45 μm nitrocellulose using the G2 fast blotter (as described in sections 2.6.2 and 2.6.5). The gels were retained and stained with a colloidal Coomassie stain (as per subsubsection 2.6.3.2). The blots were probed with GafD and developed using the SureSignal Femto chemiluminescent substrate, see Sections 2.6.8.1 and 2.6.9.

The blots were copied and bands of interest were labelled (Figure 5.9). The bands were cut from the colloidal coomassie gels by overlaying the gel with the labelled blots in a clear dish over a white light box. The collected gel pieces were subjected to an in-gel tryptic digest followed by identification on a Thermo Q-Exactive, the methods for which are described in section 2.8.

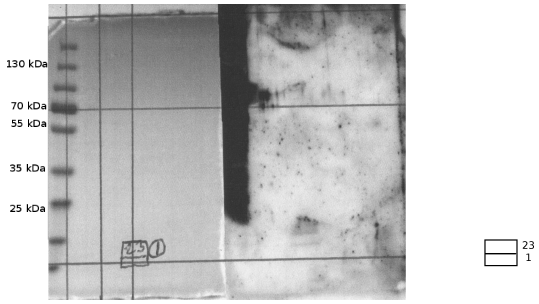

(a) Original sorted

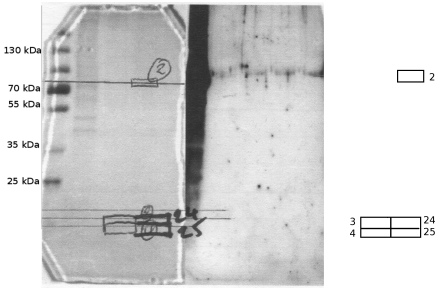

(b) Repeat sorted

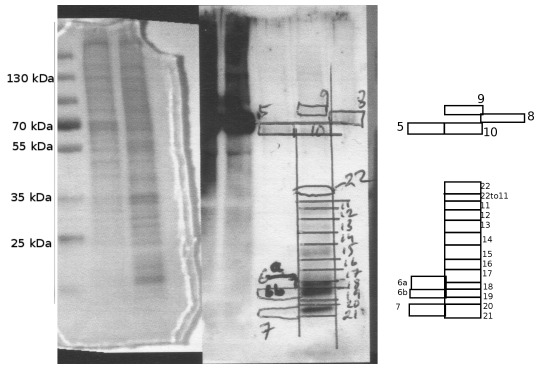

(c) Bulk unsorted

Figure 5.9: Origins of gel pieces cut for mass spectrometry. Printed copies of the blots had the bands of interest marked out such that colloidal Coomassie stained gels could be placed in a clear petri dish and aligned with the bands over a light box for excision with a scalpel. The original sorted blot (a) produced pieces 1 and 23. The repeated sorted blot (b) produced pieces 2, 3, 4, 24, 25. The bulk unsorted blot produced 5,6A,6B,7-22 and "22to11". All were prepared from Ramos lysates that had been enriched for membrane proteins through ultracentrifugation. The numbered areas are reproduced to the side of the gel for ease of reading.

The blots were copied and bands of interest were labelled (see Figure 5.9). The bands were cut from the colloidal coomassie gels by overlaying the gel with the labelled blots in a clear dish over a white light box. The collected gel pieces were subjected to an in-gel tryptic digest followed by identification

on a Thermo Q-Exactive, the methods for which are described in section 2.8.

5.4.3 Preliminary analysis of Mass Spectrometry data

Peptides measured on the Q-exactive were analysed by Proteome Discoverer (Thermo) to identify their associated proteins. Any instances of keratin discarded. This resulted in the identification of 903 proteins, of which 652 were unique. All 903 were compared with the dbOGAP's "O-GlcNAcylated proteins in dbOGAP with evidence attributions to corresponding PubMed ID(s)" database (Wang et al., 2011), resulting in 193 matches, of which 103 were unique.

A full list of the proteins identified, along with their corresponding gel piece and O-GlcNAc status can be found in Appendix D.2.

The 103 matching proteins had their UniProt accessions converted to Entrez GeneID's and uploaded to be searched against DAVID (Huang et al., 2009a,b). Information about pathways and gene ontology was collected and reported. This information is summarised in Tables 5.3, 5.5, 5.4 and 5.6.

Table 5.1: Results of proteomic searching across 27 gel pieces.

Total proteins identified	1102 (672 unique)
Total proteins after exclusion of keratins	903 (652 unique)
O-GlcNAcylated proteins identified	193 (103 unique)

Table 5.2: KEGG pathway analysis of O-GlcNAcylated proteins from mass spectrometry. Functional annotation carried out by DAVID against the KEGG pathways database. 56 proteins not clustered.

Term	Count
Ribosome	13
Glycolysis / Gluconeogenesis	7
Aminoacyl-tRNA biosynthesis	6
Antigen processing and presentation	7
Spliceosome	8
Pentose phosphate pathway	3
Pyruvate metabolism	3

As seen from Table 5.3, the identified O-GlcNAcylated proteins are predominantly acetylated and phosphorylated. This fits with the fact that O-GlcNAcylation often acts as an antagonist to PTM's such as phosphorylation (Hart & Akimoto, 2009).

Table 5.3: Top 20 keywords associated with identified O-GlcNAcylated proteins.

Term	Count
acetylation	95
phosphoprotein	89
cytoplasm	54
nucleus	42
nucleotide-binding	31
rna-binding	29
atp-binding	29
ribonucleoprotein	23
protein biosynthesis	22
dna-binding	17
disease mutation	16
mrna splicing	14
methylation	14
mrna processing	14
ribosome	13
ribosomal protein	13
Chaperone	10
ubl conjugation	10
Spliceosome	9
ATP	9

Cellular compartment results (Table 5.5) associate the identified proteins as being part of the nucleo-cytosolic compartment. Associations with the plasma membrane were not apparent from the search. In addition, many proteins were specifically associated with internal membranes such as the ribosomal membranes.

Pathway and bioprocess results (Table 5.4, Table 5.6) were most strongly associated with ribosomal functions. Protein folding proteins and chaperones are also well represented, and may have been translocated from the endoplasmic reticulum to the cell surface. The display of these proteins on the cell surface is highly immunogenic and has been linked with various auto-immune diseases and cancers (Casciola-Rosen et al., 1994; Franz et al., 2007; Wiersma et al., 2015).

Patching of the failing plasma membrane with intra-cellular membranes during late apoptosis is likely to be a mechanism by which O-GlcNAc bearing nucleo-cytosolic proteins are presented on the cells surface (Franz et al., 2007). As the plasma membrane loses area through blebbing, but the volume

Table 5.4: KEGG pathway analysis of O-GlcNAcylated proteins from mass spectrometry. Functional annotation carried out by DAVID against the KEGG pathways database. 56 proteins not clustered.

Term	Count
Ribosome	13
Glycolysis / Gluconeogenesis	7
Aminoacyl-tRNA biosynthesis	6
Antigen processing and presentation	7
Spliceosome	8
Pentose phosphate pathway	3
Pyruvate metabolism	3

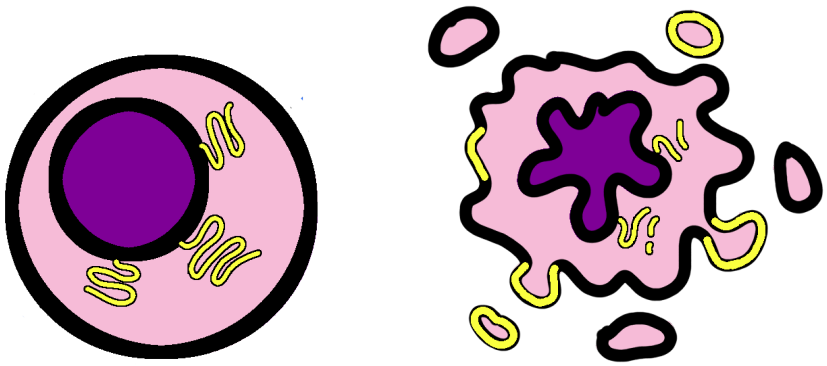

(a) Healthy cell **(b)** Late apoptotic cell

Figure 5.10: Ribosomal membranes may be transported to the surface during apoptosis. It is possible that exposure of O-GlcNAcylated proteins on the cell surface is due to the movement of ribosomal membranes (yellow), which are rich in O-GlcNAcylated proteins, to patch the degrading extracellular membrane.

of the cell is not lost at a matching rate, it is necessary for the cell to maintain its membrane through patching with internal membranes. Were the membrane to fail, the cytosolic compartment would be spilled, resulting in the exposure of normally-protected immunogenic epitopes that could lead to an autoimmune response. This would then result in the display of O-GlcNAcylated proteins on the cell surface, which may also be immunogenic, but would be a smaller quantity of exposed protein.

Table 5.5: Cellular localisation of top 20 results from DAVID against GO_CC_FAT

Term	Count
cytosol	50
ribonucleoprotein complex	38
non-membrane-bounded organelle	38
intracellular non-membrane-bounded organelle	38
membrane-enclosed lumen	32
intracellular organelle lumen	31
organelle lumen	31
nuclear lumen	26
cytosolic part	17
nucleoplasm	16
ribosome	15
nucleolus	15
cell fraction	15
soluble fraction	14
ribosomal subunit	13
cytosolic ribosome	12
cytoplasmic membrane-bounded vesicle	12
membrane-bounded vesicle	12
cytoplasmic vesicle	12
vesicle	12

Table 5.6: Bioprocess involved in identified O-GlcNAcylated proteins. Top 20 processes identified by DAVID against GO_BP_FAT database.

Term	Count
translation	24
RNA processing	24
mRNA metabolic process	20
RNA splicing	19
mRNA processing	18
macromolecular complex assembly	17
macromolecular complex subunit organization	17
translational elongation	16
RNA splicing, via transesterification reactions with bulged adenosine as nucleophile	12
nuclear mRNA splicing, via spliceosome	12
RNA splicing, via transesterification reactions	12
protein complex biogenesis	12
protein complex assembly	12
response to organic substance	11
negative regulation of macromolecule metabolic process	11
cell cycle	11
glucose metabolic process	10
protein folding	10
hexose metabolic process	10
posttranscriptional regulation of gene expression	10

5.5 Summary of GafD results

The recombinant CBP GafD was found to bind to late apoptotic B-cells as measured by flow cytometry. This finding was unexpected as GafD binds O-GlcNAc which is reported to be exclusively a post translational modification of intracellular proteins. Binding was confirmed to be specific and it appears after deterioration of cell membrane integrity as evidenced by propidium iodide uptake.

Isolation of the cell plasma membrane was carried out in order to run western blots and mass spectrometric analysis on membrane-bound proteins. This was required in order to exclude intra-cellular proteins, as it is known that many of these are O-GlcNAcylated. It was demonstrated that there is a clear difference in GafD binding to western blots of membrane enriched lysates of untreated and late apoptotic B-cells.

Mass spectrometric analysis indicated that many of the proteins collected in the membrane fraction were of nucleo-cytosolic origin. This not only explains the presence of O-GlcNAc on the cell surface but confirms existing literature that indicates that intracellular membranes, such as the endoplasmic reticulum, are recruited to the cell surface during late apoptosis (Franz et al., 2007; Casciola-Rosen et al., 1994).

The O-GlcNAcylation of proteins is reported to be transient, as it is easily degraded by lysosyme, and therefore it is possible that the full repertoire of O-GlcNAcylated proteins is not represented in this study. Further methods to clarify and confirm the presence of O-GlcNAc on the cellular surface are discussed in section 5.6.

The membrane fractionation by ultracentrifugation is a crude method for enriching plasma proteins. It is possible that some of the membrane proteins that were identified were from contaminant organelles that were not sedimented during the first 14,000 g spin. Even low levels of these contaminant proteins would be to detected by the very sensitive Orbitrap Mass Spectrometer. The clear difference in GafD binding that was seen across the blots, implies that the appearance of intracellular proteins in the membrane lysates were not due to contamination by the nucleo-cytosolic fraction during sample preparation. As discussed in section 5.6, it may be wise to perform further separation of the proteins 2D electrophoresis, prior to blotting.

5.6 Future Work on GafD

The GafD sorting and membrane fractionation should be repeated and further optimised. The membrane fraction should be subjected to a GafD pull-down and the bound proteins identified by mass spectrometry in order to confirm the results in subsection 5.4.3. Furthermore, cutting proteins from a 2D-electrophoresis gel with matching GafD blot would provide much greater resolution of the O-GlcNAcylated proteins that are displayed on the cell surface as they would be separated by both size and pI, and would resolve to spots rather than bands of many proteins. It may be possible to perform a cross-linking of the GafD to the O-GlcNAcylated surface proteins by the use of formaldehyde or gluteraldehyde as is sometimes performed for immunoprecipation of antibody binding partners (Nadeau & Carlson, 2007).

An assay to inhibit the action of neuraminidase on the cell surface therefore preventing desialyation of cell surface glycans could further demonstrate that the mechanism of GafD binding on the cell surface is due to migration of intracellular O-GlcNAc-bearing proteins to the surface rather than the cleavage of surface glycans. In addition, if inhibition of apoptotic blebbing prevented O-GlcNAc exposure on the cell surface, it would further confirm that GafD binding is due to transport of intracellular membranes to the surface.

It should also be attempted to identify GafD binding proteins in late apoptosis in a number of cell types, in order to see if O-GlcNAc exposure is specific to B-lymphocytes or a common feature of apoptosis. Of particular interest would be looking for O-GlcNAc on the surface of late apoptotic MCF-7 cells which, characteristically, do not bleb in late apoptosis as they lack -3 (Jänicke, 2009).

Mass spectrometry to confirm the O-GlcNAcylation to complement the GafD blotting should be carried out. β-elimination and Michael addition of the membrane isolates would allow identification of the O-GlcNAcylation site of the exposed protein. In addition, an alternative method such as the chemical labelling of O-GlcNAcylated proteins via the Thermo Click-IT kit should be considered, for both western blot and mass spectrometry.

Isolation of blebs could be performed to identify O-GlcNAc heavy blebs. As mentioned in (Franz et al., 2007), the intracellular-membrane patches on the cell surface tend to form blebs that are distinct from the extracellular-

membrane blebs, and it may be possible to test these for O-GlcNAcylation status.

5.6.1 Possible applications

GafD as a specific probe is another tool that may be added to the glycoanalytical tool kit. Although, the ability to identify very late apoptotic cells *in vitro* may not seem critical, it may be useful to identify very late apoptotic cells in relation to overburdened immune systems.

It may be interesting to isolate apoptotic bodies and other microparticles and attempt to identify if GafD binds to their surfaces. It may be possible to distinguish blebs that are derived from the outer membrane of the cell from those of nucleo-cytoplasmic origin. Identification of such blebs in patient samples could potentially lead to improvements in lupus diagnostics. Such highly inflamatory, late apoptotic bodies are likely to be a sign of an overburdened immune system. The late-apoptotic bodies display nucleo-cytoplamic elements which are normally hidden from the immune system. It is now hypothesised that the display of such self-antigens in conjunction with the pro-inflamatory nature of late apoptotic cells drives the autoimmune reactivity of lupus (Casciola-Rosen et al., 1994; Dye et al., 2013; Zirngibl et al., 2014).

5.7 AAL-2 binds late apoptotic Ramos B-cells

AAL-2 is a carbohydrate binding protein with similar glycan specificity to the commercially available GSL II but with a higher affinity (Jiang et al., 2012). Unlike GSL II, AAL-2 does not require ions for its binding site to function. As it is a recombinant lectin it would make a good alternative to GSL II which is purified from *Griffonia simplicifolia*. AAL-2 has six binding sites on a single monomer for terminal GlcNAc (Ren et al., 2015), whereas GSL II is composed of four subunits but is limited to binding two terminal GlcNAcs at a time.

AAL-2 was compared with GSL II for use as a flow cytometry label and as a probe for blotting. An attempt was also made to make use of its higher binding affinity to remove late apoptotic cells from culture.

5.7.1 AAL-2 binds the same population as GSL II for flow cytometry

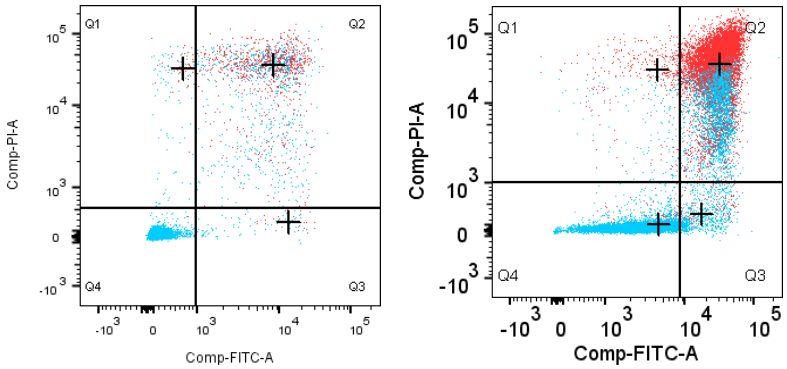

(a) AAL-2 **(b)** GSL II

Figure 5.11: Flow cytometric measurements of AAL-2 and GSL II in relation to Annexin-V and propidium iodide Apoptotic cells are labelled with Annexin-V FITC, PI and 10 μg /mL of GSL II labelled with DyLight405 or AAL-2 labelled with V450 (as described in subsection 2.3.2). Cells labelled with AAL-2 or GSL II are red, where cells that don't bind lectin are blue. Q1 is annexin-V negative / PI positive. Q2 is annexin-V positive / PI positive (late apoptotic cells). Q3 is annexin-v positive / PI negative (early apoptotic). Q4 is annexin-V negative / PI negative (healthy cells). GLS II and AAL-2 binding is predominantly seen in the late apoptotic (Q3) quadrant.

It was observed that AAL-2 and GSL II bind exclusively to late apoptotic Ramos B-cells (Figure 5.11). This is expected as both are terminal GlcNAc binders. It has been reported that desialyation in late apoptosis exposes underlying GlcNAc (Meesmann et al., 2010).

The advantage of using AAL-2 is that it is a recombinant lectin , giving a consistent production , performance and lower cost than GSL-II. In addition AAL-2 does not require ions for activity of its binding site (Jiang et al., 2012).

5.7.2 AAL-2 gives similar binding patterns to GSL II for blotting

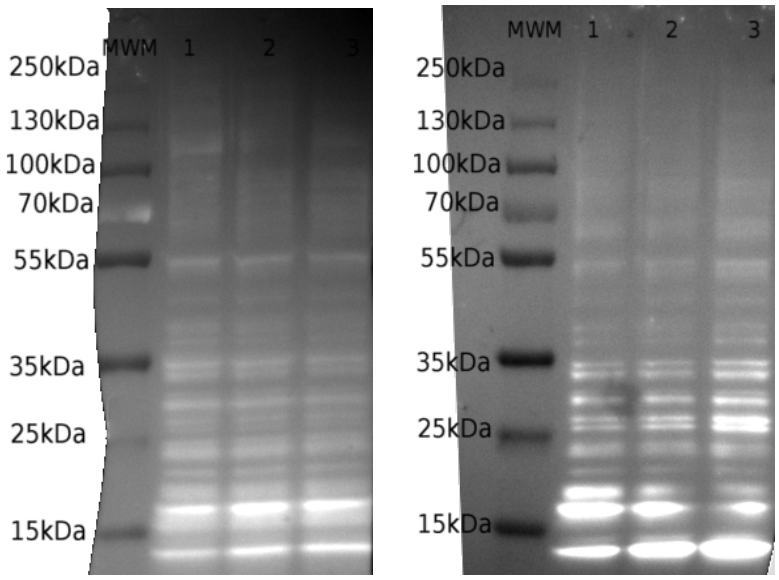

(a) AAL-2 **(b)** GSL II

Figure 5.12: Western blotting of Ramos whole cell lysates with AAL-2 and GSL II Ramos lysates were run on a 4-20 % SDS-PAGE gel with PageRuler Plus as the molecular weight marker (MWM) and transferred to 0.45 μm nitrocellulose using the Thermo Fisher G2 fast blotter (as described in sections 2.6.2 and 2.6.5). Blots were probed with AAL-2 / anti-his (a) and GSLII / anti-biotin (b) (as per subsubsection 2.6.8.1). Lanes 1 to 3 contain lysates of cells induced to apoptose for 0, 24, and 48 hours. Lanes 1 to 3 were loaded equally.

As seen in Figure 5.12, blotting with AAL-2 and GSL II yield similar bands on Ramos whole cell lysates. Differences between the sensitivities of anti-his and anti-biotin antibodies can be resolved by biotinylation of AAL-2 so the same secondary antibody can be used for both lectins.

Identical binding patterns allows future blotting with AAL-2 in place of GSL II, as AAL-2 is cheaper to produce with no requirements for ions in the buffers.

5.7.3 AAL-2 does not pull down late apoptotic cells

As AAL-2 has a higher binding affinity than GSL II, it was attempted to use AAL-2 to deplete the late apoptotic cells from a culture. Depleting the late apoptotic cell population would reduce the pro-inflammatory influence

of late apoptotic cells on the other cells in culture. In particular for suspension cultures, it can be challenging to separate dead and dying cells, whereas in adherent culture they can be simply washed away. At present, enrichment of live cells in suspension culture is carried out by centrifuging the cells at a much lower force, such that the healthy cells pellet more easily, and the lighter ragged cells that are late apoptotic remain in suspension. Positively selecting late-apoptotic cells would leave healthy cells untouched. This would remove the possibility of affecting the healthy population by activation of a host of receptors by binding with a probe.

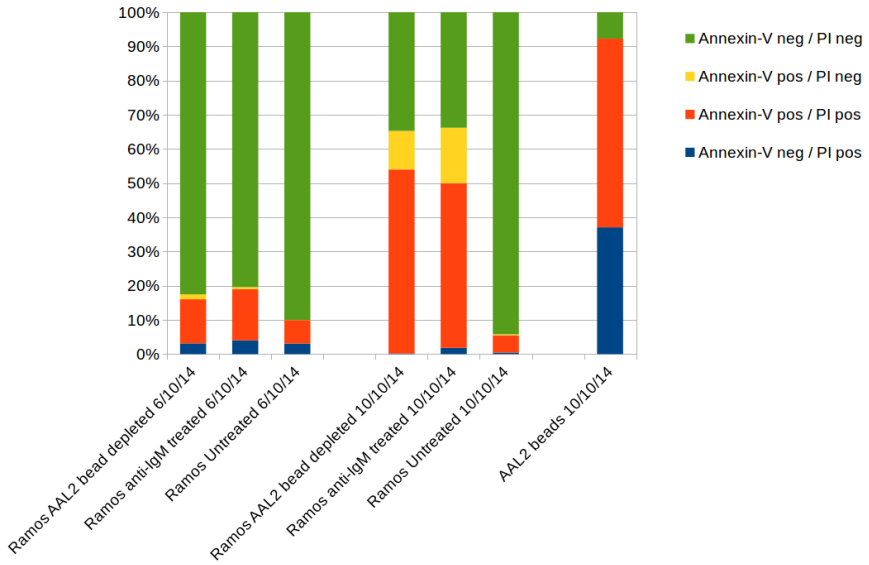

Figure 5.13: Flow cytometric analysis of purification of apoptotic Ramos B-cell suspension using AAL-2 conjugated to 10 μm magnetic beads. Samples on 6/10/14 were apoptosed for 24h. Samples on 10/10/14 were apoptosed for 48h. Bead depletion was carried out as per section 2.4. All samples were measured on a BD FACS Aria using Annexin-V FITC and propidium iodide. Analysis was performed using FlowJo. Doublets and debris were excluded using FSC-A/FSC-H. Setting of positive gates was carried out against unstained samples.

In Figure 5.13, it is shown that there is no significant difference in the fraction of annexin-V positive / PI positive cells before and after AAL-2 bead depletion. However on the beads themselves, the cells are largely the PI positive cells that would have exposed terminal GlcNAc, indicating that the beads could potentially collect or enrich a subset of cells.

It is possible that the fragile nature of the late apoptotic membrane means that although the beads have bound to the cells, the shear force

between the bead and the cell allows the bead to rip off parts of the cell membrane without pulling the entire cell out of suspension.

5.7.4 Summary of AAL-2 results

Recombinant AAL-2 is a useful alternative probe to the commercially available GSL-II for flow cytometry and western blotting. AAL-2 was shown to bind exclusively to late apoptotic cells. This was in agreement with the published literature where GSL II has previously been reported to bind to late apoptotic cells (Meesmann et al., 2010). Use of AAL-2 as a probe for western blotting also yielded similar results to GSL II.

Attempts to use AAL-2 with 10 μm magnetic beads to pull late apoptotic cells from cell suspension were unsuccessful. This is likely due to the shear force between the large magnetic particle and the fragile cell membrane.

AAL-2 has advantages as an alternative probe to GSL II as it is a recombinant protein that may be more easily produced consistently and does not require calcium ions to coordinate its binding site. However, GSL II is established and readily available, whereas AAL-2 is not commercially available and would need to be produced in-house.

5.7.5 Future Work on AAL-2

The use of AAL-2 for flow cytometry and blotting should be extended to other cell types and to microparticles, to further demonstrate its potential as an alternative to GSL II.

A Far Eastern blot may also be an interesting application of the AAL-2. Thin layer chromatography of the whole cell lysate or membrane isolate of apoptotic cells is transferred to PVDF and could be probed with AAL-2 to see if there are changes in the expression of terminal GlcNAc attached the lipids of the cell membranes(Taki et al., 1994).

A magnetic bead pull down using immobolised AAL-2 would allow for the removal of late apoptotic cells from a cell culture population. As AAL-2 only interacts with late apoptotic cells, it would not affect healthy cells and would reduce the pro-inflammatory effects of having late apoptotic cells in the culture. The magnetic bead pull down assay should be attempted with various size beads. A fine dust coating of small magnetic beads may result in less damage of the fragile cell membranes. Shear forces between cell and

large bead may result in tearing of the membrane and failure to remove the cell itself from the culture.

Microfluidic devices have been used to examine the effects of shear force on cells that are adhered to a surface or otherwise captured by antibodies (Lu et al., 2004; Christ et al., 2010; Christophis et al., 2010). The effect of shear force on the apoptotic cell membrane could be examined by coating a microfluidic channel with AAL-2, capturing apoptotic cells and identifying if the cell membranes tear or if the entire cell shears off intact.

5.7.6 Possible applications

AAL-2 is suitable as an alternative lectin to GSL-II, and has possible uses everywhere GSL-II is used to interrogate sugars.

AAL-2's affinity for late apoptotic cells is potentially very useful for separating dead cells from a culture of suspension cells. Harsh transfection protocols (Weaver, 1995) or drug screenings can result in late apoptotic cells that can adversely affect the remaining cells in culture as they become pro-inflammatory in late apoptosis. Maintaining the few transfected cells, or isolating the drug effects from the pro-inflammatory dead cells, requires a way of isolating the dead cells from the population. If magnetic capture in free solution may not be optimised, it is still possible to have a magnetic separation of apoptotic cells based on the magnet activated cell sorting method by Miltenyi Biotec (Miltenyi et al., 1990). The AAL-2 would be conjugated to kit beads, and the cells passed through a magnet activated cell sorter to perform the separation.

Use of AAL-2 as the capture protein in supermacroporous cryogels (Kumar & Srivastava, 2010) could also be an efficient, low shear method for separating apoptotic from non apoptotic cells. The procedure would be similar to affinity chromatography methods, but the supermacroporous column would permit the free movement of cells rather than being limited to smaller molecules.

Chapter 6

Conclusions

The field of glycobiology , and more specifically glycobiological analysis, is rapidly emerging as one of the most exciting areas of research in Biology. As its importance to the diagnostic and biopharmaceutical industries becomes more recognised, there is a general realisation that new and more specific methodologies for glycoanalysis are required. During the work of this thesis, novel combinations of methodologies, microfluidic platforms and new probes were investigated for their ability to interrogate cell surface glycosylation.

In particular, this work demonstrates, for the first time, the **sequential** interrogation of cell surface glycans with a unique combination of labelled lectin probes in the microfluidic platform, Lab in a Trench (LiaT). This sequential labelling of the same cell surface is made possible by the use of selective/specific release of the labelled probes by the corresponding free sugars.

This work also reports on the recombinant production of novel carbohydrate binding protein probes, namely GafD and AAL-2, which were found to be useful for the interrogation of apoptotic cells through flow cytometry and western blotting. These findings demonstrated the potential ability of this bioanalytical approach to observe changes in the glycosylation of the cell surface as they becomes apoptotic.

These new tools have the potential to transform the field of glycobiology, as the novel CBP's can be integrated into existing biological work-flows, and the LiaT system can be used with existing facilities. This helps achieve some of the aims of the Glycoscience Roadmap (of Sciences et al., 2012), whereby glycoanalytical tools would be readily available and usable by non-

glycoscience specialists to integrate into their own investigations. Changes in glycosylation may be relevant in all areas of cell biology, and these tools will make it easier for cell biologists to discover their relevance to their work.

6.1 Lab in a Trench is a new method for observing cell surface glycosylation

Lab in a Trench has allowed us to realise a powerful new method for observing cell surface glycosylation through sequential labelling and specific release of fluorophore-labelled lectins or carbohydrate binding protein probes. This method allows for the localisation of different glycans on the surfaces of individual cells and demonstrates the heterogeneous nature of cell glycosylation even in an apparently homogeneous cell line.

LiaT can allow for affordable analysis of the cell surface glycosylation, as the platform needs no special equipment to run and the sequential labelling requires only a single fluorophore label for the different lectin probes. The specific release of the bound lectin probe is simply achieved by the use of the appropriate free sugar.

The manufacture of the device has been greatly improved through lengthy optimisation of bonding conditions and surface treatments. As bursting was a common occurance after bonding fully cured PDMS layers that had been plasma treated, it was decided to use partially cured PDMS as this gives good strength between the layers during loading. Hydrophilisation of the channels through plasma treatment facilitates easier loading and reduces air bubbles.

The system at present requires an operator with empirical experience of the system, as variability of flow within the system still presents a problem. Issues of sterility and material compatibility with the cells are presently resolved through keeping experiments short, but a change in material and experimental environment may improve this in the future. The ability to carry out longer experiments would greatly increase the utility of LiaT. Similarly reducing the optical depth of the trench would enable higher resolution imaging. Use of a microscope with auto focus and a programmable stage would permit higher throughput of image capture and reduce the demands on the operative.

6.2 GafD binding demonstrates changes in the late apoptotic membrane of B-cells

GafD binds to O-GlcNAc displayed on the surface of late apoptotic B-lymphocytes. O-GlcNAc is a sugar modification seen exclusively on intracellular proteins. The likely mechanism for this exposure of O-GlcNAcylated proteins is through the transposition of intracellular membranes to the extracellular surface to patch the surface after loss of membrane through blebbing. This mechanism has been postulated by others (Casciola-Rosen et al., 1994; Franz et al., 2007) based on observations of ribosomal proteins, but this is the first demonstration through O-GlcNac binding. Membrane patching reduces the exposure of the cytosolic compartment to the immune system in the event that a late apoptotic cell has not yet been cleared.

Measurement with GafD was performed by flow cytometry in order to gather large volumes of cell data with simultaneous apoptotic marker detection. The GafD binding events corresponded to the late apoptotic population identified by propidium iodide uptake. Unfortunately, due to constraints of the LiaT system, it was not possible to perform these experiments on the system, but it is hoped they could be run on it with optimised conditions in the future.

Investigation of the proteins that bound the GafD was then carried out to identify the mechanism leading to O-GlcNAc exposure. Enrichment of cell membranes was essential to remove interfering signals from intracellular proteins which are O-GlcNAcylated. Identification of the membrane associated proteins was performed mass spectrometry, with the detection of many O-GlcNAcylated intracellular proteins. In particular many ribosome associated proteins were identified. This appears to be in accordance with existing literature (Franz et al., 2007; Casciola-Rosen et al., 1994).

Further mass spectrometric measurements to directly analyse the O-GlcNAcylation would be preferable to matching proteins against existing datasets, and would require access to a specialised source and the facilities to perform BEMAD on the samples. In addition, multiple cell lines should be tested to confirm that this is not a feature specific to the Ramos B-cell lymphoma line.

6.3 AAL-2 is a good alternative to GSL II for cell analysis

AAL-2 is an attractive alternative to GSL II for the analysis of cells. It has the same binding patterns as GSL II in western blot and flow cytometry of late apoptotic B-cells. Its advantages include higher binding affinity and the ability to produce it recombinantly. In addition, it has no requirements for ions to enable binding, making it more flexible in the buffers it can be used with. This would allow it to be used in a conjunction with a range of stains where the GSL II buffer might not be ideal.

Although AAL-2's higher affinity for terminal GlcNAc than GSL II would imply it would be good for pulling late apoptotic cells from suspension, it would seem that when conjugated to larger beads it does not succeed in this. It will be valuable to investigate the possibility of using finer magnetic particles to see if the apoptotic cells could be pulled from suspension without tearing of their membranes. Future work will include a range of magnetic bead sizes to see if this isolation method will be of use.

References

H. Alwael, et al. (2011). 'Pipette-tip selective extraction of glycoproteins with lectin modified gold nano-particles on a polymer monolithic phase.'. *The Analyst* **136**(12):2619–28.

H. J. An, et al. (2009). 'Glycomics and disease markers.'. *Current opinion in chemical biology* **13**(5-6):601–7.

R. M. Anthony & J. V. Ravetch (2010). 'A novel role for the IgG Fc glycan: The anti-inflammatory activity of sialylated IgG Fcs'. *Journal of Clinical Immunology* **30**(SUPPL. 1):9–14.

D. Apostolovic, et al. (2015). 'Red meat allergic patients have a selective IgE response to the α-Gal glycan.'. *Allergy* **70**(15):1497–1500.

R. Apweiler, et al. (1999). 'On the frequency of protein glycosylation, as deduced from analysis of the SWISS-PROT database'. *Biochimica et Biophysica Acta (BBA) - General Subjects* **1473**(1):4–8.

J. Arnaud, et al. (2013). 'Binding sugars: from natural lectins to synthetic receptors and engineered neolectins'. *Chemical Society Reviews* **42**(11):4798.

N. X. Arndt, et al. (2011). 'Differential carbohydrate binding and cell surface glycosylation of human cancer cell lines.'. *Journal of cellular biochemistry* **112**(9):2230–40.

T. Arnold & D. Linke (2008). 'The Use of Detergents to Purify Membrane Proteins'. In *Current Protocols in Protein Science*. John Wiley & Sons, Inc.

P. P. Austin Suthanthiraraj & S. W. Graves (2013). 'Fluidics'. *Current Protocols in Cytometry* (July):1–14.

D. R. e. a. Bandura (2009). 'Mass Cytometry: Technique for Real Time Single Cell Multitarget Immunoassay Based on Inductively Coupled Plasma Time-of-Flight Mass Spectrometry' **81**(16):6813–6822.

P. S. Banerjee, et al. (2013). 'Chemical approaches to study O-GlcNAcylation'. *Chem. Soc. Rev.* **42**(10):4345–4357.

Y. C. Barnes, et al. (1999). 'Sialylation of the sialic acid binding lectin sialoadhesin regulates its ability to mediate cell adhesion.'. *Blood* **93**(4):1245–52.

C. Batisse, et al. (2004). 'Lectin-based three-color flow cytometric approach for studying cell surface glycosylation changes that occur during apoptosis.'. *Cytometry. Part A : the journal of the International Society for Analytical Cytology* **62**(2):81–8.

H. Becker & C. Gärtner (2008). 'Polymer microfabrication technologies for microfluidic systems.'. *Analytical and bioanalytical chemistry* **390**(1):89–111.

M. Bergmann, et al. (1998). 'Abnormal surface expression of sialoglycans on B lymphocyte cell lines from patients with carbohydrate deficient glycoprotein syndrome I A (CDGS I A).'. *Glycobiology* **8**(10):963–72.

E. Berthier, et al. (2012). 'Engineers are from PDMS-land, Biologists are from Polystyrenia'. *Lab on a Chip* **12**(7):1224.

C. R. Bertozzi & R. Sasisekharan (2009). *Glycomics*.

R. O. Bilyy, et al. (2012). 'Macrophages discriminate glycosylation patterns of apoptotic cell-derived microparticles.'. *The Journal of biological chemistry* **287**(1):496–503.

I. Brockhausen, et al. (2009). 'O-GalNAc Glycans'. In *Essentials of Glycobiology*.

R. Burger, et al. (2015). 'An integrated centrifugo-opto-microfluidic platform for arraying, analysis, identification and manipulation of individual cells'. *Lab Chip* **15**(2):378–381.

R. Burger, et al. (2012). 'Array-based capture, distribution, counting and multiplexed assaying of beads on a centrifugal microfluidic platform.'. *Lab on a chip* **12**(7):1289–95.

M. Butler (2005). 'Animal cell cultures: Recent achievements and perspectives in the production of biopharmaceuticals'. *Applied Microbiology and Biotechnology* **68**(3):283–291.

J.-T. Cao, et al. (2012a). 'Quantum dots-based immunofluorescent microfluidic chip for the analysis of glycan expression at single-cells.'. *Analytical chemistry* **84**(22):10097–104.

J. T. Cao, et al. (2012b). 'Microfluidic Platform for the Evaluation of Multi-Glycan Expressions on Living Cells using Electrochemical Impedance Spectroscopy and Optical Microscope'. *Analytical Chemistry* **84**(15):6775–6782.

J.-T. Cao, et al. (2015). 'Versatile Microfluidic Platform for the Assessment of Sialic Acid Expression on Cancer Cells Using Quantum Dots with Phenylboronic Acid Tags'. *ACS Applied Materials & Interfaces* **7**(27):14878–14884.

D. D. Carlo, et al. (2006). 'Dynamic single cell culture array'. *Lab on a Chip* **6**(11):1445.

L. a. Casciola-Rosen, et al. (1994). 'Autoantigens targeted in systemic lupus erythematosus are clustered in two populations of surface structures on apoptotic keratinocytes.'. *The Journal of experimental medicine* **179**(4):1317–1330.

K. V. Christ, et al. (2010). 'Measurement of single-cell adhesion strength using a microfluidic assay'. *Biomedical Microdevices* **12**(3):443–455.

C. Christophis, et al. (2010). 'Quantification of the adhesion strength of fibroblast cells on ethylene glycol terminated self-assembled monolayers by a microfluidic shear force assay'. *Physical Chemistry Chemical Physics* **12**(17):4498.

R. J. Clark, et al. (2003). 'Diabetes and the accompanying hyperglycemia impairs cardiomyocyte calcium cycling through increased nuclear O-GlcNAcylation.'. *The Journal of biological chemistry* **278**(45):44230–7.

B. E. Collins & J. C. Paulson (2004). 'Cell surface biology mediated by low affinity multivalent protein-glycan interactions.'. *Current opinion in chemical biology* **8**(6):617–25.

D. J. Collins, et al. (2015). 'Two-dimensional single-cell patterning with one cell per well driven by surface acoustic waves'. *Nature Communications* **6**:8686.

R. D. Cummings & M. E. Etzler (2009). *Antibodies and Lectins in Glycan Analysis*.

R. D. Cummings & R. P. McEver (2009). *C-type Lectins*.

J. DeBlaquiere & A. Burgess (1999). 'Affinity Purification of Plasma Membranes'. *Journal of biomolecular techniques: JBT* **10**(2):64.

I. K. Dimov (2010). *Science Platform for Cell Based Assays by Gravity Driven Sequential Perfusion and Diffusion by*. Ph.D. thesis.

I. K. Dimov, et al. (2010). 'Lab-in-a-trench platform for real-time monitoring of cell surface protein expression'. In *2010 IEEE 23rd International Conference on Micro Electro Mechanical Systems (MEMS)*, pp. 96–99. IEEE.

I. K. Dimov, et al. (2011). 'Integrated microfluidic array plate (iMAP) for cellular and molecular analysis.'. *Lab on a chip* **11**(16):2701–10.

L. Douay & G. Andreu (2007). 'Ex vivo Production of Human Red Blood Cells From Hematopoietic Stem Cells: What Is the Future in Transfusion?'. *Transfusion Medicine Reviews* **21**(2):91–100.

D. H. Dube & C. R. Bertozzi (2005). 'Glycans in cancer and inflammation–potential for therapeutics and diagnostics.'. *Nature reviews. Drug discovery* **4**(6):477–88.

D. H. Dube, et al. (2006). 'Regulating Cell Surface Glycosylation with a Small-Molecule Switch'. In *Methods in enzymology*, pp. 213–229.

G. B. J. Dubelaar, et al. (1999). 'Design and first results of CytoBuoy: A wireless flow cytometer for in situ analysis of marine and fresh waters'. *Cytometry* **37**(4):247–254.

M. V. Dwek, et al. (2010). 'A sensitive assay to measure biomarker glycosylation demonstrates increased fucosylation of prostate specific antigen (PSA) in patients with prostate cancer compared with benign prostatic hyperplasia'. *Clinica Chimica Acta* **411**(23-24):1935–1939.

J. R. Dye, et al. (2013). 'The role of microparticles in the pathogenesis of rheumatoid arthritis and systemic lupus erythematosus.'. *Scandinavian journal of immunology* **78**(2):140–8.

M. a. Eddings, et al. (2008). 'Determining the optimal PDMS–PDMS bonding technique for microfluidic devices'. *Journal of Micromechanics and Microengineering* **18**(6):067001.

J. Eeva & J. Pelkonen (2004). 'Mechanisms of B cell receptor induced apoptosis.'. *Apoptosis : an international journal on programmed cell death* **9**(5):525–31.

J. C. Egrie & J. K. Browne (2001). 'Development and characterization of novel erythropoiesis stimulating protein (NESP).'. *Nephrology, dialysis, transplantation : official publication of the European Dialysis and Transplant Association - European Renal Association* **16 Suppl 3**:3–13.

M. R. Elliott & K. S. Ravichandran (2010). 'Clearance of apoptotic cells: implications in health and disease.'. *The Journal of cell biology* **189**(7):1059–70.

S. Elliott (2009). 'Cell Damage due to Hydrodynamic Stress in Fluorescence Activated Cell Sorters'. Tech. rep.

J. Etxebarria, et al. (2012). 'Lectin-array blotting: profiling protein glycosylation in complex mixtures.'. *ACS chemical biology* **7**(10):1729–37.

S. Franz, et al. (2006). 'Lectins Detect Changes of the Glycosylation Status of Plasma Membrane Constituents During Late Apoptosis'. *Cytometry* **69A**:230–239.

S. Franz, et al. (2007). 'After shrinkage apoptotic cells expose internal membrane-derived epitopes on their plasma membranes.'. *Cell death and differentiation* **14**(4):733–42.

H. H. Freeze (2001). 'Lectin analysis of proteins blotted onto filters.'. *Current protocols in molecular biology / edited by Frederick M. Ausubel ... [et al.]* **Chapter 17**(1993):Unit17.7.

H. H. Freeze & M. Aebi (2005). 'Altered glycan structures: the molecular basis of congenital disorders of glycosylation.'. *Current opinion in structural biology* **15**(5):490–8.

H. H. Freeze, et al. (2015). 'Neurological Aspects of Human Glycosylation Disorders'. *Annual Review of Neuroscience* **38**(1):105–125.

H. H. Freeze & R. S. Haltiwanger (2009). 'Other Classes of ER/Golgi-derived Glycans'. In *Essentials of Glycobiology*.

H. H. Freeze & H. Schachter (2009). 'Genetic Disorders of Glycosylation'. In A. Varki, R. D. Cummings, J. Esko, H. Freeze, P. Stanley, C. Bertozzi, G. Hart, & M. Etzler (eds.), *Essentials of Glycobiology*, chap. 42. Cold Spring Harbor Laboratory Press, 2 edn.

Y. Fuchs & H. Steller (2015). 'Live to die another way: modes of programmed cell death and the signals emanating from dying cells'. *Nature Reviews Molecular Cell Biology* **16**(6):329–344.

K. Furukawa, et al. (2001). 'Novel functions of complex carbohydrates elucidated by the mutant mice of glycosyltransferase genes.'. *Biochimica et biophysica acta* **1525**(1-2):1–12.

S. J. Gamblin & J. J. Skehel (2010). 'Influenza Hemagglutinin and Neuraminidase Membrane Glycoproteins'. *Journal of Biological Chemistry* **285**(37):28403–28409.

C. X. Gao, et al. (2005). 'Bisecting GlcNAc mediates the binding of annexin V to Hsp47'. *Glycobiology* **15**(11):1067–1075.

N. Gao & M. A. Lehrman (2006). 'Non-Radioactive Analysis of Lipid-Linked Oligosaccharide Compositions by Fluorophore-Assisted Carbohydrate Electrophoresis'. *Methods in Enzymology* **415**:3–20.

Y. Gavel & G. v. Heijne (1990). 'Sequence differences between glycosylated and non-glycosylated Asn-X-Thr/Ser acceptor sites: implications for protein engineering'. *"Protein Engineering, Design and Selection"* **3**(5):433–442.

P. Gemeiner, et al. (2009). 'Lectinomics'. *Biotechnology Advances* **27**(1):1–15.

H. Ghazarian, et al. (2011). 'A glycobiology review: carbohydrates, lectins and implications in cancer therapeutics.'. *Acta histochemica* **113**(3):236–47.

D. Ghosh, et al. (2004). 'Lectin affinity as an approach to the proteomic analysis of membrane glycoproteins'. *Journal of Proteome Research* **3**(4):841–850.

O. Gornik & G. Lauc (2007). 'Enzyme linked lectin assay (ELLA) for direct analysis of transferrin sialylation in serum samples.'. *Clinical biochemistry* **40**(9-10):718–23.

D. R. Gossett, et al. (2011). 'Sequential array cytometry: multi-parameter imaging with a single fluorescent channel.'. *Annals of biomedical engineering* **39**(4):1328–34.

E. J. Gualda, et al. (2015). 'SPIM-fluid: open source light-sheet based platform for high-throughput imaging'. *Biomedical Optics Express* **6**(11):4447.

C. Guinez, et al. (2004). '70-kDa-heat shock protein presents an adjustable lectinic activity towards O-linked N-acetylglucosamine.'. *Biochemical and biophysical research communications* **319**(1):21–6.

M. T. Guo, et al. (2012). 'Droplet microfluidics for high-throughput biological assays'. *Lab on a Chip* **12**(12):2146.

A. Gustafsson, et al. (2006). 'Carbohydrate-dependent inhibition of Helicobacter pylori colonization using porcine milk'. *Glycobiology* **16**(1):1–10.

J. a. Hanover, et al. (2010). 'The hexosamine signaling pathway: O-GlcNAc cycling in feast or famine.'. *Biochimica et biophysica acta* **1800**(2):80–95.

S. M. Hardy, et al. (2010). 'Glycoprotein microarray for the fluorescence detection of antibodies produced as a result of erythropoietin (EPO) abuse'. *Analytical Methods* **2**(1):17.

G. W. Hart & Y. Akimoto (2009). *The O-GlcNAc Modification.*

I. Häuselmann & L. Borsig (2014). 'Altered Tumor-Cell Glycosylation Promotes Metastasis.'. *Frontiers in oncology* **4**(February):28.

S. N. Hester, et al. (2013). 'Human milk oligosaccharides inhibit rotavirus infectivity in vitro and in acutely infected piglets'. *British Journal of Nutrition* **110**(07):1233–1242.

P. Heyder, et al. (2003). 'Early detection of apoptosis by staining of acid-treated apoptotic cells with FITC-labeled lectin from Narcissus pseudonarcissus.'. *Cytometry. Part A : the journal of the International Society for Analytical Cytology* **55**(2):86–93.

E. Higgins (2010). 'Carbohydrate analysis throughout the development of a protein therapeutic'. *Glycoconjugate Journal* **27**(2):211–225.

J. Hirabayashi (2008). 'Concept, strategy and realization of lectin-based glycan profiling.'. *Journal of biochemistry* **144**(2):139–47.

J. Hirabayashi, et al. (2013). 'Lectin microarrays: concept, principle and applications'. *Chemical Society Reviews* **42**(10):4443.

Y. Hu, et al. (2009). 'Increased enzymatic O-GlcNAcylation of mitochondrial proteins impairs mitochondrial function in cardiac myocytes exposed to high glucose'. *Journal of Biological Chemistry* **284**(1):547–555.

D. W. Huang, et al. (2009a). 'Systematic and integrative analysis of large gene lists using DAVID bioinformatics resources.'. *Nature Protocols* **4**(1):44–57.

D. W. Huang, et al. (2009b). 'Bioinformatics enrichment tools: Paths toward the comprehensive functional analysis of large gene lists'. *Nucleic Acids Research* **37**(1):1–13.

D. Huh, et al. (2005). 'Microfluidics for flow cytometric analysis of cells and particles.'. *Physiological measurement* **26**(3):R73–R98.

A. Imberty & A. Varrot (2008). 'Microbial recognition of human cell surface glycoconjugates.'. *Current opinion in structural biology* **18**(5):567–76.

H. Iwase, et al. (2015). 'Pig kidney graft survival in a baboon for 136 days: longest life-supporting organ graft survival to date'. *Xenotransplantation* pp. 302–309.

J. H. Jang & S. Hanash (2003). 'Profiling of the cell surface proteome.'. *Proteomics* **3**(10):1947–54.

R. U. Jänicke (2009). 'MCF-7 breast carcinoma cells do not express caspase-3'. *Breast Cancer Research and Treatment* **117**(1):219–221.

S. Jiang, et al. (2012). 'A novel lectin from Agrocybe aegerita shows high binding selectivity for terminal N-acetylglucosamine.'. *The Biochemical journal* **443**(2):369–78.

K. Kanninen, et al. (2004). 'Glycosylation changes in Alzheimer's disease as revealed by a proteomic approach'. *Neuroscience Letters* **367**(2):235–240.

D. Keogh, et al. (2014). 'Generating novel recombinant prokaryotic lectins with altered carbohydrate binding properties through mutagenesis of the PA-IL protein from Pseudomonas aeruginosa'. *Biochimica et Biophysica Acta (BBA) - General Subjects* **1840**(6):2091–2104.

G. Kijanka, et al. (2011). *Advanced Biomedical Engineering*. InTech.

G. S. Kijanka, et al. (2014). 'Real-time monitoring of cell migration, phagocytosis and cell surface receptor dynamics using a novel, live-cell opto-microfluidic technique'. *Analytica Chimica Acta* **872**:95–99.

T. R. Kline, et al. (2008). 'ABO, D blood typing and subtyping using plug-based microfluidics'. *Analytical Chemistry* **80**(16):6190–6197.

S. Kobel, et al. (2010). 'Optimization of microfluidic single cell trapping for long-term on-chip culture'. *Lab on a Chip* **10**(7):857.

B. J. Kroesen, et al. (2001). 'Induction of apoptosis through B-cell receptor cross-linking occurs via de novo generated C16-ceramide and involves mitochondria.'. *The Journal of biological chemistry* **276**(17):13606–13614.

A. Kumar & A. Srivastava (2010). 'Cell separation using cryogel-based affinity chromatography.'. *Nature protocols* **5**(11):1737–1747.

A. Kuno, et al. (2005). 'Evanescent-field fluorescence-assisted lectin microarray: a new strategy for glycan profiling.'. *Nature methods* **2**(11):851–6.

R. a. Laine (1997). 'Information capacity of the carbohydrate code'. *Pure and Applied Chemistry* **69**(9):1867–1874.

S. K. Lam & T. B. Ng (2011). 'Lectins: production and practical applications'. *Applied Microbiology and Biotechnology* **89**(1):45–55.

I. M. Lazar, et al. (2011). 'Recent advances in the MS analysis of glycoproteins: Theoretical considerations'. *ELECTROPHORESIS* **32**(1):3–13.

J. O. Lazatin, et al. (1994). 'Fucosylation in cystic fibrosis airway epithelial cells'. *Glycosylation & Disease* **1**(4):263–270.

T. W. Lebien & T. F. Tedder (2008). 'ASH 50th anniversary review B lymphocytes : how they develop and function'. *The american society of hematology* **112**(5):1570–1580.

J. A. Lee, et al. (2008). 'MIFlowCyt: The minimum information about a flow cytometry experiment'. *Cytometry Part A* **73A**(10):926–930.

J. S. Lee, et al. (2012). 'Current state and perspectives on erythropoietin production'. *Applied Microbiology and Biotechnology* **95**(6):1405–1416.

H. Li & M. d'Anjou (2009). 'Pharmacological significance of glycosylation in therapeutic proteins.'. *Current opinion in biotechnology* **20**(6):678–84.

Y. Li, et al. (2011). 'High-throughput lectin microarray-based analysis of live cell surface glycosylation.'. In *Current protocols in protein science / editorial board, John E. Coligan ... [et al.]*, vol. Chapter 12, p. Unit12.9.

L. Lin, et al. (2013). 'Microfluidic cell trap array for controlled positioning of single cells on adhesive micropatterns'. *Lab on a Chip* **13**(4):714.

S.-H. Lin & G. Guidotti (2009). 'Chapter 35 Purification of Membrane Proteins'. In *Methods in enzymology*, pp. 619–629.

F. Liu, et al. (2002). 'Role of glycosylation in hyperphosphorylation of tau in Alzheimer's disease'. *FEBS Letters* **512**(1-3):101–106.

L. Liu (2015). 'Antibody Glycosylation and Its Impact on the Pharmacokinetics and Pharmacodynamics of Monoclonal Antibodies and Fc-Fusion Proteins'. *Journal of Pharmaceutical Sciences* **104**(6):1866–1884.

Q. P. Liu, et al. (2007). 'Bacterial glycosidases for the production of universal red blood cells.'. *Nature biotechnology* **25**(4):454–464.

H. Lu, et al. (2004). 'Microfluidic shear devices for quantitative analysis of cell adhesion'. *Analytical Chemistry* **76**(18):5257–5264.

E. Lugli, et al. (2010). 'Data analysis in flow cytometry: The future just started'. *Cytometry Part A* **77**(7):705–713.

B. Y. Ma, et al. (2009). 'The lectin Jacalin induces human B-lymphocyte apoptosis through glycosylation-dependent interaction with CD45.'. *Immunology* **127**(4):477–88.

J. Ma & G. W. Hart (2014). 'O-GlcNAc profiling: from proteins to proteomes.'. *Clinical proteomics* **11**(1):8.

J. Ma, et al. (2015). 'O-GlcNAcomic Profiling Identifies Widespread O-GlcNAcylation in Oxidative Phosphorylation System Regulating Cardiac Mitochondrial Function'. *Journal of Biological Chemistry* p. jbc.M115.691741.

J. D. Marth & P. K. Grewal (2008). 'Mammalian glycosylation in immunity.'. *Nature reviews. Immunology* **8**(11):874–87.

D. a. McClain, et al. (2002). 'Altered glycan-dependent signaling induces insulin resistance and hyperleptinemia.'. *Proceedings of the National Academy of Sciences of the United States of America* **99**(16):10695–9.

H. M. Meesmann, et al. (2010). 'Decrease of sialic acid residues as an eat-me signal on the surface of apoptotic lymphocytes.'. *Journal of cell science* **123**(Pt 19):3347–56.

J. S. Mellors, et al. (2010). 'Integrated Microfluidic Device for Automated Single Cell Analysis Using Electrophoretic Separation and Electrospray Ionization Mass Spectrometry' **82**(3):967–973.

M. C. Merckel, et al. (2003). 'The Structural Basis of Receptor-binding by Escherichia coli Associated with Diarrhea and Septicemia'. *Journal of Molecular Biology* **331**(4):897–905.

I. Meyvantsson & D. J. Beebe (2008). 'Cell culture models in microfluidic systems.'. *Annual review of analytical chemistry (Palo Alto, Calif.)* **1**:423–49.

S. Miltenyi, et al. (1990). 'High gradient magnetic cell separation with MACS.'. *Cytometry* **11**(2):231–238.

K. W. Moremen, et al. (2012). 'Vertebrate protein glycosylation: diversity, synthesis and function'. *Nature Reviews Molecular Cell Biology* **13**(7):448–462.

B. Mulloy, et al. (2009). *Structural Analysis of Glycans*.

P. Nacharaju, et al. (2005). 'Surface decoration of red blood cells with maleimidophenyl-polyethylene glycol facilitated by thiolation with iminothiolane: An approach to mask A, B, and D antigens to generate universal red blood cells'. *Transfusion* **45**(3):374–383.

O. W. Nadeau & G. M. Carlson (2007). 'Protein Interactions Captured by Chemical Cross-linking: One-Step Cross-linking with Formaldehyde'. *Cold Spring Harbor Protocols* **2007**(8):pdb.prot4634–pdb.prot4634.

S. Nagrath, et al. (2007). 'Isolation of rare circulating tumour cells in cancer patients by microchip technology'. *Nature* **450**(7173):1235–1239.

Y. Nakayama, et al. (2013). 'Genetic Disorders'. In M. Puiu (ed.), *Genetic Disorders*, pp. 243–269. InTech.

J. Nilsson, et al. (2013). 'Targeting the glycoproteome'. *Glycoconjugate Journal* **30**(2):119–136.

N. O'Donnell, et al. (2004). 'Ogt-dependent X-chromosome-linked protein glycosylation is a requisite modification in somatic cell function and embryo viability.'. *Molecular and cellular biology* **24**(4):1680–90.

N. A. of Sciences, et al. (2012). 'Transforming Glycoscience: A Roadmap for the Future'. Tech. rep.

H. Ohto & K. E. Nollet (2011). 'Overview on platelet preservation: Better controls over storage lesion'. *Transfusion and Apheresis Science* **44**(3):321–325.

K. Ohtsubo & J. D. Marth (2006). 'Glycosylation in cellular mechanisms of health and disease.'. *Cell* **126**(5):855–67.

C. Oliveira, et al. (2012). 'Recombinant lectins: an array of tailor-made glycan-interaction biosynthetic tools'. *Critical Reviews in Biotechnology* **33**(February 2012):1–15.

M. L. Olsson & H. Clausen (2008). 'Modifying the red cell surface: Towards an ABO-universal blood supply'. *British Journal of Haematology* **140**(1):3–12.

T. M. O'Connell, et al. (2014). 'Sequential Glycan Profiling at Single Cell Level with the Microfluidic Lab-in-a-Trench Platform'. *Lab on a Chip* .

S. Park, et al. (2010). 'Array-based analysis of secreted glycoproteins for rapid selection of a single cell producing a glycoprotein with desired glycosylation'. *Analytical Chemistry* **82**(13):5830–5837.

D. S. Pisetsky, et al. (2012). 'Microparticles as mediators and biomarkers of rheumatic disease.'. *Rheumatology (Oxford, England)* **51**(10):1737–46.

M. E. Piyasena & S. W. Graves (2014). 'The intersection of flow cytometry with microfluidics and microfabrication'. *Lab on a Chip* **14**(6):1044.

I. O. Potapenko, et al. (2010). 'Glycan gene expression signatures in normal and malignant breast tissue; possible role in diagnosis and progression.'. *Molecular oncology* **4**(2):98–118.

X.-M. Ren, et al. (2015). 'Structural Basis of Specific Recognition of Non-Reducing Terminal N-Acetylglucosamine by an Agrocybe aegerita Lectin'. *Plos One* **10**(6):e0129608.

E. I. Rigopoulou, et al. (2012). 'Asialoglycoprotein receptor (ASGPR) as target autoantigen in liver autoimmunity: lost and found.'. *Autoimmunity reviews* **12**(2):260–9.

C. D. Rillahan & J. C. Paulson (2011). 'Glycan microarrays for decoding the glycome.'. *Annual review of biochemistry* **80**:797–823.

G. T. Roman, et al. (2006). 'Single-cell manipulation and analysis using microfluidic devices'. *Analytical and Bioanalytical Chemistry* **387**(1):9–12.

J. Roth (2011). 'Lectins for histochemical demonstration of glycans'. *Histochemistry and cell biology* **136**(2):117–30.

A. C. Rowat, et al. (2009). 'Tracking lineages of single cells in lines using a microfluidic device.'. *Proceedings of the National Academy of Sciences of the United States of America* **106**(43):18149–54.

B. Roy, et al. (2014). 'On-chip lectin microarray for glycoprofiling of different gastritis types and gastric cancer'. *Biomicrofluidics* **8**(3):034107.

N. Saady (2011). 'No Title'. *J. Appl. Sci. Environ. Sanitation* **6**(3):309–15.

S. Saarela, et al. (1996). 'The GafD protein of the G (F17) fimbrial complex confers adhesiveness of Escherichia coli to laminin.'. *Infection and immunity* **64**(7):2857–60.

F. Schwarz & M. Aebi (2011). 'Mechanisms and principles of N-linked protein glycosylation.'. *Current opinion in structural biology* **21**(5):576–82.

A. Seifinejad, et al. (2010). 'Generation of human induced pluripotent stem cells from a Bombay individual: Moving towards "universal-donor" red blood cells'. *Biochemical and Biophysical Research Communications* **391**(1):329–334.

N. Sethuraman & T. A. Stadheim (2006). 'Challenges in therapeutic glycoprotein production.'. *Current opinion in biotechnology* **17**(4):341–6.

H. M. Shapiro & W. G. Telford (2009). 'Lasers for Flow Cytometry'. *Current Protocols in Cytometry* (July):1–17.

N. Sharon (2006). 'Carbohydrates as future anti-adhesion drugs for infectious diseases.'. *Biochimica et biophysica acta* **1760**(4):527–37.

G. Simone (2014). 'Can Microfluidics boost the Map of Glycome Code?'. *Journal of Glycomics & Lipidomics* **04**(02):1–9.

A. M. Skelley, et al. (2009). 'Microfluidic control of cell pairing and fusion.'. *Nature methods* **6**(2):147–52.

S. M. Smith (2011). 'Strategies for the Purification of Membrane Proteins'. In D. Walls & S. T. Loughran (eds.), *Protein Chromatography*, chap. 29, pp. 485–496. Humana Press, 1 edn.

M. M. St. Amand, et al. (2014). 'Controllability Analysis of Protein Glycosylation in Cho Cells'. *PLoS ONE* **9**(2):e87973.

P. Stanley & R. D. Cummings (2009). 'Structures Common to Different Glycans'. In *Essentials of Glycobiology*.

P. Stanley, et al. (2009). 'N-Glycans'. In *Essentials of Glycobiology*.

L. I. Stoykova, et al. (2003). 'Alpha1,3fucosyltransferases in cystic fibrosis airway epithelial cells.'. *Biochimie* **85**(3-4):363–7.

H. Streicher & N. Sharon (2003). 'Recombinant plant lectins and their mutants.'. *Methods in enzymology* **363**:47–77.

K. H. Sun, et al. (1996). 'The expression of acidic ribosomal phosphoproteins on the surface membrane of different tissues in autoimmune and normal mice which are the target molecules for anti-double-stranded DNA antibodies.'. *Immunology* **87**(3):362–71.

T. Taki, et al. (1994). 'Bloting of glycolipids and phospholipids from a HP-TLC to a PVDF membrane'.

K. Tanabe, et al. (2006). 'A cytoplasmic peptide: N-glycanase'. In *Methods in enzymology*, pp. 46–55.

H. Tateno, et al. (2007). 'A novel strategy for mammalian cell surface glycome profiling using lectin microarray.'. *Glycobiology* **17**(10):1138–46.

N. J. Thompson, et al. (2013). 'The impact of mass spectrometry on the study of intact antibodies: from post-translational modifications to structural analysis'. *Chem. Commun.* **49**(6):538–548.

R. Thompson, et al. (2011). 'Optimization of the enzyme-linked lectin assay for enhanced glycoprotein and glycoconjugate analysis.'. *Analytical biochemistry* **413**(2):114–22.

C. R. Torres & G. W. Hart (1984). 'Topography and polypeptide distribution of terminal N-acetylglucosamine residues on the surfaces of intact lymphocytes. Evidence for O-linked GlcNAc'. *Journal of Biological Chemistry* **259**(5):3308–3317.

D. Ungar (2009). 'Golgi linked protein glycosylation and associated diseases.'. *Seminars in cell & developmental biology* **20**(7):762–9.

M. van Engeland, et al. (1998). 'A review on an apoptosis detection system based on phosphatidyserine exposure' **31**:1–9.

G. Vandenborre, et al. (2011). 'Plant lectins as defense proteins against phytophagous insects'. *Phytochemistry* **72**(13):1538–1550.

D. Vanderschaeghe, et al. (2010). 'Glycome profiling using modern glycomics technology: technical aspects and applications'. *Biological Chemistry* **391**(2/3):149–161.

A. Varki, et al. (eds.) (2009a). *Essentials of Glycobiology*. Cold Spring Harbor Laboratory Press, 2nd editio edn.

A. Varki, et al. (2009b). *Discovery and Classification of Glycan-Binding Proteins*.

A. Varki & J. B. Lowe (2009). 'Biological Roles of Glycans'. In *Essentials of Glycobiology*.

A. Vasconcelos-dos Santos, et al. (2015). 'Biosynthetic Machinery Involved in Aberrant Glycosylation: Promising Targets for Developing of Drugs Against Cancer'. *Frontiers in Oncology* **5**(June):1–23.

D. A. L. Vickers, et al. (2011). 'Lectin-mediated microfluidic capture and release of leukemic lymphocytes from whole blood'. *Biomedical Microdevices* **13**(3):565–571.

D. a. L. Vickers, et al. (2012). 'Lectin-functionalized microchannels for characterizing pluripotent cells and early differentiation.'. *Biomicrofluidics* **6**(2):24122–2412210.

K. Vosseller, et al. (2002). 'Elevated nucleocytoplasmic glycosylation by O-GlcNAc results in insulin resistance associated with defects in Akt activation in 3T3-L1 adipocytes.'. *Proceedings of the National Academy of Sciences of the United States of America* **99**(8):5313–8.

C. Wacker, et al. (2011). 'Glycosylation profiles of therapeutic antibody pharmaceuticals.'. *European journal of pharmaceutics and biopharmaceutics : official journal of Arbeitsgemeinschaft für Pharmazeutische Verfahrenstechnik e.V* **79**(3):503–7.

E. Wagner-Rousset, et al. (2008). 'The way forward, enhanced characterization of therapeutic antibody glycosylation: Comparison of three level mass spectrometry-based strategies'. *Journal of Chromatography B* **872**(1-2):23–37.

P. Walian, et al. (2004). 'No Title'. *Genome Biology* **5**(4):215.

H. H. Wandall, et al. (2008). 'Galactosylation does not prevent the rapid clearance of long-term, 4 °C-stored platelets'. *Blood* **111**(6):3249–3256.

F.-L. Wang, et al. (2009). 'High expression of alpha 2, 3-linked sialic acid residues is associated with the metastatic potential of human gastric cancer.'. *Cancer detection and prevention* **32**(5-6):437–43.

H. Wang, et al. (2008). 'Imaging glycosylation.'. *Journal of the American Chemical Society* **130**(26):8154–5.

J. Wang, et al. (2011). 'dbOGAP - An Integrated Bioinformatics Resource for Protein O-GlcNAcylation'. *BMC Bioinformatics* **12**(1):91.

Y. Wang, et al. (2001). 'Modeling human congenital disorder of glycosylation type IIa in the mouse: conservation of asparagine-linked glycan-dependent functions in mammalian physiology and insights into disease pathogenesis.'. *Glycobiology* **11**(12):1051–1070.

M. Ward, et al. (2009). 'Fundamentals of Acoustic Cytometry'. *Current Protocols in Cytometry* (July):1–12.

J. C. Weaver (1995). 'Electroporation Theory'. *Methods in Molecular Biology* **28**:3–28.

L. Wells, et al. (2002). 'Dynamic O- Glycosylation of Nuclear and Cytosolic Proteins'. *Journal of Biological Chemistry* **277**(3):1755–1761.

V. R. Wiersma, et al. (2015). 'Mechanisms of Translocation of ER Chaperones to the Cell Surface and Immunomodulatory Roles in Cancer and Autoimmunity.'. *Frontiers in oncology* **5**(January):7.

J. C. S. Wood (2009). 'Establishing and Maintaining System Linearity'. *Current Protocols in Cytometry* (January):1–14.

W. Xu, et al. (2010). 'Lectin binding assays for in-process monitoring of sialylation in protein production'. *Mol.Biotechnol.* **45**(1559-0305 (Electronic)):248–256.

J. Xue, et al. (2013). 'Regulation of galectin-3-induced apoptosis of Jurkat cells by both O-glycans and N-glycans on CD45.'. *FEBS letters* **587**(24):3986–94.

Z. Ye & J. D. Marth (2004). 'N-glycan branching requirement in neuronal and postnatal viability.'. *Glycobiology* **14**(6):547–58.

H. Yin & D. Marshall (2012). 'Microfluidics for single cell analysis'. *Current Opinion in Biotechnology* **23**(1):110–119.

A. Yoshida, et al. (2001). 'Muscular dystrophy and neuronal Migration disorder caused by mutations in a glycosyltransferase, POMGnT1'. *Developmental Cell* **1**(5):717–724.

T. Yue & B. B. Haab (2009). 'Microarrays in Glycoproteomics Research'. *Clinics in Laboratory Medicine* **29**(1):15–29.

N. E. Zachara & G. W. Hart (2006). 'Cell signaling, the essential role of O-GlcNAc!'. *Biochimica et biophysica acta* **1761**(5-6):599–617.

J. Zhao, et al. (2007). 'Glycoprotein microarrays with multi-lectin detection: unique lectin binding patterns as a tool for classifying normal, chronic pancreatitis and pancreatic cancer sera'. *Journal of proteome ...* **6**(5):1864–1874.

T. Zheng, et al. (2005). 'Lectin arrays for profiling cell surface carbohydrate expression.'. *Journal of the American Chemical Society* **127**(28):9982–3.

T. Zheng, et al. (2007). 'Lectin-modified microchannels for mammalian cell capture and purification.'. *Biomedical microdevices* **9**(4):611–7.

M. Zirngibl, et al. (2014). 'Loading of nuclear autoantigens prototypically recognized by SLE sera into late apoptotic vesicles requires intact microtubules and MLCK activity.'. *Clinical and experimental immunology* pp. 1–29.

Appendix A

Outputs

A.1 Publications

A.1.1 Journal Articles

Sequential Glycan Profiling at Single Cell Level with the Microfluidic Lab-in-a-Trench Platform

Accepted to *Lab on a Chip* on 18th July 2014.

Authors: Tríona O'Connell [1,2], Damien King [3], Chandra K. Dixit [3,4], Brendan O'Connor [1,2], Dermot Walls [1,2], Jens Ducrée [3,4]

1. School of Biotechnology, Dublin City University
2. Irish Separation Science Cluster, Dublin City University
3. School of Physics, Dublin City University
4. Biomedical Diagnostics Institute, Dublin City University

Abstract: It is now widely recognised that the earliest changes that occur on a cell when it is stressed or becoming diseased are alterations in its surface glycosylation. Current state-of-the-art technologies in glycoanalysis include mass spectrometry, protein microarray formats, techniques in cytometry and more recently, glycoquantitative polymerase chain reaction (Glyco-qPCR). Techniques for the glycoprofiling of the surfaces of single cells are either limited to the analysis of large cell populations or are unable to handle multiple and / or sequential probing. Here, we report a novel approach of single live cell glycoprofiling enabled by the microfluidic "Lab-in-a-Trench" (LiaT) platform for performing capture and retention of cells,

along with shear-free reagent loading. The significant technical improvement on state-of-the-art is the demonstration of consecutive profiling of glycans on a single cell by sequential elution of the previous lectin probe using their corresponding free sugar. We have qualitatively analysed glycan density on the surface of individual cells. This has allowed us to qualitatively co-localise the observed glycans. This approach enables exhaustive glycoprofiling and glycan mapping on the surface of individual live cells with multiple lectins. The possibility of sequentially profiling glycans on cells will be a powerful new tool to add to current glycoanalytical techniques. The LiaT platform will enable cell biologists to perform many high sensitivity assays and also will also make a significant impact on biomarker research.

A portable centrifugal analyser for liver function screening

Accepted to *Biosensors and Bioelectronics* on 17th January 2014.

*Authors:*Charles E. Nwankire [1,2], Monika Czugala[3], Robert Burger [1,2], Kevin J. Fraser [3], Tríona M. O'Connell [1], Thomas Glennon [1],Blessing E. Onwuliri [4,5],Isikaku E. Nduaguibe [5],Dermot Diamond [3],Jens Ducrée [1,2]

1. Biomedical Diagnostics Institute, National Centre for Sensor Research, Dublin City University, Ireland
2. School of Physical Sciences, Dublin City University, Ireland
3. INSIGHT: Centre for Data Analytics, National Centre for Sensor Research, Dublin City University, Ireland
4. PEPFAR Centralised Laboratory, Abia State University Teaching Hospital, Aba, Nigeria
5. Department of Chemical Pathology, Abia State University Teaching Hospital, Aba, Nigeria a

Abstract: Mortality rates of up to 50 % have been reported after liver failure due to drug-induced hepatotoxicity and certain viral infections (Gao et al., 2008). These adverse conditions frequently affect HIV and tuberculosis patients on regular medication in resource-poor settings. Here, we report full integration of sample preparation with the read-out of a 5-parameter liver assay panel (LAP) on a portable, easy-to-use, fast and cost-efficient centrifugal microfluidic analysis system (CMAS). Our unique, dissolvable-film based centrifugo-pneumatic valving was employed to provide sample-to-answer fashion automation for plasma extraction (from finger-prick of

blood), metering and aliquoting into separate reaction chambers for parallelized colorimetric quantification during rotation. The entire LAP completes in less than 20min while using only a tenth the reagent volumes when compared with standard hospital laboratory tests. Accuracy of in-situ liver function screening was validated by 96 separate tests with an average coefficient of variance (CV) of 7.9 % compared to benchtop and hospital lab tests. Unpaired two sample statistical t-tests were used to compare the means of CMAS and benchtop reader, on one hand; and CMAS and hospital tests on the other. The results demonstrate no statistical difference between the respective means with 94 % and 92 % certainty of equivalence, respectively. The portable platform thus saves significant time, labour and costs compared to established technologies, and therefore complies with typical restrictions on lab infrastructure, maintenance, operator skill and costs prevalent in many field clinics of the developing world. It has been successfully deployed to a centralised lab in Nigeria.

A.1.2 Conference presentations

Irish Cytometry Society Annual meeting

University College Dublin. 25th - 26th February 2014.

Poster Title: A novel method for glycoprofiling live cells using Lab in a Trench

Authors: Tríona M. O'Connell [1,2], Damien King [3], Chandra K. Dixit [3,4], Brendan O'Connor [1,2], Dermot Walls [1,2], Jens Ducrée [3,4]

1. School of Biotechnology, Dublin City University
2. Irish Separation Science Cluster, Dublin City University
3. School of Physics, Dublin City University
4. Biomedical Diagnostics Institute, Dublin City University

Abstract:

Lab in a Trench (LiaT) is a microfluidic system that allows repeated probing of cells captured in a shear-free environment. We have demonstrated a novel method of sequentially glycoprofiling live B-cells using LiaT and an epifluorescent microscope. Lectins are carbohydrate binding proteins that can identify specific glycans on a cell surface. Cells were captured with LiaT and incubated in appropriate buffer. Commercially available plant lectins

were labelled with DyLight 488, introduced into the system and allowed time to bind to the cells. These lectins were then eluted using the appropriate free sugar and further lectins were used to probe the cell.Lab in a Trench analyses can be carried out in parallel, with the analysis of up to four trenches of cells at a time. Each trench captures between 5 and 30 cells. The compact platform is compatible with standard laboratory reagents and microscopes. Measurements of the cell fluorescence were taken at various timepoints after addition of the lectin probe and its elution by sugar. Images were analysed using ImageJ. Sequential images were overlaid to demonstrate localisation of the lectins and the glycans to which they bind. Image analysis allows semi-quantitative comparison of glycan density on cells. This is the first demonstration of sequential analysis of glycan distribution on the surface of live cells.

CYTO 2015 - 30th Congress of the International Society for Advancement of Cytometry

Glasgow, Scotland. June 26 - 30, 2015.

Poster Title: Observing surface glycosylation changes on apoptotic B-cells using the lab in a trench platform

Authors: Tríona M. O'Connell [1,2], Damien King [3], Chandra K. Dixit [3,4], Brendan O'Connor [1,2], Jens Ducrée [3,4], Dermot Walls [1,2]

1. School of Biotechnology, Dublin City University
2. Irish Separation Science Cluster, Dublin City University, Glasnevin, Dublin 9, Ireland
3. School of Physics, Dublin City University, Glasnevin, Dublin 9, Ireland
4. Biomedical Diagnostics Institute, Dublin City University , Glasnevin, Dublin 9, Ireland

Abstract:

Lab in a Trench (LiaT) is a microfluidic system that allows repeated probing of cells captured in a shear-free environment. We have demonstrated a novel method of sequentially glycoprofiling live B-cells using LiaT and an epifluorescent microscope. Lectins are carbohydrate binding proteins that can identify specific glycans on a cell surface.

Cells were captured with LiaT and incubated in appropriate buffer. Commercially available plant lectins were labelled with compatible fluor-

phores, introduced into the system and allowed time to bind to the cells. These lectins can then be eluted using the appropriate free sugar and further lectins were used to probe the cell.

Lab in a Trench analyses can be carried out in parallel, with the analysis of up to four trenches of cells at a time. Each trench captures between 5 and 30 cells. The compact platform is compatible with standard laboratory reagents and microscopes.

Measurements of the cell fluorescence were taken at various timepoints after addition of the lectin probe and its elution by sugar. Images were analysed using ImageJ. Sequential images were overlaid to demonstrate localisation of the lectins and the glycans to which they bind. Image analysis allows semi-quantitative comparison of glycan density on cells.

By inducing apoptosis while cells are in the trenches, the lectin binding profile of the cells can be monitored in real time. It has been reported (Meesmann, 2010) that de-sialyation of cell surface glycans exposes terminal N-acetylglucosamine. Here, we can probe this exposure of terminal GlcNAc as we observe the cells in the trench. Confirmation of this lectin specificity can be controlled by eluting the lectins with free GlcNAc.

References: H. M. Meesmann et al., Journal of cell science 123, 3347-3356 (2010).

Society for Glycobiology Annual Meeting

San Francisco. December 1-4th, 2015.

Poster Title: Lab in a Trench: a flexible microfluidic system for single cell imaging using lectins

Authors: Tríona M. O'Connell [1,2], Arnaud Coudray[3,4] , Damien King [3], Laura Santana González [3,4], Jens Ducrée [3,4], Brendan O'Connor [1,2], Dermot Walls [1,2]

1. School of Biotechnology, Dublin City University, Glasnevin, Dublin 9, Ireland
2. Irish Separation Science Cluster, Dublin City University, Glasnevin, Dublin 9, Ireland
3. School of Physics, Dublin City University, Glasnevin, Dublin 9, Ireland
4. Biomedical Diagnostics Institute, Dublin City, Glasnevin, Dublin 9, Ireland University

Abstract:

Lab in a Trench is a microfluidic platform that captures cells by a gravity dependant principle. Cells captured in the trench are in shear free conditions and can be probed by simply flowing labels into the system. We have previously demonstrated a method for sequentially labelling single cells with fluorophore labelled lectins [1], and have extended the system to demonstrate the binding patterns of lectins to cells before and after fixation. We have also used the system to induce apoptosis in the trench and monitor the binding rate of GSL II in comparison to propidium iodide uptake.

Cell surface glycosylation is often examined using fluorescently labelled lectins. By labelling the cells with lectin and then eluting with free sugar, the image of the labelled live cell can be captured. The cell can then be fixed with a variety of fixing agents, including 4 % formaldehyde, and then reprobed in order to compare the binding patterns of lectins on the same cell surface. This allows a mix of live and fixed assays to be carried out on the same cell, while understanding some of the changes in binding that may occur after fixation.

Captured cells can also be treated and monitored for surface changes over time. B-lymphocytes are captured in the trench and induced to apoptose using anti-IgM. Stains such as propidium iodide and labelled lectins are then flowed through the system and their rate of binding monitored.

[1] O'Connell, Tríona M., et al. "Sequential glycan profiling at single cell level with the microfluidic lab-in-a-trench platform: a new era in experimental cell biology." Lab on a Chip 14.18 (2014): 3629-3639.

Society for Glycobiology Annual Meeting

San Francisco. December 1-4th, 2015.

Poster Title: O-linked β-N-acetylglucosamine is exposed on the surface of B-lymphocytes in late apoptosis

Authors: Tríona M. O'Connell [1,2], Ruth LArragy [1,2], ,Grainne O'Keefe [3],,Seán Doyle[3], Brendan O'Connor [1,2], Dermot Walls [1,2]

1. School of Biotechnology, Dublin City University, Glasnevin, Dublin 9, Ireland
2. Irish Separation Science Cluster, Dublin City University, Glasnevin, Dublin 9, Ireland

3. Maynooth University Department of Biology, Maynooth University, Maynooth, Co. Kildare,
   Ireland

Abstract:

It is known that apoptosis induces changes in the surface glycosylation of cells. In particular, exposure of terminal N-acetylglucosamine (GlcNAc) is characteristic of late apoptosis. Using the bacterial lectin GafD, and flow cytometry, we have demonstrated the exposure of O-linked β- GlcNAc in late apoptosis.

Ramos cells (ATCC no. CRL-1596), a B cell line of Burkitt's lymphoma origin, were used as a model of apoptosis. Anti-IgM binds to the B cell receptor, and in the absence of co-signalling by CD40, induces apoptosis in the cells.

GafD, a fimbrial protein from E. coli with O-β-GlcNAc binding specificity, was biotinylated and labelled with streptavidin conjugated BV421 (BioLegend). Confirmation of binding specificity was carried out by inhibiting lectin binding using free GlcNAc.

Apoptotic cells were incubated with BV421 GafD for 30 minutes, washed, and labelled with Annexin V-FITC and propidium iodide(BD Biosciences). Cells were then measured on a BD FACS Aria and analysed with FlowJo. A sub population of late apoptotic cells were identified that were positive for GafD labelling.

These cells exhibiting GafD binding were isolated through cell sorting. As O-β-GlcNAc is a common intracellular sugar residue, it was necessary to isolate the outer membrane of the cells by ultracentrifugation in order to identify the O-β-GlcNAc bearing protein. Membrane proteins were analysed by western blot and the relevant GafD binding proteins excised from matching gels for identification by mass spectrometry.

A.2 Outreach Activities

Represented Irish Science Separation Cluster at the national finals of Thesis in Three (2012) with "Sugar Coated Cells".

Delivered a public talk on my work at Pint of Science 2014, PubhD Dubin (April 2015) and at Soapbox Science Belfast 2015.

National finalist in FameLab competition in 2013 and 2014.

Appendix B

Lectins

Table B.1: Lectin specificities

Lectin	**Specificity**	**Mol. Wt.**	**Inhibiting Sugar**
ConA	α-mannose, α-glucose	104 kDa	Mannose
ECL	Galβ4GlcNAc	54 kDa	Lactose
LCA	α-mannose, α-glucose	50 kDa	Mannose
NPL	α-mannose	59 kDa	Mannose
WGA	GlcNAc	36 kDa	GlcNAc
GSL II	α or β GlcNAc	113 kDa	GlcNAc

Appendix C

Materials

C.1 Common Buffers

C.1.1 10X TBS

- 24 g Tris Base
- 88 g NaCl

Dissolve in 800 mL dH_20. Adjust pH to 7.4 with HCl. Add dH_2O to a final volume of 1 L.

C.1.2 1X TBST

Dilute 1 part 10X TBS in 9 parts dH_2O, autoclave if needed. Add 0.1 % Tween-20 and mix.

C.1.3 PBS

C.2 SDS-PAGE

C.2.1 1.5M Tri HCl pH 8.3

- 157.6 g Tris HCl

Dissolve Tris HCl in 180 mL dH_2O. Adjust pH to 8.3. Add dH_2O to a final volume of 200 mL.

C.2.2 0.5M Tris HCl pH 6.8

- 3.94 g Tris HCl

Dissolve in 45 mL dH_2O. Adjust pH to 6.8 with HCl. Make up to 50 mL with dH_2O

C.2.3 Laemelli buffer (6X)

- 7 mL 0.5 M Tris 6.8
- 3 mL Glycerol
- 1 g SDS
- 50 μL Bromophenol Blue (2.5 % stock solution)

Mix well and store at room temperature.

To use add 18.6 g DTT per 200 μL or 12 μL beta mercaptoethanol per 108 μL of buffer. Add the reducing agent fresh on the day of use.

C.2.4 SDS PAGE running buffer (10X)

- 30 g Tris
- 144 g glycine
- 100 mL 10 % SDS

Mix well and make up to 1 L with dH_2O. Leave the stock solution stirring until it has fully dissolved. Make up 1 part to 9 parts dH_2O for working solution.

C.2.5 Coomassie Stain

- 45 mL methanol
- 10 mL glacial acetic acid
- 45 mL dH_2O
- 300 mg Coomassie Brilliant Blue R250

Add the acetic acid to the dH_2O. Dissolve the Coomassie in methanol before mixing with the water and acetic acid. Filter and store. Coomassie stain can be recycled.

C.2.6 Coomassie Destain

- 225 mL methanol
- 50 mL glacial acetic acid
- 225 mL dH_2O

Add the acid to the water, then add the methanol. Discard appropriately after destaining of the gels.

C.2.7 Colloidal Coomassie stain

- 20 g O-Phosphoric Acid
- 100 g Ammonium Sulphate
- 1 g Coomassie Brilliant Blue G-250

Dissolve the phosphoric acid and ammonium sulphate in 800 mL of dH_2O. Add the Coomassie while stirring. Make up to 1L with dH_2O and allow the stock solution to stir for at least 24 hours.

Immediately before use, make a working solution by diluting four parts of stock solution to one part of methanol.

C.2.8 IPG strip rehydration buffer

- 7 M Urea
- 2 M Thiourea
- 2 % w/v CHAPS
- 0.002 % w/v Bromophenol blue
- 20mM DTT (added just prior to use)
- 0.5 % v/v IPG carrier ampholytes 3-10

C.2.9 IPG strip equilibration buffer

- 50 mM Tris
- 6 M Urea
- 30 % w/v Glycerol
- 2 % w/v SDS
- 0.002 % w/v Bromophenol blue

Mixed and pH to 8.8.

C.3 Western Blot

C.3.1 Semi-Dry transfer buffer

- 2.9 g Glycine
- 5.8 g Tris Base
- 3.7 mL 10 % w/v SDS
- 800 mL dH_2O
- 200 mL methanol

Dissolve the glycine and Tris in the dH_2O and SDS. Add the methanol. Mix well and store at 4 °C .

C.4 Cell Culture materials

C.4.1 Heat inactivation of Serum

Serum is defrosted at 37 °C in a water bath until there is no ice remaining. The serum is then removed from the bath which is set to 56 °C . When the bath has reached temperature, the serum is placed in the bath for 30 minutes with occasional agitation.

The serum is then filtered to remove any particulates. The filtered, heat inactivated serum is aliquoted into 50 mL and stored at -20 °C .

C.4.2 Freezing stock solution

- 5 mL DMSO
- 10 mL heat inactivated FBS
- 35mL RPMI 1640 (freshly supplemented)

Mix well and filter sterilise through a 0.2 μm syringe filter. Aliquot into 10 mL and freeze at -20 °C until required.

Appendix D

Data

D.1 Flow Cytometry Plots

D.1.1 Supplementary Flow for LiaT paper

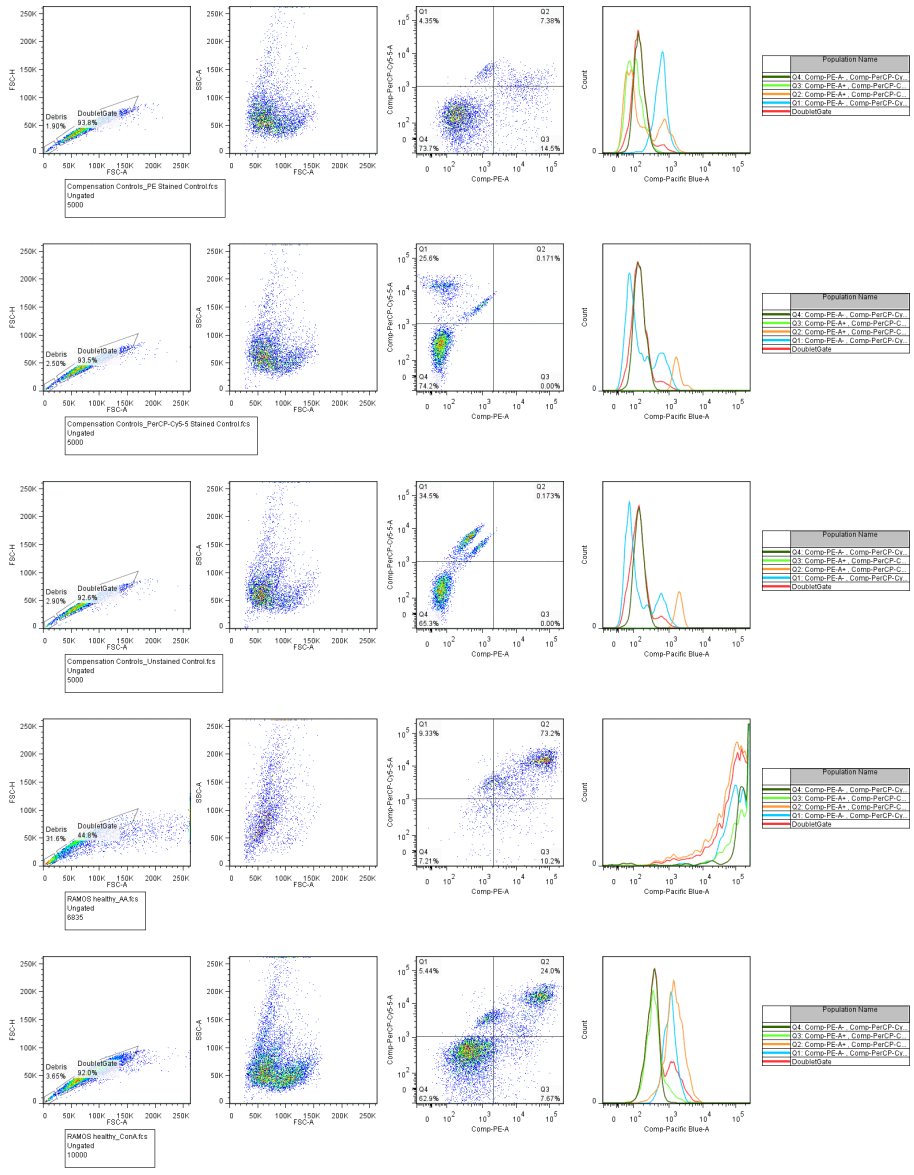

Figure D.1: Measuring apoptosis of untreated cells alongside various lectins. Cells were stained with Annexin V-PE and 7AAD to determine apoptotic state. Lectins were labelled with BD V450.

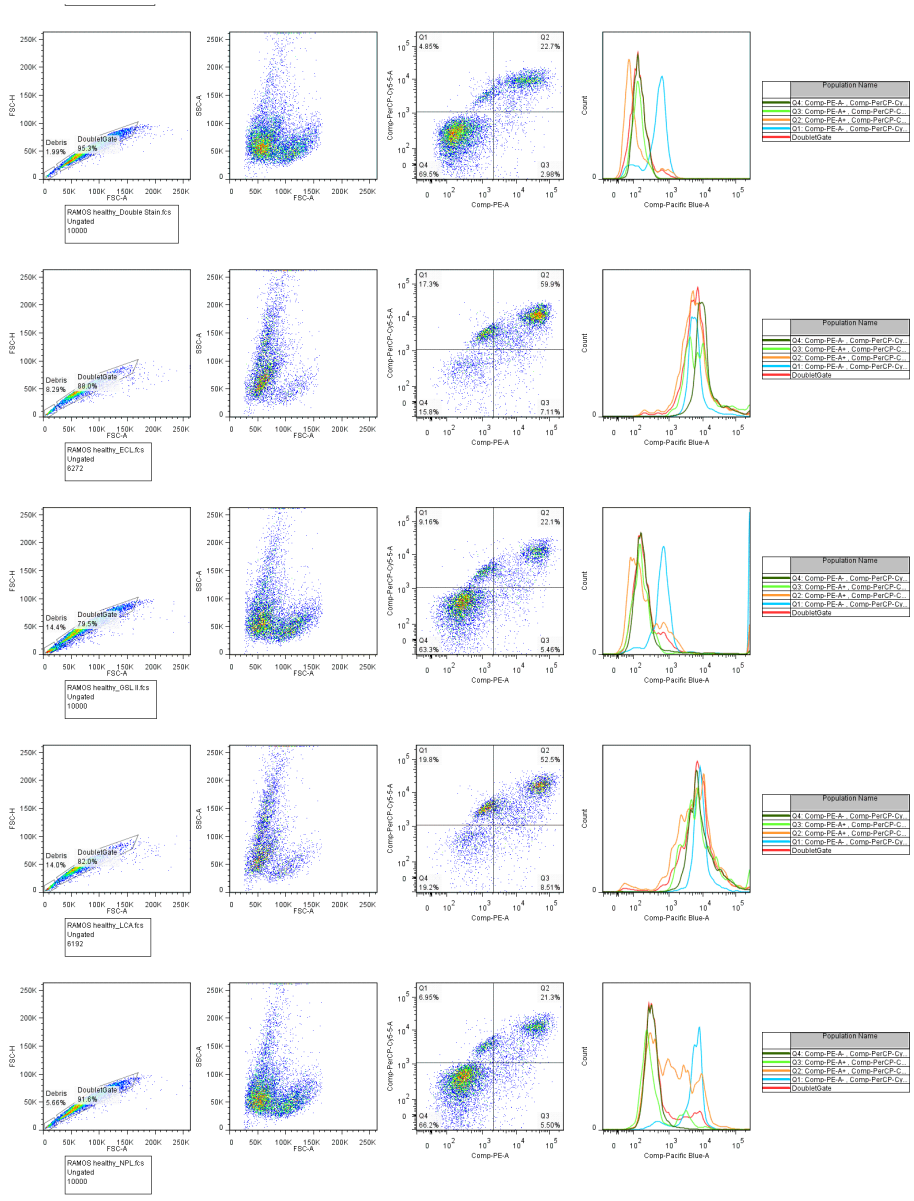

Figure D.1 continued.

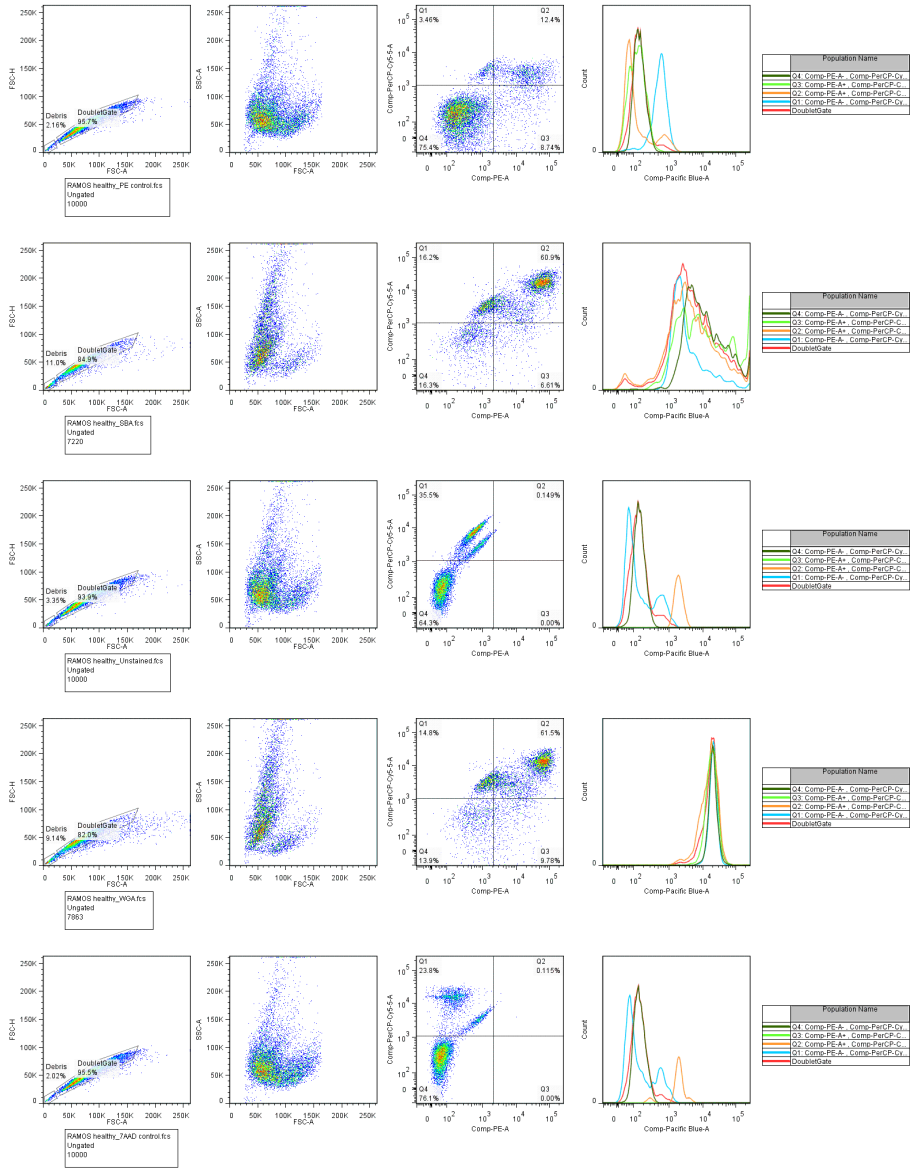

Figure D.1 continued.

D.2 Proteomic Data

Table D.1: List of all proteins identified in mass spectrometry (exclusive of keratins), correlated with gel piece number, PMID where the protein is known to be O-GlcNAcylated (PMID) and Site of O-GlcNAcylation where known (Site).

Gel Piece	Accession	Description	PMID	Site
1	P60709	Actin, cytoplasmic 1	20305658	
2	P10809	60 kDa heat shock protein, mitochondrial		
5	P62191	26S protease regulatory subunit 4		
5	O43242	26S proteasome non-ATPase regulatory subunit 3		
5	P10809	60 kDa heat shock protein, mitochondrial		
5	Q01518	Adenylyl cyclase-associated protein 1		
5	Q06203	Amidophosphoribosyltransferase		
5	C9JM09	Asparagine synthetase [glutamine-hydrolyzing] (Fragment)		
5	P14868	Aspartate–tRNA ligase, cytoplasmic		
5	P25705	ATP synthase subunit alpha, mitochondrial		
5	I3L0H8	ATP-dependent RNA helicase DDX19A		
5	O00571	ATP-dependent RNA helicase DDX3X		
5	P07814	Bifunctional glutamate/proline–tRNA ligase	16408927	
5	P04040	Catalase	18984734	S114;S254
5	C9JFE4	COP9 signalosome complex subunit 1		
5	O43175	D-3-phosphoglycerate dehydrogenase	16408927	
5	P81605	Dermcidin		
5	P15924	Desmoplakin		
5	U3KQB9	DNA primase large subunit		
5	J3KQ69	DNA replication licensing factor MCM3		
5	B4DXV1	Elongator complex protein 3		
5	P55884	Eukaryotic translation initiation factor 3 subunit B	16408927	
5	B4DVY1	Eukaryotic translation initiation factor 3 subunit D		
5	Q9Y262	Eukaryotic translation initiation factor 3 subunit L		
5	P11413	Glucose-6-phosphate 1-dehydrogenase	16408927	
5	P06744	Glucose-6-phosphate isomerase	16408927	
5	E9PKE3	Heat shock cognate 71 kDa protein		
5	Q5T6W5	Heterogeneous nuclear ribonucleoprotein K		
5	Q00839	Heterogeneous nuclear ribonucleoprotein U	16408927	

Table D.1: (continued)

Gel Piece	Accession	Description	PMID	Site
5	B3KRS5	Histone deacetylase		
5	P16403	Histone H1.2	20305658	
5	P52292	Importin subunit alpha-1	16408927	
5	H0Y4R1	Inosine-5'-monophosphate dehydrogenase 2 (Fragment)		
5	C9J381	Inosine-5'-monophosphate dehydrogenase		
5	F5GWP8	Junction plakoglobin		
5	Q9UKX7	Nuclear pore complex protein Nup50		
5	H0YHC3	Nucleosome assembly protein 1-like 1 (Fragment)		
5	B4E363	Phenylalanine–tRNA ligase alpha subunit		
5	P11940	Polyadenylate-binding protein 1	20305658	
5	K7EK45	Polypyrimidine tract-binding protein 1 (Fragment)		
5	Q9UMS4	Pre-mRNA-processing factor 19		
5	B4DLW8	Probable ATP-dependent RNA helicase DDX5		
5	G5EA52	Protein disulfide isomerase family A, member 3, isoform CRA_b		
5	P07237	Protein disulfide-isomerase		
5	Q9P258	Protein RCC2	16408927	
5	P14618	Pyruvate kinase PKM	16408927	
5	F5H4D6	Ras GTPase-activating protein-binding protein 1		
5	Q9Y265	RuvB-like 1		
5	Q12874	Splicing factor 3A subunit 3		
5	K7ENG2	Splicing factor U2AF 65 kDa subunit		
5	P17987	T-complex protein 1 subunit alpha	16408927	
5	P78371	T-complex protein 1 subunit beta		
5	P50991	T-complex protein 1 subunit delta	16408927	
5	B7ZAR1	T-complex protein 1 subunit epsilon		
5	Q99832	T-complex protein 1 subunit eta		
5	B4DUR8	T-complex protein 1 subunit gamma		
5	P50990	T-complex protein 1 subunit theta	16408927;17614351	
5	P40227	T-complex protein 1 subunit zeta	16408927	
5	Q9UJA5	tRNA (adenine(58)-N(1))-methyltransferase non-catalytic subunit TRM6		

Table D.1: (continued)

Gel Piece	Accession	Description	PMID	Site
5	Q9Y3I0	tRNA-splicing ligase RtcB homolog		
5	J3QSA3	Ubiquitin (Fragment)		
5	A6NJA2	Ubiquitin carboxyl-terminal hydrolase		
5	Q16851	UTP–glucose-1-phosphate uridylyltransferase		
5	Q8WU90	Zinc finger CCCH domain-containing protein 15		
8	P81605	Dermcidin		
8	P15924	Desmoplakin		
8	Q5D862	Filaggrin-2		
9	K7EJ81	116 kDa U5 small nuclear ribonucleoprotein component		
9	Q99460	26S proteasome non-ATPase regulatory subunit 1	16408927	
9	F5GZS6	4F2 cell-surface antigen heavy chain		
9	Q01813	6-phosphofructokinase type C		
9	P17858	6-phosphofructokinase, liver type		
9	P08237	6-phosphofructokinase, muscle type	16408927	
9	P11021	78 kDa glucose-regulated protein	16408927	
9	Q99798	Aconitate hydratase, mitochondrial		
9	P13798	Acylamino-acid-releasing enzyme		
9	F8WBH3	Aldehyde dehydrogenase family 16 member A1		
9	H0YN42	Annexin (Fragment)		
9	B4E3P0	ATP-citrate synthase		
9	Q08211	ATP-dependent RNA helicase A		
9	Q92499	ATP-dependent RNA helicase DDX1	16408927	
9	Q9NVP1	ATP-dependent RNA helicase DDX18		
9	Q9BQ39	ATP-dependent RNA helicase DDX50		
9	P25098	Beta-adrenergic receptor kinase 1		
9	P07814	Bifunctional glutamate/proline–tRNA ligase	16408927	
9	K7ES02	Bleomycin hydrolase (Fragment)		
9	P27824	Calnexin		
9	G3V153	Caprin-1		
9	P31944	Caspase-14		

Table D.1: (continued)

Gel Piece	Accession	Description	PMID	Site
9	E5RHJ4	Cell cycle and apoptosis regulator protein 2 (Fragment)		
9	Q12996	Cleavage stimulation factor subunit 3		
9	P53621	Coatomer subunit alpha	16408927	
9	O75534	Cold shock domain-containing protein E1	20305658	
9	E9PHA2	Condensin complex subunit 2		
9	Q5JY65	Crooked neck-like protein 1		
9	K4DI93	Cullin 4B, isoform CRA_e		
9	Q13616	Cullin-1		
9	Q13618	Cullin-3		
9	A8MVQ3	Cysteine–tRNA ligase, cytoplasmic		
9	Q08554	Desmocollin-1		
9	Q02413	Desmoglein-1		
9	P15924	Desmoplakin		
9	J3KQ69	DNA replication licensing factor MCM3		
9	P33992	DNA replication licensing factor MCM5		
9	Q14566	DNA replication licensing factor MCM6	16408927	
9	P33993	DNA replication licensing factor MCM7	16408927	
9	Q99543	DnaJ homolog subfamily C member 2		
9	F5GXT0	Double-strand break repair protein MRE11A		
9	G8JLD5	Dynamin-1-like protein		
9	P13639	Elongation factor 2	16408927	
9	Q92556	Engulfment and cell motility protein 1		
9	K7EM90	Enolase (Fragment)		
9	P58107	Epiplakin		
9	F5H335	Eukaryotic translation initiation factor 3 subunit A		
9	P55884	Eukaryotic translation initiation factor 3 subunit B	16408927	
9	H3BRV0	Eukaryotic translation initiation factor 3 subunit C		
9	E7EQR4	Ezrin		
9	Q92945	Far upstream element-binding protein 2	16408927	
9	P20930	Filaggrin		

Table D.1: (continued)

Gel Piece	Accession	Description	PMID	Site
9	Q5D862	Filaggrin-2		
9	P51116	Fragile X mental retardation syndrome-related protein 2		
9	P47929	Galectin-7		
9	E7EPR3	Gamma-interferon-inducible protein 16		
9	P78347	General transcription factor II-I		
9	Q06210	Glutamine–fructose-6-phosphate aminotransferase [isomerizing] 1		
9	P04406	Glyceraldehyde-3-phosphate dehydrogenase	18794846	
9	P41250	Glycine–tRNA ligase	16408927	
9	P13807	Glycogen [starch] synthase, muscle	18174169	
9	O00178	GTP-binding protein 1		
9	P04792	Heat shock protein beta-1		
9	P07900	Heat shock protein HSP 90-alpha	16408927	
9	P08238	Heat shock protein HSP 90-beta	16408927	
9	Q5SWC8	Heterochromatin protein 1-binding protein 3 (Fragment)		
9	P52272	Heterogeneous nuclear ribonucleoprotein M		
9	O43390	Heterogeneous nuclear ribonucleoprotein R	20305658	
9	Q00839	Heterogeneous nuclear ribonucleoprotein U	16408927	
9	Q1KMD3	Heterogeneous nuclear ribonucleoprotein U-like protein 2		
9	F8W0V1	Histidine ammonia-lyase (Fragment)		
9	P01871	Ig mu chain C region		
9	Q12906	Interleukin enhancer-binding factor 3	20305658	
9	J3KR24	Isoleucine–tRNA ligase, cytoplasmic		
9	F5GWP8	Junction plakoglobin		
9	C9J315	Lanosterol synthase (Fragment)		
9	Q4G0J3	La-related protein 7		
9	D6REM6	Matrin-3		
9	G5E9X5	Methylcrotonoyl-CoA carboxylase subunit alpha, mitochondrial		
9	P35579	Myosin-9	16408927	
9	P43007	Neutral amino acid transporter A		
9	Q15758	Neutral amino acid transporter B(0)		

Table D.1: (continued)

Gel Piece	Accession	Description	PMID	Site
9	Q09161	Nuclear cap-binding protein subunit 1		
9	Q7Z417	Nuclear fragile X mental retardation-interacting protein 2	20305658	
9	Q9Y3T9	Nucleolar complex protein 2 homolog		
9	F5H6G7	Nucleolar protein 10		
9	Q9NR30	Nucleolar RNA helicase 2	16408927	
9	Q13835	Plakophilin-1		
9	B1ANR0	Poly(A) binding protein, cytoplasmic 4 (Inducible form), isoform CRA_e		
9	Q8TCS8	Polyribonucleotide nucleotidyltransferase 1, mitochondrial		
9	O94906	Pre-mRNA-processing factor 6		
9	E9PIF2	Probable ATP-dependent RNA helicase DDX10		
9	C9JMU5	Probable ATP-dependent RNA helicase DDX17		
9	Q9BUQ8	Probable ATP-dependent RNA helicase DDX23		
9	Q9Y4C8	Probable RNA-binding protein 19		
9	Q9NY61	Protein AATF		
9	Q8WVV4	Protein POF1B		
9	Q13123	Protein Red		
9	E7EW05	Protein SDA1 homolog		
9	B3KXI2	Protein transport protein Sec23A		
9	Q15437	Protein transport protein Sec23B	20305658	
9	Q08188	Protein-glutamine gamma-glutamyltransferase E		
9	Q96PZ0	Pseudouridylate synthase 7 homolog		
9	O43143	Putative pre-mRNA-splicing factor ATP-dependent RNA helicase DHX15	16408927	
9	P46087	Putative ribosomal RNA methyltransferase NOP2		
9	B1ALK7	Rho guanine nucleotide exchange factor 7		
9	O76094	Signal recognition particle subunit SRP72		
9	P23246	Splicing factor, proline- and glutamine-rich	20305658	
9	Q5R363	SRSF protein kinase 1		
9	Q9Y5Y6	Suppressor of tumorigenicity 14 protein		
9	P52888	Thimet oligopeptidase		
9	Q96FV9	THO complex subunit 1		

Table D.1: (continued)

Gel Piece	Accession	Description	PMID	Site
9	H7C072	THO complex subunit 5 homolog (Fragment)		
9	P26639	Threonine–tRNA ligase, cytoplasmic	16408927	
9	A2T926	Thymopentin		
9	Q13263	Transcription intermediary factor 1-beta		
9	J3KNP2	Transducin beta-like protein 3 (Fragment)		
9	P55072	Transitional endoplasmic reticulum ATPase		
9	P40939	Trifunctional enzyme subunit alpha, mitochondrial		
9	E7ET15	U2 snRNP-associated SURP motif-containing protein		
9	E7EVD1	U4/U6 small nuclear ribonucleoprotein Prp3		
9	J3QSA3	Ubiquitin (Fragment)		
9	B4DWJ2	Uncharacterized protein		
9	Q96QK1	Vacuolar protein sorting-associated protein 35		
9	P26640	Valine–tRNA ligase	16408927	
9	Q15061	WD repeat-containing protein 43		
9	P13010	X-ray repair cross-complementing protein 5	16408927	
9	Q7Z2W4	Zinc finger CCCH-type antiviral protein 1		
10	O43242	26S proteasome non-ATPase regulatory subunit 3		
10	P10809	60 kDa heat shock protein, mitochondrial		
10	P11021	78 kDa glucose-regulated protein	16408927	
10	O95782	AP-2 complex subunit alpha-1		
10	K7EJ01	AP-2 complex subunit beta (Fragment)		
10	P54136	Arginine–tRNA ligase, cytoplasmic		
10	F8WEJ5	Asparagine synthetase [glutamine-hydrolyzing]		
10	O43776	Asparagine–tRNA ligase, cytoplasmic	16408927	
10	P61221	ATP-binding cassette sub-family E member 1		
10	B4E3P0	ATP-citrate synthase		
10	P46063	ATP-dependent DNA helicase Q1		
10	Q08211	ATP-dependent RNA helicase A		
10	Q9NVP1	ATP-dependent RNA helicase DDX18		
10	O00571	ATP-dependent RNA helicase DDX3X		

Table D.1: (continued)

Gel Piece	Accession	Description	PMID	Site
10	F5H5U2	ATP-dependent RNA helicase DDX55		
10	O43252	Bifunctional 3'-phosphoadenosine 5'-phosphosulfate synthase 1		
10	Q3LXA3	Bifunctional ATP-dependent dihydroxyacetone kinase/FAD-AMP lyase (cyclizing)		
10	P07814	Bifunctional glutamate/proline–tRNA ligase	16408927	
10	P31939	Bifunctional purine biosynthesis protein PURH	16408927	
10	E9PLA9	Caprin-1 (Fragment)		
10	Q9NXV6	CDKN2A-interacting protein	20068230	S348;T322
10	Q9UJX2	Cell division cycle protein 23 homolog		
10	Q969X6	Cirhin		
10	F8WJN3	Cleavage and polyadenylation-specificity factor subunit 6		
10	O75534	Cold shock domain-containing protein E1	20305658	
10	E7EN77	Condensin complex subunit 1 (Fragment)		
10	P17812	CTP synthase 1		
10	Q9Y3Z3	Deoxynucleoside triphosphate triphosphohydrolase SAMHD1		
10	H0YDD4	Dihydrolipoyllysine-residue acetyltransferase component of pyruvate dehydrogenase complex, mitochondrial (Fragment)		
10	Q16555	Dihydropyrimidinase-related protein 2		
10	P33993	DNA replication licensing factor MCM7	16408927	
10	P11387	DNA topoisomerase 1		
10	B7Z4L4	Dolichyl-diphosphooligosaccharide–protein glycosyltransferase subunit 1		
10	Q9H4M9	EH domain-containing protein 1		
10	Q9H223	EH domain-containing protein 4		
10	P13639	Elongation factor 2	16408927	
10	P55884	Eukaryotic translation initiation factor 3 subunit B	16408927	
10	O15371	Eukaryotic translation initiation factor 3 subunit D		
10	Q9Y262	Eukaryotic translation initiation factor 3 subunit L		
10	E7EQR4	Ezrin		
10	Q92945	Far upstream element-binding protein 2	16408927	
10	Q96I24	Far upstream element-binding protein 3		
10	P49327	Fatty acid synthase		

Table D.1: (continued)

Gel Piece	Accession	Description	PMID	Site
10	F5H1C6	Fermitin family homolog 3 (Fragment)		
10	B4DXZ6	Fragile X mental retardation syndrome-related protein 1		
10	Q06210	Glutamine–fructose-6-phosphate aminotransferase [isomerizing] 1		
10	O00178	GTP-binding protein 1		
10	Q9BVP2	Guanine nucleotide-binding protein-like 3		
10	O60832	H/ACA ribonucleoprotein complex subunit 4		
10	H3BQZ7	HCG2044799		
10	P08107	Heat shock 70 kDa protein 1A/1B	16177265, 17645866	
10	P34932	Heat shock 70 kDa protein 4	16408927	
10	P11142	Heat shock cognate 71 kDa protein	16408927	
10	B4DY72	Heat shock protein 105 kDa		
10	P08238	Heat shock protein HSP 90-beta	16408927	
10	Q5SSJ5	Heterochromatin protein 1-binding protein 3		
10	P14866	Heterogeneous nuclear ribonucleoprotein L	20305658	
10	P52272	Heterogeneous nuclear ribonucleoprotein M		
10	O60506	Heterogeneous nuclear ribonucleoprotein Q	20305658	
10	O43390	Heterogeneous nuclear ribonucleoprotein R	20305658	
10	Q00839	Heterogeneous nuclear ribonucleoprotein U	16408927	
10	P01871	Ig mu chain C region		
10	P52294	Importin subunit alpha-5		
10	Q9NZI8	Insulin-like growth factor 2 mRNA-binding protein 1		
10	Q9Y6M1	Insulin-like growth factor 2 mRNA-binding protein 2		
10	O00425	Insulin-like growth factor 2 mRNA-binding protein 3		
10	P19525	Interferon-induced, double-stranded RNA-activated protein kinase		
10	Q12906	Interleukin enhancer-binding factor 3	20305658	
10	O00139	Kinesin-like protein KIF2A		
10	Q9UQ13	Leucine-rich repeat protein SHOC-2		
10	Q8N1G4	Leucine-rich repeat-containing protein 47		
10	P09960	Leukotriene A-4 hydrolase	16408927	
10	B4DJ96	Luc7-like protein 3		

Table D.1: (continued)

Gel Piece	Accession	Description	PMID	Site
10	Q15046	Lysine–tRNA ligase	20305658	
10	D6REM6	Matrin-3		
10	P55081	Microfibrillar-associated protein 1		
10	H0YN19	Myelin expression factor 2 (Fragment)		
10	P35579	Myosin-9	16408927	
10	P23368	NAD-dependent malic enzyme, mitochondrial		
10	Q9BXJ9	N-alpha-acetyltransferase 15, NatA auxiliary subunit		
10	C9JEM7	Negative elongation factor A (Fragment)		
10	Q15758	Neutral amino acid transporter B(0)		
10	E9PIN3	Nuclear RNA export factor 1 (Fragment)		
10	E9PFK5	Nucleolar protein 14		
10	O00567	Nucleolar protein 56		
10	Q9Y2X3	Nucleolar protein 58		
10	Q86U38	Nucleolar protein 9		
10	Q9NR30	Nucleolar RNA helicase 2	16408927	
10	E9PKP7	Nucleolar transcription factor 1		
10	Q8WXF1	Paraspeckle component 1		
10	B4DJV5	Periodic tryptophan protein 1 homolog		
10	B5MCF9	Pescadillo homolog		
10	Q9NSD9	Phenylalanine–tRNA ligase beta subunit		
10	Q16822	Phosphoenolpyruvate carboxykinase [GTP], mitochondrial		
10	Q9H307	Pinin		
10	P13796	Plastin-2		
10	P09874	Poly [ADP-ribose] polymerase 1	16408927	
10	Q9UHX1	Poly(U)-binding-splicing factor PUF60		
10	E7ERJ7	Polyadenylate-binding protein 1		
10	Q6UN15	Pre-mRNA 3'-end-processing factor FIP1		
10	Q5SRN1	Pre-mRNA-processing factor 17		
10	E9PIF2	Probable ATP-dependent RNA helicase DDX10		
10	C9JMU5	Probable ATP-dependent RNA helicase DDX17		

Table D.1: (continued)

Gel Piece	Accession	Description	PMID	Site
10	B4DLW8	Probable ATP-dependent RNA helicase DDX5		
10	A8MTP9	Probable ATP-dependent RNA helicase DDX52		
10	H7C3E9	Probable ATP-dependent RNA helicase DDX56 (Fragment)		
10	O60678	Protein arginine N-methyltransferase 3		
10	B4DV00	Protein arginine N-methyltransferase 5		
10	Q96GA3	Protein LTV1 homolog		
10	Q96PZ0	Pseudouridylate synthase 7 homolog		
10	K7EMM8	Putative oxidoreductase GLYR1 (Fragment)		
10	O43143	Putative pre-mRNA-splicing factor ATP-dependent RNA helicase DHX15	16408927	
10	P46087	Putative ribosomal RNA methyltransferase NOP2		
10	P14618	Pyruvate kinase PKM	16408927	
10	Q9BZI7	Regulator of nonsense transcripts 3B		
10	I3L4R8	Replication protein A 70 kDa DNA-binding subunit (Fragment)		
10	J3QSV6	Ribosomal L1 domain-containing protein 1 (Fragment)		
10	Q14692	Ribosome biogenesis protein BMS1 homolog		
10	Q96PK6	RNA-binding protein 14	20068230	S244;S254;S256;S280
10	E1P5S2	RNA-binding protein 39		
10	P57772	Selenocysteine-specific elongation factor		
10	Q08170	Serine/arginine-rich splicing factor 4		
10	P10398	Serine/threonine-protein kinase A-Raf		
10	Q9BVS4	Serine/threonine-protein kinase RIO2		
10	P30153	Serine/threonine-protein phosphatase 2A 65 kDa regulatory subunit A alpha isoform	16408927	
10	P30154	Serine/threonine-protein phosphatase 2A 65 kDa regulatory subunit A beta isoform		
10	F5H5Y3	Signal recognition particle subunit SRP68		
10	G3V4X8	SNW domain-containing protein 1		
10	Q9NQZ2	Something about silencing protein 10		
10	Q15459	Splicing factor 3A subunit 1		
10	E9PJ04	Splicing factor 3B subunit 2 (Fragment)		
10	Q15393	Splicing factor 3B subunit 3	16408927	
10	P23246	Splicing factor, proline- and glutamine-rich	20305658	

Table D.1: (continued)

Gel Piece	Accession	Description	PMID	Site
10	Q7KZF4	Staphylococcal nuclease domain-containing protein 1	16408927	
10	P38646	Stress-70 protein, mitochondrial	16408927	
10	F5H0T1	Stress-induced-phosphoprotein 1		
10	Q9UH65	Switch-associated protein 70		
10	P17987	T-complex protein 1 subunit alpha	16408927	
10	B7ZAR1	T-complex protein 1 subunit epsilon		
10	Q99832	T-complex protein 1 subunit eta		
10	B4DUR8	T-complex protein 1 subunit gamma		
10	P50990	T-complex protein 1 subunit theta	16408927;17614351	
10	P40227	T-complex protein 1 subunit zeta	16408927	
10	H3BR06	Telomeric repeat-binding factor 2 (Fragment)		
10	B4E022	Transketolase		
10	Q9UI10	Translation initiation factor eIF-2B subunit delta		
10	Q08J23	tRNA (cytosine(34)-C(5))-methyltransferase		
10	Q9UIG0	Tyrosine-protein kinase BAZ1B		
10	P08621	U1 small nuclear ribonucleoprotein 70 kDa		
10	Q9Y5J1	U3 small nucleolar RNA-associated protein 18 homolog		
10	Q9NYH9	U3 small nucleolar RNA-associated protein 6 homolog		
10	B9A018	U4/U6.U5 tri-snRNP-associated protein 2		
10	J3QSA3	Ubiquitin (Fragment)		
10	P49748	Very long-chain specific acyl-CoA dehydrogenase, mitochondrial		
10	B7Z1R5	V-type proton ATPase catalytic subunit A		
10	P13010	X-ray repair cross-complementing protein 5	16408927	
10	P12956	X-ray repair cross-complementing protein 6		
10	Q96KR1	Zinc finger RNA-binding protein	20068230	S148;S195;T202
11	P62258	14-3-3 protein epsilon		
11	C9J9M4	26S proteasome non-ATPase regulatory subunit 1 (Fragment)		
11	P49406	39S ribosomal protein L19, mitochondrial		
11	P15880	40S ribosomal protein S2	18794846	
11	F2Z2S8	40S ribosomal protein S3		

Table D.1: (continued)

Gel Piece	Accession	Description	PMID	Site
11	D6RG13	40S ribosomal protein S3a (Fragment)		
11	P62701	40S ribosomal protein S4, X isoform		
11	P62753	40S ribosomal protein S6	20305658	
11	C9J9K3	40S ribosomal protein SA (Fragment)		
11	F8VU65	60S acidic ribosomal protein P0 (Fragment)		
11	P46777	60S ribosomal protein L5	18794846	
11	P18124	60S ribosomal protein L7		
11	P62424	60S ribosomal protein L7a		
11	E9PKZ0	60S ribosomal protein L8 (Fragment)		
11	O15144	Actin-related protein 2/3 complex subunit 2		
11	Q9UIV1	CCR4-NOT transcription complex subunit 7		
11	B5MDQ4	Cell differentiation protein RCD1 homolog		
11	Q9Y3Y2	Chromatin target of PRMT1 protein		
11	Q96CT7	Coiled-coil domain-containing protein 124		
11	F5H7C6	COP9 signalosome complex subunit 7a (Fragment)		
11	J3KQ34	COP9 signalosome complex subunit 7b		
11	P81605	Dermcidin		
11	P29692	Elongation factor 1-delta		
11	K7EM90	Enolase (Fragment)		
11	Q5RKV6	Exosome complex component MTR3		
11	Q9NQT5	Exosome complex component RRP40		
11	D6RAU2	Guanine nucleotide-binding protein subunit beta-2-like 1		
11	D6R9P3	Heterogeneous nuclear ribonucleoprotein A/B		
11	Q13151	Heterogeneous nuclear ribonucleoprotein A0	20305658	
11	F8W6I7	Heterogeneous nuclear ribonucleoprotein A1		
11	P51991	Heterogeneous nuclear ribonucleoprotein A3	16408927	
11	H0YA96	Heterogeneous nuclear ribonucleoprotein D0 (Fragment)		
11	Q5T6W2	Heterogeneous nuclear ribonucleoprotein K (Fragment)		
11	O60506	Heterogeneous nuclear ribonucleoprotein Q	20305658	
11	P22626	Heterogeneous nuclear ribonucleoproteins A2/B1	20305658	

Table D.1: (continued)

Gel Piece	Accession	Description	PMID	Site
11	G3V4W0	Heterogeneous nuclear ribonucleoproteins C1/C2 (Fragment)		
11	P26583	High mobility group protein B2		
11	P16403	Histone H1.2	20305658	
11	P16401	Histone H1.5	20305658	
11	Q92522	Histone H1x	20305658	
11	P13761	HLA class II histocompatibility antigen, DRB1-7 beta chain		
11	Q9UBB5	Methyl-CpG-binding domain protein 2		
11	Q9UKD2	mRNA turnover protein 4 homolog		
11	Q9HAN9	Nicotinamide mononucleotide adenylyltransferase 1		
11	C9JW96	Prohibitin (Fragment)		
11	P12004	Proliferating cell nuclear antigen		
11	H0YNE3	Proteasome activator complex subunit 1		
11	H0YM70	Proteasome activator complex subunit 2		
11	K7EMD0	Proteasome activator complex subunit 3 (Fragment)		
11	V9GYH7	Proteasome assembly chaperone 2		
11	P25786	Proteasome subunit alpha type-1		
11	Q9BXY0	Protein MAK16 homolog		
11	O95478	Ribosome biogenesis protein NSA2 homolog		
11	Q9NRX1	RNA-binding protein PNO1		
11	Q9UKM9	RNA-binding protein Raly		
11	Q07955	Serine/arginine-rich splicing factor 1		
11	B7Z2F4	T-complex protein 1 subunit delta		
11	P50990	T-complex protein 1 subunit theta	16408927;17614351	
11	Q86V81	THO complex subunit 4		
11	P67936	Tropomyosin alpha-4 chain		
11	Q9BQE3	Tubulin alpha-1C chain		
11	Q5JP53	Tubulin beta chain		
11	K7EP07	Tubulin-folding cofactor B (Fragment)		
11	P09661	U2 small nuclear ribonucleoprotein A'		
11	Q5VU59	Uncharacterized protein		

Table D.1: (continued)

Gel Piece	Accession	Description	PMID	Site
11	G3V2S6	V-type proton ATPase subunit D		
11	P16989	Y-box-binding protein 3		
12	P31946	14-3-3 protein beta/alpha	16408927	
12	P31946	14-3-3 protein beta/alpha	16408927	
12	P62258	14-3-3 protein epsilon		
12	Q04917	14-3-3 protein eta		
12	P61981	14-3-3 protein gamma		
12	P27348	14-3-3 protein theta		
12	P63104	14-3-3 protein zeta/delta		
12	K7EJR3	26S proteasome non-ATPase regulatory subunit 8 (Fragment)		
12	C9IY40	39S ribosomal protein L2, mitochondrial		
12	P15880	40S ribosomal protein S2	18794846	
12	P23396	40S ribosomal protein S3		
12	D6RG13	40S ribosomal protein S3a (Fragment)		
12	P62701	40S ribosomal protein S4, X isoform		
12	A2A3R5	40S ribosomal protein S6		
12	Q5JR95	40S ribosomal protein S8		
12	C9J9K3	40S ribosomal protein SA (Fragment)		
12	P05388	60S acidic ribosomal protein P0		
12	P26373	60S ribosomal protein L13	20305658	
12	Q02878	60S ribosomal protein L6		
12	A8MUD9	60S ribosomal protein L7		
12	Q5T8U3	60S ribosomal protein L7a (Fragment)		
12	Q6DKI1	60S ribosomal protein L7-like 1		
12	M0R261	6-phosphogluconolactonase (Fragment)		
12	Q9UKK9	ADP-sugar pyrophosphatase		
12	Q9HB71	Calcyclin-binding protein		
12	Q9NX58	Cell growth-regulating nucleolar protein		
12	O00299	Chloride intracellular channel protein 1		
12	P27707	Deoxycytidine kinase		

Table D.1: (continued)

Gel Piece	Accession	Description	PMID	Site
12	P24534	Elongation factor 1-beta		
12	E7EUT5	Glyceraldehyde-3-phosphate dehydrogenase		
12	D6R9P3	Heterogeneous nuclear ribonucleoprotein A/B		
12	Q13151	Heterogeneous nuclear ribonucleoprotein A0	20305658	
12	F8W6I7	Heterogeneous nuclear ribonucleoprotein A1		
12	P51991	Heterogeneous nuclear ribonucleoprotein A3	16408927	
12	H0YA96	Heterogeneous nuclear ribonucleoprotein D0 (Fragment)		
12	Q5T6W5	Heterogeneous nuclear ribonucleoprotein K		
12	P22626	Heterogeneous nuclear ribonucleoproteins A2/B1	20305658	
12	G3V5X6	Heterogeneous nuclear ribonucleoproteins C1/C2 (Fragment)		
12	P16403	Histone H1.2	20305658	
12	Q96GX9	Methylthioribulose-1-phosphate dehydratase		
12	B8ZZL5	MIT domain-containing protein 1 (Fragment)		
12	P06748	Nucleophosmin	16408927	
12	Q9BRP8	Partner of Y14 and mago		
12	P18669	Phosphoglycerate mutase 1		
12	P13796	Plastin-2		
12	Q15365	Poly(rC)-binding protein 1		
12	Q9UL46	Proteasome activator complex subunit 2	16408927	
12	H0YLC2	Proteasome subunit alpha type		
12	P25788	Proteasome subunit alpha type-3		
12	O14818	Proteasome subunit alpha type-7		
12	Q9BPW8	Protein NipSnap homolog 1		
12	H0Y6C3	Pyrroline-5-carboxylate reductase 3 (Fragment)		
12	J3KRE2	Rho GDP-dissociation inhibitor 1		
12	Q5VU10	Ribonuclease P protein subunit p30 (Fragment)		
12	Q92979	Ribosomal RNA small subunit methyltransferase NEP1		
12	H0Y6E7	RNA-binding motif protein, X chromosome, N-terminally processed (Fragment)		
12	Q5QPM1	RNA-binding protein Raly (Fragment)		
12	M0R0P1	rRNA 2'-O-methyltransferase fibrillarin (Fragment)		

Table D.1: (continued)

Gel Piece	Accession	Description	PMID	Site
12	Q5JRI1	Serine/arginine-rich-splicing factor 10		
12	O75940	Survival of motor neuron-related-splicing factor 30		
12	P40227	T-complex protein 1 subunit zeta	16408927	
12	F8WBV5	Thioredoxin domain-containing protein 9		
12	Q86V81	THO complex subunit 4		
12	P62995	Transformer-2 protein homolog beta		
12	D6R904	Tropomyosin alpha-3 chain		
12	F8VVB9	Tubulin alpha-1B chain (Fragment)		
12	P09661	U2 small nuclear ribonucleoprotein A'		
12	G3V4C6	UPF0568 protein C14orf166		
12	P16989	Y-box-binding protein 3		
13	P27348	14-3-3 protein theta		
13	J3QKW2	28S ribosomal protein S7, mitochondrial		
13	Q5H928	3-hydroxyacyl-CoA dehydrogenase type-2		
13	E9PPU1	40S ribosomal protein S3		
13	Q5JR95	40S ribosomal protein S8		
13	P46781	40S ribosomal protein S9	18794846	
13	C9J9K3	40S ribosomal protein SA (Fragment)		
13	F8VPE8	60S acidic ribosomal protein P0 (Fragment)		
13	F8W7C6	60S ribosomal protein L10		
13	P62906	60S ribosomal protein L10a		
13	P26373	60S ribosomal protein L13	20305658	
13	P40429	60S ribosomal protein L13a	18794846	
13	P50914	60S ribosomal protein L14		
13	P61313	60S ribosomal protein L15		
13	P62424	60S ribosomal protein L7a		
13	E9PKZ0	60S ribosomal protein L8 (Fragment)		
13	P67870	Casein kinase II subunit beta	20305658	
13	O43809	Cleavage and polyadenylation specificity factor subunit 5		
13	P81605	Dermcidin		

Table D.1: (continued)

Gel Piece	Accession	Description	PMID	Site
13	P19388	DNA-directed RNA polymerases I, II, and III subunit RPABC1		
13	P24534	Elongation factor 1-beta		
13	P20042	Eukaryotic translation initiation factor 2 subunit 2		
13	P04406	Glyceraldehyde-3-phosphate dehydrogenase	18794846	
13	Q8TAE8	Growth arrest and DNA damage-inducible proteins-interacting protein 1		
13	P62826	GTP-binding nuclear protein Ran		
13	E9PI65	Heat shock cognate 71 kDa protein (Fragment)		
13	D6R9P3	Heterogeneous nuclear ribonucleoprotein A/B		
13	Q13151	Heterogeneous nuclear ribonucleoprotein A0	20305658	
13	F8W6I7	Heterogeneous nuclear ribonucleoprotein A1		
13	P51991	Heterogeneous nuclear ribonucleoprotein A3	16408927	
13	D6RF44	Heterogeneous nuclear ribonucleoprotein D0 (Fragment)		
13	E9PCY7	Heterogeneous nuclear ribonucleoprotein H		
13	P22626	Heterogeneous nuclear ribonucleoproteins A2/B1	20305658	
13	P16403	Histone H1.2	20305658	
13	Q5SRN7	HLA class I histocompatibility antigen, A-68 alpha chain		
13	P00492	Hypoxanthine-guanine phosphoribosyltransferase	20305658	
13	F8VZJ2	Nascent polypeptide-associated complex subunit alpha, muscle-specific form		
13	D6RIC3	Nucleolar protein 16		
13	H7C3T4	Peroxiredoxin-4 (Fragment)		
13	P30041	Peroxiredoxin-6		
13	O75934	Pre-mRNA-splicing factor SPF27		
13	P25787	Proteasome subunit alpha type-2		
13	P28066	Proteasome subunit alpha type-5	18984734	S198
13	P60900	Proteasome subunit alpha type-6		
13	H0Y586	Proteasome subunit alpha type-7 (Fragment)		
13	B7Z972	Protein-L-isoaspartate O-methyltransferase		
13	H3BMH2	Ras-related protein Rab-11A (Fragment)		
13	P51148	Ras-related protein Rab-5C		
13	P49247	Ribose-5-phosphate isomerase		

Table D.1: (continued)

Gel Piece	Accession	Description	PMID	Site
13	J3QR09	Ribosomal protein L19		
13	Q92979	Ribosomal RNA small subunit methyltransferase NEP1		
13	H0Y6E7	RNA-binding motif protein, X chromosome, N-terminally processed (Fragment)		
13	P60174	Triosephosphate isomerase	20305658	
13	P08579	U2 small nuclear ribonucleoprotein B”		
13	Q9Y224	UPF0568 protein C14orf166		
13	P16989	Y-box-binding protein 3		
14	Q9Y3B7	39S ribosomal protein L11, mitochondrial		
14	E9PPU1	40S ribosomal protein S3		
14	P62081	40S ribosomal protein S7		
14	Q5JR95	40S ribosomal protein S8		
14	P46781	40S ribosomal protein S9	18794846	
14	C9J9K3	40S ribosomal protein SA (Fragment)		
14	F8W7C6	60S ribosomal protein L10		
14	P26373	60S ribosomal protein L13	20305658	
14	P50914	60S ribosomal protein L14		
14	P61313	60S ribosomal protein L15		
14	F8VWC5	60S ribosomal protein L18		
14	C9JXB8	60S ribosomal protein L24		
14	Q02878	60S ribosomal protein L6		
14	D6RAN4	60S ribosomal protein L9 (Fragment)		
14	A8MX94	Glutathione S-transferase P		
14	P04406	Glyceraldehyde-3-phosphate dehydrogenase	18794846	
14	F8W6I7	Heterogeneous nuclear ribonucleoprotein A1		
14	P22626	Heterogeneous nuclear ribonucleoproteins A2/B1	20305658	
14	P16403	Histone H1.2	20305658	
14	P62805	Histone H4		
14	Q12905	Interleukin enhancer-binding factor 2		
14	F8VZJ2	Nascent polypeptide-associated complex subunit alpha, muscle-specific form		
14	Q06830	Peroxiredoxin-1	16408927	

Table D.1: (continued)

Gel Piece	Accession	Description	PMID	Site
14	P20618	Proteasome subunit beta type-1		
14	P28070	Proteasome subunit beta type-4		
14	P28074	Proteasome subunit beta type-5		
14	P61224	Ras-related protein Rap-1b		
14	H0Y6E7	RNA-binding motif protein, X chromosome, N-terminally processed (Fragment)		
14	B7Z9L0	T-complex protein 1 subunit delta		
15	Q9NWU5	39S ribosomal protein L22, mitochondrial		
15	F5H702	39S ribosomal protein L48, mitochondrial		
15	M0QZC5	40S ribosomal protein S11		
15	F2Z2S8	40S ribosomal protein S3		
15	P62081	40S ribosomal protein S7		
15	Q5JR95	40S ribosomal protein S8		
15	P46781	40S ribosomal protein S9	18794846	
15	P05388	60S acidic ribosomal protein P0		
15	Q5VVC9	60S ribosomal protein L11 (Fragment)		
15	P30050	60S ribosomal protein L12		
15	P50914	60S ribosomal protein L14		
15	J3QS96	60S ribosomal protein L17 (Fragment)		
15	F8VUA6	60S ribosomal protein L18 (Fragment)		
15	P46778	60S ribosomal protein L21	20305658	
15	P62750	60S ribosomal protein L23a		
15	C9JXB8	60S ribosomal protein L24		
15	J3KTJ8	60S ribosomal protein L26 (Fragment)		
15	P47914	60S ribosomal protein L29		
15	A8MUD9	60S ribosomal protein L7		
15	E9PKZ0	60S ribosomal protein L8 (Fragment)		
15	D6RAN4	60S ribosomal protein L9 (Fragment)		
15	Q9Y221	60S ribosome subunit biogenesis protein NIP7 homolog		
15	F8VR50	Actin-related protein 2/3 complex subunit 3 (Fragment)		
15	F8WDD7	Actin-related protein 2/3 complex subunit 4		

Table D.1: (continued)

Gel Piece	Accession	Description	PMID	Site
15	F5H0C7	ADP-ribosylation factor 3 (Fragment)		
15	Q92572	AP-3 complex subunit sigma-1		
15	Q9NVP1	ATP-dependent RNA helicase DDX18		
15	E9PJK1	CD81 antigen		
15	F8WJN3	Cleavage and polyadenylation-specificity factor subunit 6		
15	G3V1A4	Cofilin 1 (Non-muscle), isoform CRA_a		
15	Q02413	Desmoglein-1		
15	P15924	Desmoplakin		
15	Q9NRW3	DNA dC-¿dU-editing enzyme APOBEC-3C		
15	P62487	DNA-directed RNA polymerase II subunit RPB7		
15	P68104	Elongation factor 1-alpha 1	16408927	
15	O43324	Eukaryotic translation elongation factor 1 epsilon-1		
15	P02792	Ferritin light chain		
15	P20930	Filaggrin		
15	Q5D862	Filaggrin-2		
15	P47929	Galectin-7		
15	D6R9P3	Heterogeneous nuclear ribonucleoprotein A/B		
15	F8W6I7	Heterogeneous nuclear ribonucleoprotein A1		
15	P22626	Heterogeneous nuclear ribonucleoproteins A2/B1	20305658	
15	G3V4C1	Heterogeneous nuclear ribonucleoproteins C1/C2		
15	P16403	Histone H1.2	20305658	
15	P16401	Histone H1.5	20305658	
15	Q86YZ3	Hornerin		
15	Q96AZ6	Interferon-stimulated gene 20 kDa protein		
15	F5GWP8	Junction plakoglobin		
15	P00338	L-lactate dehydrogenase A chain		
15	H3BNT4	M-phase phosphoprotein 6		
15	P19105	Myosin regulatory light chain 12A		
15	Q96J17	NOLC1 protein		
15	P67809	Nuclease-sensitive element-binding protein 1	20305658	

Table D.1: (continued)

Gel Piece	Accession	Description	PMID	Site
15	P06748	Nucleophosmin	16408927	
15	P23284	Peptidyl-prolyl cis-trans isomerase B	20305658	
15	H0YM70	Proteasome activator complex subunit 2		
15	A2ACR1	Proteasome subunit beta type		
15	P28074	Proteasome subunit beta type-5		
15	Q5JNW7	Proteasome subunit beta type-8		
15	P51149	Ras-related protein Rab-7a		
15	P61224	Ras-related protein Rap-1b		
15	Q86V81	THO complex subunit 4		
15	F8VRK0	Tubulin alpha-1B chain (Fragment)		
15	Q9NV31	U3 small nucleolar ribonucleoprotein protein IMP3		
16	P46783	40S ribosomal protein S10		
16	M0QZC5	40S ribosomal protein S11		
16	J3KMX5	40S ribosomal protein S13		
16	K7EQJ5	40S ribosomal protein S15		
16	P0CW22	40S ribosomal protein S17-like		
16	P62269	40S ribosomal protein S18	20305658	
16	P62266	40S ribosomal protein S23	16408927	
16	E7ETK0	40S ribosomal protein S24		
16	P62851	40S ribosomal protein S25		
16	E9PQ96	40S ribosomal protein S3		
16	P05388	60S acidic ribosomal protein P0		
16	P30050	60S ribosomal protein L12		
16	F8VUA6	60S ribosomal protein L18 (Fragment)		
16	G3V1B3	60S ribosomal protein L21		
16	K7EMA7	60S ribosomal protein L23a		
16	P61254	60S ribosomal protein L26	20305658	
16	P61353	60S ribosomal protein L27		
16	E9PJD9	60S ribosomal protein L27a		
16	H0YLP6	60S ribosomal protein L28		

Table D.1: (continued)

Gel Piece	Accession	Description	PMID	Site
16	F2Z388	60S ribosomal protein L35		
16	E9PKZ0	60S ribosomal protein L8 (Fragment)		
16	Q9BPX5	Actin-related protein 2/3 complex subunit 5-like protein		
16	E9PLJ3	Cofilin-1 (Fragment)		
16	K7ELV6	Cold-inducible RNA-binding protein (Fragment)		
16	H0YNW5	Deoxyuridine 5'-triphosphate nucleotidohydrolase, mitochondrial		
16	P81605	Dermcidin		
16	C9JBJ6	DNA-directed RNA polymerases I, II, and III subunit RPABC3		
16	D6R9P3	Heterogeneous nuclear ribonucleoprotein A/B		
16	F8W6I7	Heterogeneous nuclear ribonucleoprotein A1		
16	P22626	Heterogeneous nuclear ribonucleoproteins A2/B1	20305658	
16	G3V5X6	Heterogeneous nuclear ribonucleoproteins C1/C2 (Fragment)		
16	K7ELW9	Histone chaperone ASF1B		
16	P16403	Histone H1.2	20305658	
16	P16401	Histone H1.5	20305658	
16	P06748	Nucleophosmin	16408927	
16	P15531	Nucleoside diphosphate kinase A		
16	P20290	Transcription factor BTF3		
17	J3KMX5	40S ribosomal protein S13		
17	H0YB22	40S ribosomal protein S14 (Fragment)		
17	I3L3P7	40S ribosomal protein S15a		
17	M0R210	40S ribosomal protein S16		
17	P0CW22	40S ribosomal protein S17-like		
17	P39019	40S ribosomal protein S19	20305658	
17	P62851	40S ribosomal protein S25		
17	E9PQ96	40S ribosomal protein S3		
17	Q5JR95	40S ribosomal protein S8		
17	P30050	60S ribosomal protein L12		
17	F8VUA6	60S ribosomal protein L18 (Fragment)		
17	P62750	60S ribosomal protein L23a		

Table D.1: (continued)

Gel Piece	Accession	Description	PMID	Site
17	E9PJD9	60S ribosomal protein L27a		
17	P22626	Heterogeneous nuclear ribonucleoproteins A2/B1	20305658	
17	P06899	Histone H2B type 1-J		
17	K7EMV3	Histone H3		
17	J3QQQ9	KRAB-A domain-containing protein 2		
17	P15531	Nucleoside diphosphate kinase A		
18	P46783	40S ribosomal protein S10		
18	P62244	40S ribosomal protein S15a		
18	M0R3H0	40S ribosomal protein S16		
18	P39019	40S ribosomal protein S19	20305658	
18	P60866	40S ribosomal protein S20		
18	P05387	60S acidic ribosomal protein P2	20305658	
18	P62829	60S ribosomal protein L23		
18	K7EMA7	60S ribosomal protein L23a		
18	P49207	60S ribosomal protein L34		
18	P16403	Histone H1.2	20305658	
18	C9J0D1	Histone H2A		
18	Q16777	Histone H2A type 2-C		
18	O60814	Histone H2B type 1-K		
18	F8W1R7	Myosin light polypeptide 6		
18	F8W1N5	Nascent polypeptide-associated complex subunit alpha, muscle-specific form (Fragment)		
18	H7BY16	Nucleolin (Fragment)		
18	H0YLA2	Signal recognition particle 14 kDa protein		
18	P62314	Small nuclear ribonucleoprotein Sm D1		
19	P62244	40S ribosomal protein S15a		
19	Q5JR95	40S ribosomal protein S8		
19	P05387	60S acidic ribosomal protein P2	20305658	
19	J3QSB4	60S ribosomal protein L13 (Fragment)		
19	J3KTJ3	60S ribosomal protein L23		
19	P62750	60S ribosomal protein L23a		

Table D.1: (continued)

Gel Piece	Accession	Description	PMID	Site
19	E9PJD9	60S ribosomal protein L27a		
19	E5RI99	60S ribosomal protein L30 (Fragment)		
19	P16403	Histone H1.2	20305658	
19	C9J0D1	Histone H2A		
19	P06899	Histone H2B type 1-J		
19	P62805	Histone H4		
19	P31025	Lipocalin-1		
19	K7EJ44	Profilin 1, isoform CRA_b		
19	Q9Y3B4	Splicing factor 3B subunit 6		
19	H0YJW7	SRA stem-loop-interacting RNA-binding protein, mitochondrial (Fragment)		
20	P62750	60S ribosomal protein L23a		
20	P62805	Histone H4		
21	P05387	60S acidic ribosomal protein P2	20305658	
21	A6NCN2	Putative keratin-87 protein		
22	O00487	26S proteasome non-ATPase regulatory subunit 14		
22	P55036	26S proteasome non-ATPase regulatory subunit 4		
22	K7EKI4	39S ribosomal protein L4, mitochondrial		
22	Q9H9J2	39S ribosomal protein L44, mitochondrial		
22	C9J9K3	40S ribosomal protein SA (Fragment)		
22	P05388	60S acidic ribosomal protein P0		
22	P39023	60S ribosomal protein L3		
22	H3BM89	60S ribosomal protein L4		
22	P46777	60S ribosomal protein L5	18794846	
22	Q02878	60S ribosomal protein L6		
22	P60709	Actin, cytoplasmic 1	20305658	
22	O15143	Actin-related protein 2/3 complex subunit 1B		
22	Q9ULW3	Activator of basal transcription 1		
22	O00170	AH receptor-interacting protein		
22	P06733	Alpha-enolase	16408927	
22	Q13155	Aminoacyl tRNA synthase complex-interacting multifunctional protein 2		

Table D.1: (continued)

Gel Piece	Accession	Description	PMID	Site
22	P25705	ATP synthase subunit alpha, mitochondrial		
22	B4DT24	B-lymphocyte antigen CD20		
22	B4DDF4	Calponin-2		
22	Q9NX58	Cell growth-regulating nucleolar protein		
22	O14579	Coatomer subunit epsilon		
22	Q92905	COP9 signalosome complex subunit 5		
22	Q8WXX5	DnaJ homolog subfamily C member 9		
22	Q15717	ELAV-like protein 1	20305658	
22	P68104	Elongation factor 1-alpha 1	16408927	
22	P29692	Elongation factor 1-delta		
22	P05198	Eukaryotic translation initiation factor 2 subunit 1		
22	P20042	Eukaryotic translation initiation factor 2 subunit 2		
22	O75822	Eukaryotic translation initiation factor 3 subunit J	20305658	
22	A3KFL1	Exosome complex component RRP4 (Fragment)		
22	Q15024	Exosome complex component RRP42		
22	Q96B26	Exosome complex component RRP43		
22	P52907	F-actin-capping protein subunit alpha-1		
22	P04406	Glyceraldehyde-3-phosphate dehydrogenase	18794846	
22	P63244	Guanine nucleotide-binding protein subunit beta-2-like 1	16408927;18794846	
22	E9PKE3	Heat shock cognate 71 kDa protein		
22	B0QZK4	Heterochromatin protein 1-binding protein 3 (Fragment)		
22	D6R9P3	Heterogeneous nuclear ribonucleoprotein A/B		
22	Q13151	Heterogeneous nuclear ribonucleoprotein A0	20305658	
22	F8W6I7	Heterogeneous nuclear ribonucleoprotein A1		
22	P51991	Heterogeneous nuclear ribonucleoprotein A3	16408927	
22	F5H6R6	Heterogeneous nuclear ribonucleoprotein D0		
22	O14979	Heterogeneous nuclear ribonucleoprotein D-like	20305658	
22	H0YB39	Heterogeneous nuclear ribonucleoprotein H (Fragment)		
22	P31942	Heterogeneous nuclear ribonucleoprotein H3		
22	Q5T6W1	Heterogeneous nuclear ribonucleoprotein K		

Table D.1: (continued)

Gel Piece	Accession	Description	PMID	Site
22	O60506	Heterogeneous nuclear ribonucleoprotein Q	20305658	
22	P22626	Heterogeneous nuclear ribonucleoproteins A2/B1	20305658	
22	G3V4W0	Heterogeneous nuclear ribonucleoproteins C1/C2 (Fragment)		
22	Q5SRN7	HLA class I histocompatibility antigen, A-68 alpha chain		
22	H0Y4R1	Inosine-5'-monophosphate dehydrogenase 2 (Fragment)		
22	O75569	Interferon-inducible double-stranded RNA-dependent protein kinase activator A		
22	Q01650	Large neutral amino acids transporter small subunit 1		
22	P00338	L-lactate dehydrogenase A chain		
22	P07195	L-lactate dehydrogenase B chain	20305658	
22	G3XAL0	Malate dehydrogenase		
22	P40925	Malate dehydrogenase, cytoplasmic	16408927	
22	Q9BYG3	MKI67 FHA domain-interacting nucleolar phosphoprotein		
22	Q9BU76	Multiple myeloma tumor-associated protein 2		
22	H7C3G9	N-acetyl-D-glucosamine kinase		
22	F8VZJ2	Nascent polypeptide-associated complex subunit alpha, muscle-specific form		
22	Q8NEJ9	Neuroguidin		
22	P67809	Nuclease-sensitive element-binding protein 1	20305658	
22	P06748	Nucleophosmin	16408927	
22	D6RF62	Phosphoribosylaminoimidazole carboxylase		
22	E5RHG7	Polyadenylate-binding protein 1 (Fragment)		
22	Q15007	Pre-mRNA-splicing regulator WTAP		
22	Q9UNQ2	Probable dimethyladenosine transferase		
22	Q99848	Probable rRNA-processing protein EBP2		
22	Q9NPF4	Probable tRNA N6-adenosine threonylcarbamoyltransferase		
22	F5H3X6	Prohibitin-2 (Fragment)		
22	Q9Y315	Putative deoxyribose-phosphate aldolase		
22	Q9Y383	Putative RNA-binding protein Luc7-like 2		
22	Q504U3	Pyruvate kinase		
22	P60891	Ribose-phosphate pyrophosphokinase 1		
22	Q15050	Ribosome biogenesis regulatory protein homolog		

Table D.1: (continued)

Gel Piece	Accession	Description	PMID	Site
22	Q5VXN0	Ribosome production factor 2 homolog (Fragment)		
22	H0Y6E7	RNA-binding motif protein, X chromosome, N-terminally processed (Fragment)		
22	B4DHE8	RNA-binding protein Musashi homolog 2		
22	Q9UKM9	RNA-binding protein Raly		
22	P22087	rRNA 2'-O-methyltransferase fibrillarin		
22	P04279	Semenogelin-1		
22	Q07955	Serine/arginine-rich splicing factor 1		
22	Q13243	Serine/arginine-rich splicing factor 5		
22	Q13247	Serine/arginine-rich splicing factor 6		
22	Q5JRI1	Serine/arginine-rich-splicing factor 10		
22	C9JAB2	Serine/arginine-rich-splicing factor 7		
22	P62714	Serine/threonine-protein phosphatase 2A catalytic subunit beta isoform		
22	O00743	Serine/threonine-protein phosphatase 6 catalytic subunit		
22	Q96SI9	Spermatid perinuclear RNA-binding protein		
22	Q15427	Splicing factor 3B subunit 4		
22	B7Z2F4	T-complex protein 1 subunit delta		
22	K7ER96	Thioredoxin-like protein 1 (Fragment)		
22	P62995	Transformer-2 protein homolog beta		
22	Q9BQE3	Tubulin alpha-1C chain		
22	Q5JP53	Tubulin beta chain		
22	M0R268	U1 small nuclear ribonucleoprotein A (Fragment)		
22	B9A008	U3 small nucleolar ribonucleoprotein protein IMP4 (Fragment)		
22	E9PQI8	U4/U6.U5 tri-snRNP-associated protein 1		
23	P62805	Histone H4		
24	P05387	60S acidic ribosomal protein P2	20305658	
24	P15924	Desmoplakin		
24	P14923	Junction plakoglobin	12847106	
24	P02768	Serum albumin		
25	Q5D862	Filaggrin-2		
22to11	Q9BYD6	39S ribosomal protein L1, mitochondrial		

Table D.1: (continued)

Gel Piece	Accession	Description	PMID	Site
22to11	Q9P015	39S ribosomal protein L15, mitochondrial		
22to11	P15880	40S ribosomal protein S2	18794846	
22to11	P61247	40S ribosomal protein S3a		
22to11	P08865	40S ribosomal protein SA		
22to11	P05388	60S acidic ribosomal protein P0		
22to11	P36578	60S ribosomal protein L4	16408927	
22to11	P46777	60S ribosomal protein L5	18794846	
22to11	Q02878	60S ribosomal protein L6		
22to11	P62424	60S ribosomal protein L7a		
22to11	O15144	Actin-related protein 2/3 complex subunit 2		
22to11	P36542	ATP synthase subunit gamma, mitochondrial		
22to11	P11836	B-lymphocyte antigen CD20		
22to11	Q9NX58	Cell growth-regulating nucleolar protein		
22to11	O14579	Coatomer subunit epsilon		
22to11	P06493	Cyclin-dependent kinase 1		
22to11	Q8WXX5	DnaJ homolog subfamily C member 9		
22to11	Q15717	ELAV-like protein 1	20305658	
22to11	P29692	Elongation factor 1-delta		
22to11	Q13868	Exosome complex component RRP4		
22to11	P04406	Glyceraldehyde-3-phosphate dehydrogenase	18794846	
22to11	P63244	Guanine nucleotide-binding protein subunit beta-2-like 1	16408927;18794846	
22to11	Q99729	Heterogeneous nuclear ribonucleoprotein A/B		
22to11	Q13151	Heterogeneous nuclear ribonucleoprotein A0	20305658	
22to11	Q32P51	Heterogeneous nuclear ribonucleoprotein A1-like 2		
22to11	P51991	Heterogeneous nuclear ribonucleoprotein A3	16408927	
22to11	Q14103	Heterogeneous nuclear ribonucleoprotein D0	16408927	
22to11	O43390	Heterogeneous nuclear ribonucleoprotein R	20305658	
22to11	P22626	Heterogeneous nuclear ribonucleoproteins A2/B1	20305658	
22to11	P07910	Heterogeneous nuclear ribonucleoproteins C1/C2	20305658	
22to11	P16403	Histone H1.2	20305658	

Table D.1: (continued)

Gel Piece	Accession	Description	PMID	Site
22to11	P16401	Histone H1.5	20305658	
22to11	P01903	HLA class II histocompatibility antigen, DR alpha chain		
22to11	Q15181	Inorganic pyrophosphatase		
22to11	P07195	L-lactate dehydrogenase B chain	20305658	
22to11	P22234	Multifunctional protein ADE2	20305658	
22to11	Q13765	Nascent polypeptide-associated complex subunit alpha	20305658	
22to11	Q9H2J4	Phosducin-like protein 3		
22to11	Q9UNQ2	Probable dimethyladenosine transferase		
22to11	P32322	Pyrroline-5-carboxylate reductase 1, mitochondrial		
22to11	Q96C36	Pyrroline-5-carboxylate reductase 2		
22to11	O76021	Ribosomal L1 domain-containing protein 1		
22to11	Q07955	Serine/arginine-rich splicing factor 1		
22to11	O75494	Serine/arginine-rich splicing factor 10		
22to11	Q01130	Serine/arginine-rich splicing factor 2		
22to11	Q13435	Splicing factor 3B subunit 2		
22to11	Q01081	Splicing factor U2AF 35 kDa subunit		
22to11	P50990	T-complex protein 1 subunit theta	16408927;17614351	
22to11	Q9P031	Thyroid transcription factor 1-associated protein 26		
22to11	Q9BQE3	Tubulin alpha-1C chain		
22to11	P07437	Tubulin beta chain		
22to11	P16989	Y-box-binding protein 3		
6a	I3L3P7	40S ribosomal protein S15a		
6a	P62829	60S ribosomal protein L23		
6a	Q16777	Histone H2A type 2-C		
6a	P62314	Small nuclear ribonucleoprotein Sm D1		
6a	B4DUR8	T-complex protein 1 subunit gamma		
6b	P62851	40S ribosomal protein S25		
6b	P05387	60S acidic ribosomal protein P2	20305658	
6b	Q16777	Histone H2A type 2-C		
6b	P62805	Histone H4		

Table D.1: (continued)

Gel Piece	Accession	Description	PMID	Site
6b	P00338	L-lactate dehydrogenase A chain		
6b	P07737	Profilin-1	16408927	
6b	P62316	Small nuclear ribonucleoprotein Sm D2	20305658	
6b	Q9Y3B4	Splicing factor 3B subunit 6		
6b	F5GYQ2	tRNA methyltransferase 112 homolog		

Appendix E

Sequential glycan profile at single cell level with the microfluidic lab-in-a-trench platform.

Lab on a Chip

PAPER

View Article Online
View Journal

Cite this: DOI: 10.1039/c4lc00618f

Sequential glycan profiling at single cell level with the microfluidic lab-in-a-trench platform: a new era in experimental cell biology†

Tríona M. O'Connell,‡[ab] Damien King,‡[c] Chandra K. Dixit,‡[cd] Brendan O'Connor,[ab] Dermot Walls[ab] and Jens Ducrée*[cd]

Received 26th May 2014,
Accepted 18th July 2014

DOI: 10.1039/c4lc00618f

www.rsc.org/loc

It is now widely recognised that the earliest changes that occur on a cell when it is stressed or becoming diseased are alterations in its surface glycosylation. Current state-of-the-art technologies in glycoanalysis include mass spectrometry, protein microarray formats, techniques in cytometry and more recently, glyco-quantitative polymerase chain reaction (Glyco-qPCR). Techniques for the glycoprofiling of the surfaces of single cells are either limited to the analysis of large cell populations or are unable to handle multiple and/or sequential probing. Here, we report a novel approach of single live cell glycoprofiling enabled by the microfluidic "Lab-in-a-Trench" (LiaT) platform for performing capture and retention of cells, along with shear-free reagent loading and washing. The significant technical improvement on state-of-the-art is the demonstration of consecutive, spatio-temporally profiling of glycans on a single cell by sequential elution of the previous lectin probe using their corresponding free sugar. We have qualitatively analysed glycan density on the surface of individual cells. This has allowed us to qualitatively co-localise the observed glycans. This approach enables exhaustive glycoprofiling and glycan mapping on the surface of individual live cells with multiple lectins. The possibility of sequentially profiling glycans on cells will be a powerful new tool to add to current glycoanalytical techniques. The LiaT platform will enable cell biologists to perform many high sensitivity assays and also will also make a significant impact on biomarker research.

Introduction

In this report we present a novel method for sequential cell surface glycoprofiling at a single cell level that allows for the mapping of multiple glycans on a cell's surface. Here we demonstrate the method itself by using a microfluidic LiaT platform. Analysis of the surface glycosylation profile of a single cell is crucial for disease biomarker research in order to correctly elucidate the alteration of expression of a given biomarker.[1] This is important because the abundance of a given biomarker depends on several factors, the most important of which are regulatory molecules, such as chemo/cytokines and an abundance of other biomolecules on neighbouring cells that may affect the biomarker synergistically. Current methods mainly focus on the co-expression of two or more biomarkers, which are an important aspect for prognosis and understanding cell population signalling dynamics. However, this may lead to a loss of specific information about an individual biomarker.[2] Major classes of biomarkers currently employed in disease diagnosis are genetic and proteomic in nature. More recently, glycans or more specifically cell surface glycoproteins have been reported to be excellent early biomarkers for some disease states.[3]

Carbohydrates are one of the most abundant, naturally occurring organic molecules; they are central to the synthesis and metabolism of all living systems. Glycans are highly complex carbohydrate molecules and, unlike proteins, they are not encoded directly by the genome.[4] Instead, they are processed and incorporated at specific sites on proteins and lipids in various combinations during post-translational modification by tightly regulated, enzyme-mediated pathways. Their ability to form complexes within themselves and with other biomolecules, such as proteins, makes them a key component of cellular physiology. Examples of glycan-mediated signalling include embryonic development, cell differentiation and growth, cell–cell recognition, contact inhibition and cell signalling. They also have been shown to play a role in immune functions including host–pathogen interactions and appropriate immune response generation.[5,6]

[a] School of Biotechnology, Dublin City University, Glasnevin, Dublin 9, Ireland
[b] Irish Separation Science Cluster, Dublin City University, Glasnevin, Dublin 9, Ireland
[c] School of Physical Sciences, Dublin City University, Glasnevin, Dublin 9, Ireland. E-mail: jens.ducree@dcu.ie; Fax: +353 1 700 7873; Tel: +353 1 700 7870
[d] Biomedical Diagnostics Institute, National Centre for Sensor Research, Dublin City University, Glasnevin, Dublin 9, Ireland

† Electronic supplementary information (ESI) available. See DOI: 10.1039/c4lc00618f

‡ Authors contributed equally.

Glycans therefore constitute an advanced class of information molecules and the full potential of glycan bio-profiling has yet to be realized.

There are several challenges that must be overcome to further the field of glyco-biology as described in a recent report by the National Academy of Science and Engineering.[7,8] An important challenge is the identification of glycans as potential disease biomarkers, and investigations on their distribution and altered expression between various cell states. A significant hurdle in biological glycoanalysis is the limited availability of glycan-recognition biomolecules. Currently, lectins are the most commonly used probes for glycan analysis. Lectins are proteins that recognise and bind reversibly to specific glycan structures.[9] Although lectin binding affinities for monosaccharaides are generally quite low, they do bind to disaccharides and more complex oligosaccharide structures with significantly higher affinities and exquisite specificity.[9] The binding specificity of lectins can depend not only on specific sugar residues, but also on whether the residue is located at the terminus or within the carbohydrate structure, and on the positions and anomeric configurations (α- or β-) of the linkages between the constituent monosaccharide subunits.[9]

The limited repertoire of methods for glycoanalysis is also a major challenge. State-of-the-art glycoanalytical techniques include mass spectrometry (MS), lectin-based methods,[10] modified microarrays,[11,12] western blotting (protein immunoblotting) and whole cell cytometry methods[13] such as mass cytometry. More recently, glyco-quantitative polymerase chain reaction (Glyco-qPCR) has been developed for the ultrasensitive detection and quantification of glycans in biological samples.[14] Glyco-PCR offers the potential to study low-abundance glycans on cell surfaces and to quantitatively analyse interactions between carbohydrates and proteins that are important for the development and progress of a disease.

However, in spite of the above methodologies, glycan profiling of individual cells is not yet possible due to the limited amount of sample involved; analytical techniques such as microarrays and mass spectrometry need concentrated and high purity glycan fractions which are usually prepared by lysis and concentration of the glycoprotein extracts from a cell population. Thus the potential for single cell resolution and the identification of heterogeneity within the sample are lost. Flow cytometry or Fluorescence Activated Cell Sorting (FACS) demands a comparatively large number of cells (usually 50 000–100 000), and recovery and identification of individual cells for sequential analysis is again not possible. In addition cells are either destroyed (mass spectrometry, mass cytometry, Glyco-qPCR and microarray) or are subjected to large hydrodynamic shear forces (FACS and microarray). Therefore, these techniques are not appropriate for sequential lectin-based glycoanalysis. Furthermore, and most importantly, the samples involved are usually non-recoverable (Table 1). Glyco-qPCR is limited to glycans with a free reducing end and a carboxyl group.[14] Although these properties are common in *N*-glycans, *O*-glycans, and glycosaminoglycans, some glycans lack carboxyl groups. The various drawbacks to established methods for extensive glycoprofiling at the single live cell are summarised in Table 1.

In this paper we present a novel method of lectin-based glycoanalysis with single cell resolution by the use of a microfluidic LiaT platform.[15,16] This analytical approach for the first time permits repeated probing of the cell surface glycome through the sequential binding and elution of a series of labelled lectins. The key problems that are addressed by employing this approach are:

(i) Glycan profiling of live cells either requires many thousands of cells (FACS) or is restricted to probing only one glycan per cell (microarray). We address this issue by using a LiaT platform that allows for the sequential introduction of reagents by regulating the fluid properties in the microchannels in a low-volume (4 nL), shear-free platform. Thus, using LiaT allowed us to handle smaller cell samples and to deliver low-affinity reagents to the cell surface under vanishing flow field, both prerequisites for the successful implementation of the developed glycoprofiling method.

(ii) The binding of multiple lectins on the cell surface at the same time may result in inaccuracies due to inter-lectin steric hindrance. We address and eliminate this issue by sequentially probing glycans one after another using one lectin at a time. The ability to exchange lectins through sequential elution reduces the problem of steric hindrance between two adjacent binding sites.

(iii) The specificity of lectin binding on the cell surface is confirmed by a reduction in the level of cell-bound fluorescence following elution with the corresponding lectin-specific monosaccharide.

(iv) The cost of analysis can be significantly reduced through the use of a single fluorophore for all lectin types, thereby permitting analysis with a very basic fluorescence microscopy setup. The LiaT system does not require any specialist pumps or other auxiliary equipment. The simple architecture allows cost-efficient mass manufacture of the microfluidic chips.

Furthermore, it has been demonstrated that our method and the LiaT platform can be employed for several other applications.[17] In summary, we show that the LiaT-based multi-lectin technology described here is a significant advance that enables glycan profiling at the level of a single live cell.

Theory

Principles of lab in a trench

Lab-in-a-Trench (LiaT) is a microfluidic platform previously developed by Dimov *et al.*[15,16] in which cells are contained and analysed in a shear-free environment. We reasoned that LiaT would permit glycoprofiling at a single cell level. Several other single cell analysis platforms are available, including constricted channel-based,[18] cup-based,[19] and cylindrical trap-based systems.[20] Most of these alternative (non-LiaT) systems are either shear-based, continuous flow-based or open (several cell traps in a given area) systems. It has been

Table 1 Comparison of state-of-the-art technologies for glycoanalysis

Glycoprofiling strategies	Limitations	Advantages	Ref.
Whole cell-based approaches			
Flow cytometry	Requires huge number of cells Works at population level Costly instrumentation Inability to localise multiple glycans on cell surface and on protein domains Cells are exposed to tremendous pressures that may induce changes leading to false characterization Inability to correlate the retrieved cells to their FACS data for further validation	High-throughput and quantitative Routinely employed in clinical set-ups and industries	6–8
Microscopy	Inability to perform multi-lectin glycoprofiling Multiple staining is laborious with a high probability of inter-stain steric hindrance	Possible to localise glycans on cell surface	9
Crude cell lysate-based approaches			
Microarray	Homogeneous cell population required Inability to classify sub-populations Inability to allow single cell multi-lectin glycoprofiling Expensive, labour-intensive High detection limits and narrow detection ranges Of limited diagnostic value	High throughput Visual; quantitative	10–12
Purified cell lysate-based approaches			
Mass spectrometry	Virtually impossible to analyse intact molecules Challenging data-interpretation due to glycan complexity, proton/cation exchange and loss of sulfo groups Limited availability of computer assisted programs for complexity analysis	High-throughput Confirmatory	13–14
NMR	Inability to distinguish isomers Laborious and time consuming method of sample preparation Loss of surface sugars mainly *O*-linked along with some *N*-linked glycans during sample preparation Inability to analyse whole cells and live cell Costly instrumentation		

well established that even slight alterations in biophysical conditions, including hydrodynamic forces, can trigger changes in cellular morphology and physiology.[21] As the LiaT system allows the merely diffusion-based delivery of lectins, cells can be probed in a shear-free environment.

The LiaT platform contains a deep, micron-scale indentation within a continuous channel that enables the capture and retention of cells purely based on gravity[15,16] (Fig. 1). LiaT follows a well-known working principle that is based on the Camp–Hazen model of a settling basin.[22] In this model, the velocity of cells over the trench is the most critical parameter for ensuring their gravity-driven capture.

Lab in a trench – microfluidic theory

We consider particle trapping in the trench according to the *critical trajectory model* for a Camp–Hazen type settling tank (Fig. 1a). Cells are suspended in a flow of PBS buffer of density $\rho = 1.0 \times 10^3$ kg m^{-3} and viscosity $\eta = 1.09 \times 10^{-3}$ Pa s under the impact of the gravitational acceleration $g = 9.81$ m s^{-2}. A pressure head $\Delta p = 1.5$ hPa built up by a pipette filled to a liquid level $\sigma = 1.5$ cm applies across the main channel has total length $l_{\mathrm{channel}} = 14$ mm, constant height $h_{\mathrm{channel}} = 35$ μm and width $w_{\mathrm{channel}} = 40$ μm which broadens to $w_{\mathrm{trench}} = 250$ μm above the trench of stream-wise length $l_{\mathrm{trench}} = 100$ μm (Fig. 1b). Neglecting the trench section, the (average) flow of velocity then amounts to

$$v_{\mathrm{channel}} = \frac{h_{\mathrm{channel}} w_{\mathrm{channel}} \Delta p}{C_{\mathrm{nc}} \eta l_{\mathrm{channel}}} \approx 430\ \mu\mathrm{m\ s}^{-1}$$

with the numerical coefficient for the rectangular channel $C_{\mathrm{nc}} \approx 32.14$. The (average) flow velocity even reduces to

$$v_{\mathrm{trench}} = \frac{w_{\mathrm{channel}}}{w_{\mathrm{trench}}} \cdot v_{\mathrm{channel}} \approx 70\ \mu\mathrm{m\ s}^{-1}$$

within the sector above the trench. The resulting Reynolds number

$$\mathrm{Re} = \frac{\rho v w}{\eta} \ll 1$$

indicates that flow conditions are strictly laminar within the channel as well as in the trench for typical flow speeds v and widths w. Hence, streamlines will only penetrate into the uppermost region of the trench and molecular (reagent) transport across streamlines into the trench occurs solely through diffusion[15] (Fig. 1a).

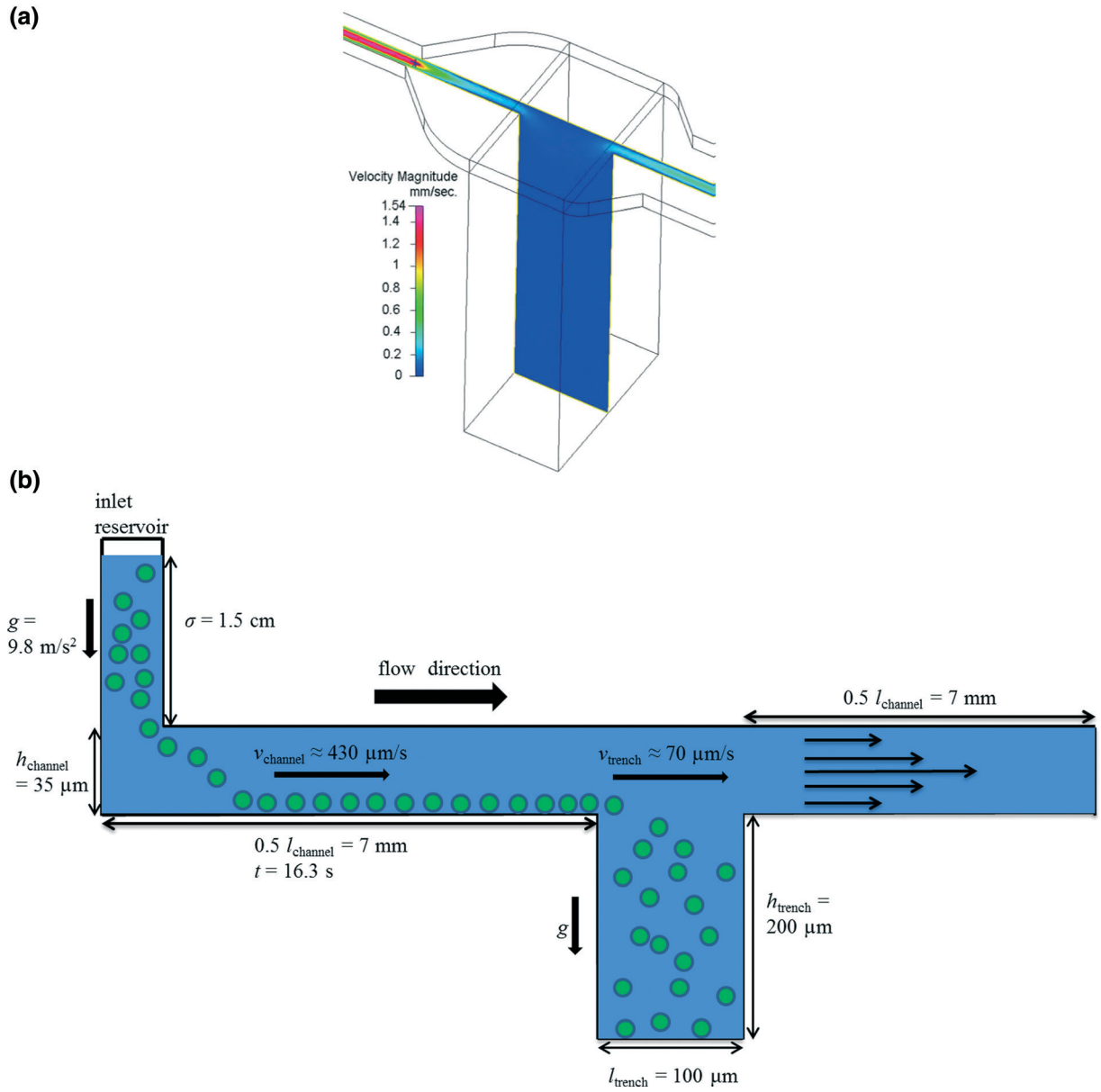

Fig. 1 Principles of the lab in a trench microfluidic platform: (a) simulation of cell capture based on sedimentation of cells to the bottom of the trench structure.[15] (b) Operating principle of the lab in a trench platform. Reagents are exchanged by diffusion permitting a shear-free environment at the bottom of the trench structure.

With the speed of sedimentation

$$v_{sed} = \frac{gd^2}{18\eta}(\rho_{cell} - \rho)$$

for cells of density ρ_{cell} and diameter d we can determine the ratio

$$\frac{t_{sed}}{t_{in}} = \frac{18\eta h_{channel}}{gd^2(\rho_{cell} - \rho)} \cdot \frac{v_{channel}}{(l_{channel}/2)}$$

between the sedimentation time t_{sed} $(h) = h_{channel}/v_{sed}$ across the entire channel height $h_{channel}$ and the (minimum) residence time of the cells in the incoming segment $t_{in} = 0.5l_{channel}/v_{channel}$ located at about $0.5l_{channel}$ after the inlet.

For Ramos cells with a density of $\rho_{cell} = 1.02 \times 10^3$ kg m^{-3} and a typical diameter $d = 10$ µm suspended in PBS buffer, this ratio is much smaller than unity so that the entire population of Ramos cells will have settled to the bottom of the channel way before reaching the downstream trench (Fig. 1b).

Due to the parabolic flow profile, their speed of cell migration will hence be significantly reduced with respect to the above calculated (average) flow velocity v_{trench}. The cell velocity in the trench region

$$v_{cell} \approx 2v_{trench}\left(\frac{h_{cell}}{h_{channel}/2}\right)^2 = 8v_{chansnel}\frac{w_{channel}}{w_{trench}}\left(\frac{h_{cell}}{h_{channel}}\right)^2$$

depends on the distance of the cell from the bottom of the channel h_{cell}. If, for instance, a cell was touching the bottom of the channel (Fig. 1b), *i.e.* $h_{cell} = d/2$, their speed of horizontal migration would amount to $v_{cell} \approx 10\ \mu m\ s^{-1}$, only.

For efficient trapping, the ratio

$$\frac{t_{sed}}{t_{res}} = \frac{18\eta h}{gd^2(\rho_{cell} - \rho)} \cdot \frac{v_{cell}}{l_{trench}} \approx \frac{18\eta h}{gd^2(\rho_{cell} - \rho)} \cdot \frac{2v_{channel} w_{channel}}{w_{trench} l_{trench}} \left(\frac{d}{h_{trench}}\right)^2 < 1$$

of the cell sedimentation time (to a depth d into the trench) and the cell residence time in the trench region needs to be lower than unity. This implies an upper limit

$$v_{channel}^* = \frac{g(\rho_{cell} - \rho) w_{trench} l_{trench} h_{trench}^2}{36\eta h w_{channel}}$$

for the flow speed in the (main) channel. Assuming that the cell will be irreversibly trapped after penetrating a distance corresponding to the channel height into the trench, *i.e.* $h = h_{channel}$, we obtain a speed limit of $v_{channel}^* = 545\ \mu m\ s^{-1} > v_{channel} = 430\ \mu m\ s^{-1}$ as calculated above. Please note that while the derived equations are quite instructive for the understanding of the system and we even obtain a speed limit compliant with an experimentally observed flow rate at which trapping occurs, these "back-of-the-envelope" calculations are just coarse, order-of-magnitude estimates in a more quantitative picture.

COMSOL simulations

Liquid flow profiles (Fig. 1a) obtained for channels of these dimensions have been comprehensively simulated by COMSOL modelling.[15]

Lab in a trench – micro-fabrication

The platform is a two layer polydimethylsiloxane (PDMS) system whereby a lower PDMS panel holds structures (channel and trenches), while an upper panel has reservoirs. In brief, PDMS (Dow Corning) was mixed with curing agent in a ratio of 5 : 1 for the trenches and 20 : 1 for the lid, followed by degassing for a minimum of 30 min under vacuum. Degassed PDMS was then poured on the appropriate silicon masters and partially cured for 3–4 hours at room temperature under vacuum. Inlet holes (diameter: 1 mm) were then punched in the lid structure. The two PDMS layers containing the channels and reservoirs were then aligned, bonded and cured at 70 °C for 24 hours.

Gravity driven flow

Gravity driven flow was implemented by fitting a vertically aligned, standard pipette tip in the inlet hole of the LiaT chip and loading it with input fluid. The flow velocity was determined by the height of the liquid column which was kept at roughly $\sigma = 1.5$ cm over the course of the experiment.

Device priming and cell loading

The fabricated LiaT was O_2 plasma treated for 5 min. Then channels and trenches were immediately primed with 100 mM Tris-buffered saline (TBS), pH = 7.4, containing 1 mM $CaCl_2$. Each inlet was then loaded with cells by adding 0.4 μl of culture (10^5 cells per mL) to the 20 μL of TBS already present in the gravity pump.

Capture efficiency close to 100% was routinely achieved within the system by keeping the flow velocity at the inlet within the range of $\leq 430\ \mu m\ s^{-1}$ and ensuring that the channel to trench depth ratio was kept above 1 : 5. It has been shown by Manbachi *et al.* that a shear stress-free environment exists within the trench under such conditions[23] and, as a consequence, flow velocities are at least three times lower at the bottom of the trench relative to the top.[15,23]

Three times the required number of cells to be captured was loaded. By operating in the critical flow velocity range of $\leq 430\ \mu m\ s^{-1}$, the required number of cells can be captured in the trench. Surplus cells were then removed by increasing the flow velocity ($>430\ \mu m\ s^{-1}$) at the inlet and these then passed over the top of the trench and travelled to the waste chamber at the bottom of the chip.

Briefly, Ramos cells were suspended in TBS buffer by adding ~1500 cells to a 20 mL solution of TBS. Cell suspensions and reagents were loaded and pumped through the system with a hydrostatic pressure-head[17] created by liquid level in the pipette tip. Theoretically, a trench can hold approximately 60 non-overlapping cells and up to 200 cells if there is no requirement for such a monolayer. Reagents were introduced at higher speeds to establish a fixed concentration on top of the trench. The laminar flow in the channel ensured an abruptly vanishing flow field below the plane of the upper flow channel, *i.e.* essentially throughout the entire trench (Fig. 1). Therefore, shortly after the cells have entered the trench, they are irreversibly retained in a flow-free environment; as they maintain their location at the bottom of the trench and can hence be individually observed over time. Access of reagents and wash buffer to the trench-trapped cells therefore solely occurs by diffusion and so the hydrodynamic stress to which these captured cells are exposed, are negligible. In addition, trench depths as small as 200 μm (with typical volumes of 4 nL) allow continuous loading of reagents and nutrients to provide efficient on-chip cell culturing.

Experimental

Reagents

Biotinylated lectins (WGA, ConA, ECL, LCA, NPL) were obtained from Vector Laboratories. These were labelled with DyLight 488 – streptavidin (Vector Laboratories) according to the manufacturer's instructions. Fucose, mannose, galactose and *N*-acetylglucosamine were purchased from Sigma. All lectins and sugars were suspended in TBS pH 7.4 with 1 mM $CaCl_2$.

Cell culture

Ramos cells (ATCC no. CRL-1596), a B cell line of Burkitt's lymphoma origin, were cultured in RPMI 1640 (Sigma) supplemented with 10% heat inactivated foetal calf serum (Gibco) and 1% penicillin/streptomycin (Sigma). Cells were incubated at 37 °C with 5% CO_2, split every two to three days and seeded at a density of 2.5×10^5 cells ml^{-1}.

Sequential glycan profiling

Each Dylight488-conjugated lectin (1 μl of 0.1 mg mL^{-1}) was introduced in the inlet with 20 μl buffer reserve. The lectin flows with the buffer in the channel. The typical time for the (near) completion of lectin diffusion from the inlet to the bottom of the trench was 20 s. Lectin binding to cells was monitored by fluorescence microscopy every 5 min. After reaching binding saturation, which was different for each lectin, free sugar (20 μl of buffer with 2 μL 1 M sugar giving a working concentration of 100 mM) was introduced into the system to elute bound lectin from the cell surface (Fig. 2). Elution sugar was chosen according to the specificity of each lectin as shown in ESI† Table S1. The elution sugar of a preceding lectin does not hinder the binding of the next incoming lectin unless both lectins have an affinity for the same sugar. In this case, the liquid in the system was replaced with fresh TBS. LCA, ConA and NPL bind specifically to mannose and its derivative arrangements, thus in those cases there was a need to change inlet buffer after each elution.

Fluorescence microscopy

The trench was imaged with an Olympus IX81 motorized inverted microscope with an attached Hamamatsu ORCA – ER digital camera C4742-80 using a 10× objective. The microscope platform was maintained at 5% CO_2 and a temperature of 37 °C for the duration of the experiments. After the introduction of each lectin into the channel, focus was maintained on the cells for the duration of each lectin binding and elution event. Images were captured at that focus after 5 min in TIFF format in order to preserve the original pixel densities of the image (Fig. 2).

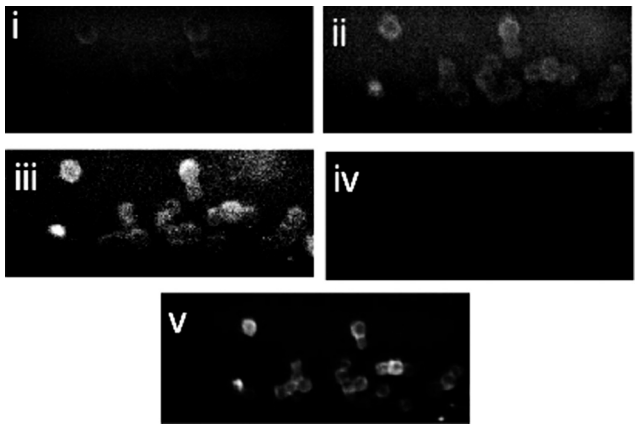

Fig. 2 Series of images of sequential elution of fluorophore-labelled lectin off Ramos cells: images i, ii, iii show diffusion of LCA into the channel and staining of the cells after 0, 5, 10 minutes. Image iv shows the cells after free mannose had been diffused into the system. Image v was taken after ECL had been added to the system.

Image analysis with ImageJ

Images were analysed by the software ImageJ (version 1.46r). Fluorescence intensity was quantitated by 'region of interest (ROI)' analysis. An average intensity was obtained for each cell through the time series. Fluorescent images of the final time point of each lectin series were used to create overlays of individual cells. This allowed a visual depiction of the glycan distribution across the surface of the cells. Examples of the overlaid images are shown in Fig. 3b, 4b and 5b.

Results and discussion

Sequential glycan probing

The LiaT platform was employed to examine the surface glycosylation of Ramos B lymphoma cells, and benchmarked with characterization of the same features by flow cytometry (ESI† Fig. S1). Ramos cell surface glycans were thus sequentially probed by a panel of four fluorescently-labelled lectins, categorized as mannose- (LCA, NPL and ConA), galactose- (ECL) and *N*-acetylglucosamine- (GlcNAc) binders (WGA). A summary of the sequential experiments undertaken is presented in Table 2. The interference of free sugar from previous stains was assessed with three mannose-binding lectins, namely, LCA, ConA and NPL (ESI† Table S1). An additional wash step was incorporated between sugar elution and addition of the next lectin in the sequence.

Each trench was loaded with 15–20 cells in TBS with 1 mM $CaCl_2$. Each DyLight488-labelled lectin was introduced in the LiaT at a concentration of 11 μg μL^{-1} and diffused to the cells at the bottom of each trench in less than 30 s, as also shown to be the case in the COMSOL simulations performed by Dimov *et al.*[15] The resultant lectin concentration effectively available for cells to bind was therefore 13 pg in each 4 nl trench. Lectin-binding events were then recorded over time by epifluorescence microscopy. They are presented here in 5 min time steps (Fig. 3–5) as a function of increasing fluorescence signal until saturation established. This was followed by elution with the specific sugar substrate of the bound lectin. A summary of the different sequential profiling experiments performed is given in Table 2.

In the first experiment with the two lectins LCA and ECL, stronger signals were detected with LCA indicating a denser mannose distribution at the cell surface when compared to ECL, which has an affinity for galactose residues (Fig. 3). This is in agreement with general cell surface glycan structures because galactose is known to be either protected or partially exposed on live healthy cells which results in poor ECL binding and hence lower equilibrium concentrations and reduced signals.[24]

In a second experiment involving three mannose-binding lectins, the successive binding of the second and third lectins

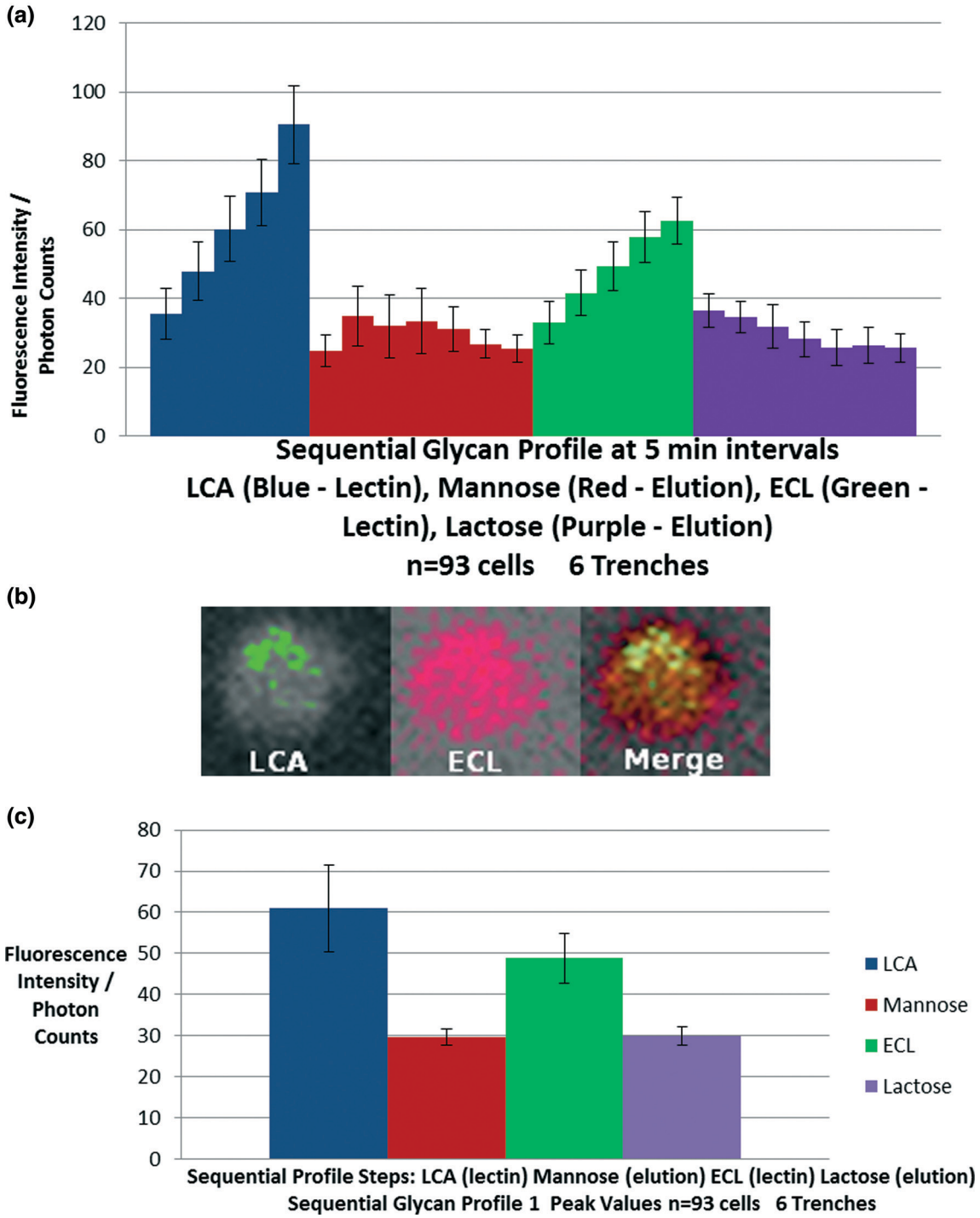

Fig. 3 (a) Average intensity of individual cell staining as calculated by ImageJ. Each lectin and elution step is represented by an individual colour. Each step within each colour on the plot represents a 5 minute time interval. Images collected at 5 minute intervals after addition of LCA (blue), mannose (red), ECL (green) and lactose (purple). (b) An example of a cell stained sequentially with LCA and ECL, and resulting overlay. (c) Average peak intensity values of individual cell staining.

was not affected by the presence of mannose during earlier steps in the probing sequence, *i.e.* indicating the effectiveness of the preceding wash step (Fig. 4). The peak fluorescence of LCA and ConA was comparable to those achieved in the next experiment (Fig. 5) also including ConA and WGA. In this 4-lectin experiment, a higher signal was obtained with the latter and an intermediate signal with the former (Fig. 5). This experiment confirmed high GlcNAc and core mannose levels on the cell surface. When mannose binders (LCA and ConA) were compared, the amount of bound LCA was found to be lower than that of bound ConA. This is likely to reflect the known difference in affinity between LCA and ConA,

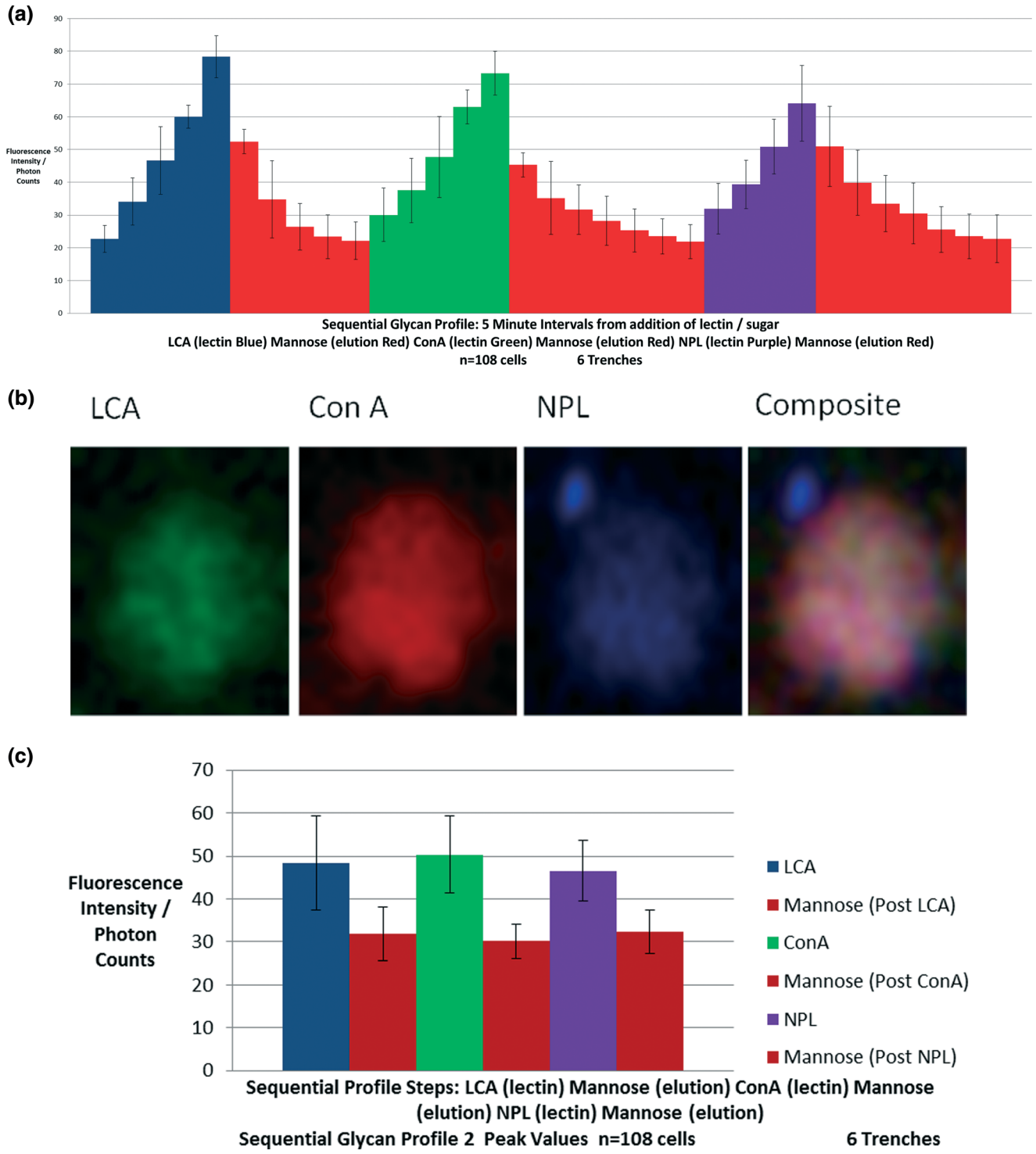

Fig. 4 (a) Average intensity of individual cell staining as calculated by ImageJ. Each lectin and elution step is represented by an individual colour. Each step within each colour on the plot represents a 5 minute interval. The images were collected at 5 minute intervals after addition of LCA (blue), ConA (green), NPL (purple) and mannose (red). (b) An example of a cell sequentially stained with LCA, ConA and NPL and resulting overlay. (c) Average peak intensity values of individual cell staining.

where the former only recognizes α-linked fucosylated mannose. GlcNAc presented with the highest density among all the exogenous glycans that were probed.

As the lectins were added in an order such that sugar elution would not interfere with the following lectin, we were able to image individual cells without the requirement for wash steps. This allowed us to create spatio-temporal glycan density profiles of the cell surface using regular image analysis (ESI† Fig. S2). In addition, the order of lectins was selected so as to minimise impact on the cells, based on the

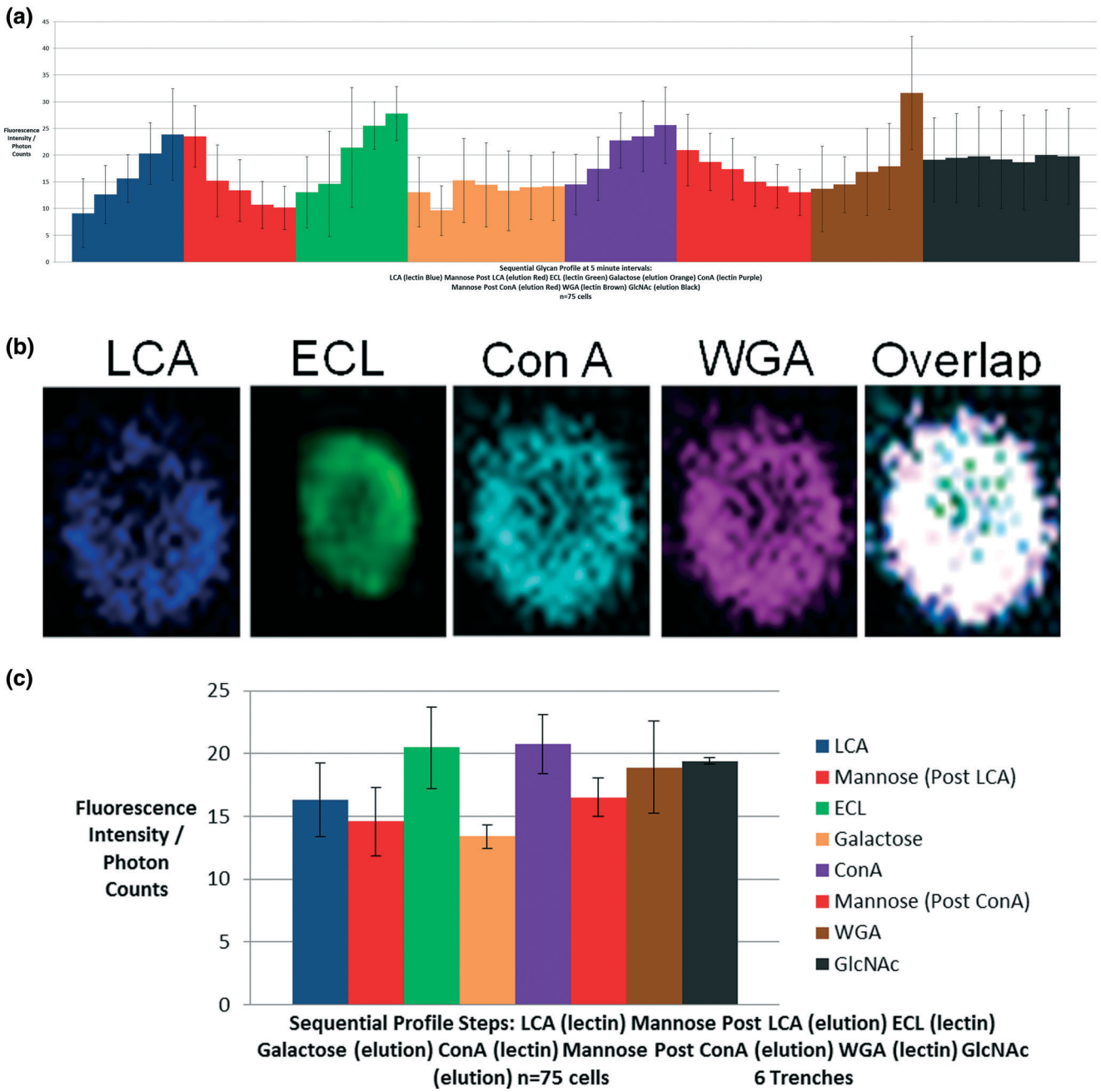

Fig. 5 (a) Each lectin and elution step is represented by a distinct colour. Each step within each colour on the plot represents a 5 minute time interval. Sequential profile steps (5 minute intervals): LCA (lectin-blue), mannose (elution-red), ECL (lectin-green), galactose (elution-orange), ConA (lectin-purple), mannose (elution-red), WGA (lectin-brown), GlcNAc (elution-black). (b) An example of a cell sequentially stained with LCA, ECL, ConA and WGA and resulting images overlaid. (c) Average peak intensity values of individual cell staining.

Table 2 Summary of experimental procedures

No. of lectins	Lectins	No. of elutions	Elutions	No. of cells	No. of trenches on chip
2	LCA, ECL	2	Mannose, galactose	93	6
3	LCA, ConA, NPL	3	Mannose (3×)	108	6
4	LCA, ECL, ConA, WGA	4	Mannose (2×), galactose, GlcNAc	75	6

changes observed when using each lectin in flow cytometry (ESI† Fig. S1). The sugar elution steps were rapid (in the order of minutes), thus minimising any potential physiological impact on the cells in the trenches. It can be noted that in experiments 2 and 3, LCA was followed directly or indirectly by ConA (Fig. 4 and 5). In experiment 3, similar observations

were made to experiment 2, indicating that the fucose elution of ECL in experiment 3 had not interfered with the cells' binding of ConA.

Qualitative cellular glycan map

Through the software Image-J we have generated a qualitative glycan map by simple co-localisation of individual lectins and an overlap of all bound lectins (Fig. 3b, 4b and 5b). In general, a cell population was profiled at successive points in time and the resulting images were then overlaid with computational tools to produce the glycan map.

In-trench lectin specificity

We have confirmed that the free sugars can be washed from the system such that they do not interfere with the following lectin. This has been demonstrated by targeting a common carbohydrate (mannose in this case) with three different lectins (LCA, ConA and NPL) that probe mannose and exhibit similar specificities. We found binding of all lectins to similar positions on the cell surface but with varying intensities (Fig. 4b).

Heterogeneity analysis: single cell *versus* cell population

The results generated were then analysed with a view to understanding glycan heterogeneity at the single-cell level. An difference was observed at the inter-cellular (n = 12) level in the glycan-probing behaviours of lectins on individual cells as demonstrated by their NPL lectin profile (ESI† Fig. S3). Lectins are usually low-affinity binders with their dissociation rate constants (K_d) ranging from 10^{-4} to 10^{-7} mol^{-1} s^{-1}. The impact of glycan structure and complexity has been known for a long time but its functional interpretation has only begun to be addressed in the last few years.[25–27]

The sequential lectin-elution method has thus enabled us to detect multiple sugars over time on a given live cell and that is a considerable technical advancement over current state-of-the-art methods. We show here that the LiaT platform also permits the differential characterization of diverse glycosylation features at the single cell as well as at a population level. By overlaying the images of different lectin probes, one could also effectively perform various other qualitative and quantitative analyses like the kinetics of lectin binding to cell-bound sugars and the development of sugar distribution profiles (ESI† Fig. S4). Coupled to LiaT platforms, this strategy has the potential to significantly impact on the advancement of glycoanalysis.

Conclusions

Due to minimisation of cell translocation as well as alterations to the physiological dynamics at their surface, the sequential binding of lectin probes to glycans on the surface of individual cells within a population can be analysed the novel LiaT platform. Furthermore, the simple geometry allows very cost-efficient mass manufacture. Beyond the here presented application in glycoscience, the LiaT platform thus also bears a significant potential to expand the analytical toolbox of cell biology and biomarker discovery.

Notes and references

1 S. J. Altschuler and L. F. Wu, *Cell*, 2010, **141**, 559–563.
2 V. Almendro, A. Marusyk and K. Polyak, *Annu. Rev. Pathol.: Mech. Dis.*, 2013, **8**, 277–302.
3 D. H. Dube and C. R. Bertozzi, *Nat. Rev. Drug Discovery*, 2005, **4**, 477–488.
4 A. Varki, R. D. Cummings, J. D. Esko, H. H. Freeze, P. Stanley, C. R. Bertozzi, G. W. Hart and M. E. Etzler, *Essentials of Glycobiology*, Cold Spring Harbor Laboratory Press, Cold Spring Harbor (NY), 2nd edn, 2009.
5 K. Ohtsubo and J. D. Marth, *Cell*, 2006, **126**, 855–867.
6 H. Ghazarian, B. Idoni and S. B. Oppenheimer, *Acta Histochem.*, 2011, **113**, 236–247.
7 National Academy of Sciences National Academy of Engineering Institute of Medicine National Research Council, *Transforming Glycoscience: A Roadmap for the Future*, 2012.
8 J. F. Rakus and L. K. Mahal, *Annu. Rev. Anal. Chem.*, 2011, **4**, 367–392.
9 M. Ambrosi, N. R. Cameron and B. G. Davis, *Org. Biomol. Chem.*, 2005, **3**, 1593–1608.
10 J. Hirabayashi, A. Kuno and H. Tateno, *Electrophoresis*, 2011, **32**, 1118–1128.
11 A. Kuno, N. Uchiyama, S. Koseki-Kuno, Y. Ebe, S. Takashima, M. Yamada and J. Hirabayashi, *Nat. Methods*, 2005, **2**, 851–856.
12 H.-H. Jeong, Y.-G. Kim, S.-C. Jang, H. Yi and C.-S. Lee, *Lab Chip*, 2012, **12**, 3290–3295.
13 D. R. Gossett, W. M. Weaver, N. S. Ahmed and D. Di Carlo, *Ann. Biomed. Eng.*, 2011, **39**, 1328–1334.
14 S. J. Kwon, K. B. Lee, K. Solakyildirim, S. Masuko, M. Ly, F. Zhang, L. Li, J. S. Dordick and R. J. Linhardt, *Angew. Chem., Int. Ed.*, 2012, **51**, 11800–11804.
15 I. K. Dimov, G. Kijanka, Y. Park, J. Ducrée, T. Kang and L. P. Lee, *Lab Chip*, 2011, **11**, 2701–2710.
16 G. Kijanka, R. Burger, I. K. Dimov, R. Padovani, K. Lawler, R. O'Kennedy and J. Ducrée, *Advanced Biomedical Engineering*, InTech, 2011.
17 I. K. Dimov, G. Kijanka and J. Ducree, in *2010 IEEE 23rd International Conference on Micro Electro Mechanical Systems (MEMS)*, IEEE, 2010, pp. 96–99.
18 A. C. Rowat, J. C. Bird, J. J. Agresti, O. J. Rando and D. A. Weitz, *Proc. Natl. Acad. Sci. U. S. A.*, 2009, **106**, 18149–18154.
19 A. M. Skelley, O. Kirak, H. Suh, R. Jaenisch and J. Voldman, *Nat. Methods*, 2009, **6**, 147–152.
20 L. Lin, Y.-S. Chu, J. P. Thiery, C. T. Lim and I. Rodriguez, *Lab Chip*, 2013, **13**, 714–721.
21 S. Elliott, *Cell Damage due to Hydrodynamic Stress in Fluorescence Activated Cell Sorters*, The Ohio State University, 2009.
22 N. M. C. Saady, *J. Appl. Sci. Environ. Sanit.*, 2011, **6**, 309–315.

23 A. Manbachi, S. Shirvastava, M. Cioffi, B. G. Chung, M. Moretti, U. Demirchi, M. Yliperttula and A. Khademhosseini, *Lab Chip*, 2008, **8**, 747–754.
24 H. Tateno, N. Uchiyama, A. Kuno, A. Togayachi, T. Sato, H. Narimatsu and J. Hirabayashi, *Glycobiology*, 2007, **17**, 1138–1146.
25 N. Sethuraman and T. A. Stadheim, *Curr. Opin. Biotechnol.*, 2006, **17**, 341–346.
26 J.-T. Cao, Z.-X. Chen, X.-Y. Hao, P.-H. Zhang and J.-J. Zhu, *Anal. Chem.*, 2012, **84**, 10097–10104.
27 J. Hirabayashi, M. Yamada, A. Kuno and H. Tateno, *Chem. Soc. Rev.*, 2013, **42**, 4443–4458.